Comparative transcriptomic analysis of *Zymoseptoria tritici* reveals interaction-specific gene expression patterns during susceptible, resistant, and non-host interactions

Sandra V. Gomez-Gutierrez,[1] Cassidy R. Million,[2] Namrata Jaiswal,[2] Michael Gribskov,[3] Matthew Helm,[2] and Stephen B. Goodwin[2, †]

[1] Department of Botany and Plant Pathology, 915 Mitch Daniels Blvd., Purdue University, West Lafayette, IN 47907-2054

[2] Crop Production and Pest Control Research Unit, USDA–Agricultural Research Service, 915 Mitch Daniels Blvd., West Lafayette, IN 47907-2054

[3] Department of Biological Sciences, 915 Mitch Daniels Blvd., Purdue University, West Lafayette, IN 47907-2054

[†] Corresponding author: S. B. Goodwin; Steve.Goodwin@USDA.gov

***Zymoseptoria tritici* is responsible for Septoria tritici blotch, a disease causing significant annual yield losses in wheat. To investigate infection phase-specific gene expression in the pathogen, we analyzed gene expression during infection of susceptible (Taichung 29) and resistant (Veranopolis and Israel 493) wheat cultivars, plus the non-host species barley at 1, 3, 6, 10, 17 and 23 days post inoculation (DPI). There were dramatic differences in pathogen gene expression at 10 DPI in the susceptible compared to both resistant interactions. The most pronounced differences in pathogen gene expression were observed at 3 DPI in both the susceptible and resistant host interactions compared to the non-host interaction.**

Thirty-one putative effectors showed early expression during the susceptible interaction compared to the non-host interaction, and six effectors were selected for subcellular localization studies. Using *Agrobacterium*-mediated transient expression in *Nicotiana benthamiana*, subcellular localization assays revealed that two candidate effectors, Mycgr3109710 and Mycgr394290, localized to putative mobile cytosolic bodies when expressed without their signal peptides, suggesting potential roles in intracellular signaling or host gene regulation. When expressed with their native signal peptides, four candidate effectors localized to the cytosol, while one effector, Mycgr3107904, did not accumulate to detectable levels, as shown by immunoblot analysis, indicating degradation. Comparison of pathogen gene expression in the susceptible host to expression in the resistant hosts, allowed us to identify genes that are expressed during the transition from biotrophic to necrotrophic growth at 10 DPI. Comparison of pathogen gene expression in resistant and susceptible hosts, versus in the non-host barley, allowed us to identify genes involved in initial colonization and host recognition. In addition, our study contributes to understanding candidate effectors that are activated early during infection and may play a role in the initial suppression of plant immunity, making them strong candidates for functional characterization.

Keywords: differential expression, effectors, fungal pathogen, localization, RNA sequencing, RNAseq, wheat*, Zymoseptoria tritici*

Zymoseptoria tritici is a fungal pathogen in the class Dothideomycetes that causes Septoria tritici blotch (STB) disease of bread (*Triticum aestivum*) and durum (*T. turgidum* subsp. *durum*) wheat (Kettles & Kanyuka, 2016; Palma-Guerrero et al., 2017). STB is one of the most

47 yield-limiting diseases of wheat globally and may result in fifty percent yield loss, especially in
48 regions with high humidity and mild temperatures (Mekonnen et al., 2020; Yang et al., 2022). *Z.*
49 *tritici* is a hemibiotroph that transitions from biotrophic to necrotrophic growth after a prolonged
50 7- to 10-day latent period (Ponomarenko et al., 2011; Rudd et al., 2015). During the biotrophic
51 growth phase, the pathogen circumvents recognition through suppression of host immune re-
52 sponses, likely by translocating virulence (effector) proteins. During the necrotrophic phase, the
53 fungus degrades host tissue and presumably extracts nutrients from host plant cells (Marshall et
54 al., 2011; Steinberg, 2015). The hemibiotrophic lifestyle of *Z. tritici* coupled with the availability
55 of a complete, chromosome-level genome (Goodwin et al., 2011) makes this fungal pathogen an
56 attractive model to investigate infection phase-specific gene expression.

57 Though *Z. tritici* is a hemibiotroph, our knowledge of its infection strategy and lifestyle
58 transition remains limited. Nevertheless, comprehensive RNA sequencing analyses have pro-
59 vided insights into host and pathogen gene expression during a susceptible interaction (Rudd et
60 al., 2015; Yang et al., 2013), transcriptome signatures associated with blastospore and mycelial
61 growth (Francisco et al., 2019), as well as differences in gene expression among *Z. tritici* strains
62 (Palma-Guerrero et al., 2017). Studies have also assessed plant gene expression in resistant-host
63 (incompatible) and non-host interactions (Orton et al., 2017; Reilly et al., 2021), and one study
64 compared the pathogen gene expression profile during infection in a susceptible host (*T. aes-*
65 *tivum* L.) and a non-host (*Brachypodium distachyon*) (Kellner et al., 2014). Kellner et al. (2014)
66 found that many *Z. tritici* genes that are up-regulated in wheat encode proteins with putative se-
67 cretion signals and therefore may play a functional role in host invasion. The most highly differ-
68 entially expressed genes (DEGs) in *Z. tritici* in the comparison of the susceptible and the non-
69 host interactions showed signatures of positive selection and can be considered candidates for

70 potential roles in host specialization of this pathogen (Kellner et al., 2014).

71 Differential responses of pathogens to susceptible, resistant, and non-host species are of-
72 ten determined by the molecular mechanisms underlying the interactions, as well as virulence
73 (effector) proteins (Selin et al., 2016). Pathogens often secrete effectors, in part, to circumvent
74 host innate immune responses (Petit-Houdenot & Fudal, 2017; Selin et al., 2016). Once translo-
75 cated to the host apoplast or cytosol, effector proteins interfere with cell surface-mediated and
76 intracellular-mediated immune responses, thereby promoting pathogenesis and disease develop-
77 ment. In *Z. tritici*, some effector proteins have been functionally characterized (Motteram et al.,
78 2009; Marshall et al., 2011; Mirzadi Gohari et al., 2015; Rudd et al., 2015; Ben M'barek et al.,
79 2015; Karki et al., 2021; Thynne et al., 2024). For example, the *Z. tritici* effector Mg3LysM is
80 expressed during early disease development and suppresses chitin-induced defense responses in
81 wheat (Marshall et al., 2011; Rudd et al., 2015). Furthermore, Karki et al. (2021) recently identi-
82 fied an effector from *Z. tritici*, ZtSSP2, that is expressed at 2 days post inoculation (DPI) and in-
83 teracts with a wheat E3 ubiquitin ligase (TaE3UBQ). Intriguingly, virus-induced gene silencing
84 of TaE3UBQ resulted in increased *Z. tritici* susceptibility, suggesting its encoded protein may
85 function as a regulator of wheat defense responses, and that ZtSSP2 may suppress TaE3UBQ lig-
86 ase activity to promote *Z. tritici* pathogenicity (Karki et al., 2021).

87 In wheat, twenty-four *Z. tritici* resistance genes (R genes) have been reported (Saintenac
88 et al., 2021; Yang et al., 2022). *Stb6* encodes a conserved, wall-associated kinase (WAK) with an
89 extracellular domain that recognizes the apoplastic AvrStb6 effector from *Z. tritici* (Brown et al.,
90 2015; Saintenac et al., 2018; Zhong et al., 2017). AvrStb6 accumulates in epiphytic hyphae of *Z.*
91 *tritici* in close proximity to the stomata, and its recognition triggers the induction of genes re-

92 sponsible for stomatal closure in resistant cultivars (Alassimone et al., 2024). The resistance pro-
93 tein *Stb16q* also encodes a cysteine-rich, wall-associated-like receptor kinase that presumably
94 recognizes a fungal carbohydrate to trigger a resistance response (Saintenac et al., 2021). Intri-
95 guingly, *Stb16q* confers full broad-spectrum resistance against 64 geographically diverse isolates
96 of *Z. tritici* (Saintenac et al., 2021). Moreover, the *Stb9* resistance protein recognizes AvrStb9*,* a
97 secreted, protease-like protein with a predicted S41 conserved domain and triggers an immune
98 response following the gene-for-gene model (Amezrou et al., 2023). However, the function of
99 *Stb9* is still not clear as it might be acting as a classical receptor protein, an inhibitor of AvrStb9
100 protease activity, or as the guard protein of the AvrStb9 target protein (Amezrou et al., 2023).
101 Recently, a genome-wide association study (GWAS) identified a 99-kb region containing
102 six candidate genes and led to eventual cloning of the *Stb15* resistance gene. *Stb15* encodes an
103 intronless G-type lectin receptor-like kinase (LecRK) with an intracellular serine/threonine re-
104 ceptor-like protein kinase and three extracellular domains (Hafeez et al., 2025). The G-type lec-
105 tin domain of *Stb15* likely binds mannose and may play a role in basal plant immunity, as
106 demonstrated previously in *Arabidopsis thaliana,* where lectins play a role in stomatal innate im-
107 munity responses (Singh and Zimmerli, 2013). *Stb15* could function as part of a guard/guardee
108 pair, triggering isolate-specific resistance, or it may bind glycoproteins, similar to other LecRKs
109 that interact with secreted proteins. A candidate for the corresponding *AvrStb15* gene, potentially
110 a small, secreted protein, has been proposed, but further research is needed to confirm this inter-
111 action and its underlying mechanisms (Hafeez et al., 2025).
112 Non-host resistance (NHR) is commonly broad spectrum and, hence, likely more durable
113 than that provided by classical R genes (Ayliffe & Sørensen, 2019; Gill et al., 2015). Several
114 types of NHR involve a hypersensitive response, as is seen in qualitative resistance conferred by

Avr recognition (Panstruga & Moscou, 2020). Evidence that Avr recognition is involved in NHR was found by studying the closest homologs of the *Z. tritici* Avr3D1 gene in sister fungal species that are nonpathogenic in wheat (Meile et al., 2023). The homologous genes induce a strong defense response in wheat when expressed in a virulent mutant strain of *Z. tritici*, suggesting they contribute to establishing host range and are involved in NHR (Meile et al., 2023). Barley (*Hordeum vulgare* subsp. *vulgare*) is closely related to wheat and is infected by *Z. passerinii* (Feurtey et al., 2020; Goodwin & Zismann, 2001), a species that is closely related to *Z. tritici.* Barley is a non-host of *Z. tritici* and thus shows strong resistance to this pathogen. Identifying and comparing DEGs in *Z. tritici* during a non-host interaction with barley is central to testing whether similar virulence factors and molecular pathways are expressed during susceptible, resistant (R gene) and non-host interactions. In addition, studying pathogen gene expression during a non-host interaction with a closely related grass species of wheat can identify candidate effectors that determine host specificity, and may lead to the identification of host target proteins. This information can be transferred from barley into the *Z. tritici* – wheat pathosystem to provide additional sources for breeding resistance in wheat.

In the present study, we investigate pathogen gene responses during interactions with susceptible, resistant, and non-host cultivars, using a time course of transcriptomic data covering distinct phases of the infection process. We examine three types of interaction: susceptible interaction with wheat cultivar Taichung 29; two resistant interactions with wheat cultivars Veranopolis and Israel 493; and a non-host interaction with barley to test the hypothesis that *Z. tritici* expresses different sets of genes tailored to each type of interaction. We identified thirty-one putative effectors that are upregulated during early disease development in a susceptible interaction compared to a non-host interaction. From these, six candidate effectors were selected based on

138 their expression profiles across time points in the replicates of the susceptible interaction, and
139 their subcellular localization was investigated using *Agrobacterium*-mediated transient expres-
140 sion in *Nicotiana benthamiana*.
141
142 **Results**
143
144 **Gene expression analysis during the interaction of *Z. tritici* and its wheat host**
145 Differential gene expression in *Z. tritici* was determined between three types of host in-
146 teractions: (1) a susceptible interaction with the wheat cultivar Taichung 29; (2) a resistant inter-
147 action with the wheat cultivar Veranopolis, which carries the *Stb2* and *Stb6* resistance genes; and
148 (3) a resistant interaction with the wheat cultivar Israel 493, which carries the *Stb3* and *Stb6* re-
149 sistance genes (Table 1). Comparison of pathogen gene expression in the susceptible host versus
150 the resistant hosts, allowed us to identify genes that are necessary for the transition from bio-
151 trophic to necrotrophic growth. We measured the gene expression at six time points: 1, 3, 6, 10,
152 17 and 23 days post inoculation (DPI). Previous studies have established that the transition from
153 biotrophic to necrotrophic growth in *Z. tritici* takes place at approximately 10 DPI (Palma-Guer-
154 rero et al., 2017; Rudd et al., 2015; Yang et al., 2013).
155 Close to two billion reads were collected for the susceptible interaction and resistant in-
156 teraction with cultivar Veranopolis, in total, over all time points and replications, while more
157 than two billion reads were obtained for the resistant interaction with cultivar Israel 493 (Supple-
158 mentary Table 1). At 1 and 3 DPI, the percentage of reads mapped to the fungal genome relative
159 to the total was similar between the susceptible and resistant interactions. However, in the sus-
160 ceptible interaction, this percentage increased at 6 and 10 DPI, aligning with the expected rise in

161 fungal biomass preceding the transition to necrotrophy. In contrast, for both resistant interac-
162 tions, at 6 and 10 DPI, the proportion of fungal reads remained comparable to the levels observed
163 at 3 DPI (Supplementary Table 1). At 17 and 23 DPI, the susceptible interaction with cultivar
164 Taichung 29 showed a significant increase in fungal reads, corresponding to the proliferation of
165 macroscopic symptoms on leaves. Conversely, in both resistant interactions, the numbers of
166 reads mapped to the *Z. tritici* genome remained at the lowest levels, consistent with the absence
167 of visible symptoms and the limited proliferation of fungal biomass in the resistant cultivars (Ad-
168 hikari et al., 2025). Overall, at 1, 3 and 6 DPI, only a small percentage (less than 1%) of the total
169 reads aligned to the fungal genome in both susceptible and resistant interactions. However, from
170 10 DPI onward, the proportion of mapped fungal reads increased in the susceptible interaction,
171 reaching its peak at 23 DPI, where it exceeded 40% in two replicates.

172 Gene expression patterns in the susceptible and the two resistant interactions were ex-
173 plored with principal component analysis (PCA). The PCA plots for 1, 3, 6 and 10 DPI (Fig. 1)
174 and for 17 and 23 DPI (Fig. 2.) were generated separately because normalization had to be per-
175 formed in two groups due to the very few reads in the resistant interactions at 17 and 23 DPI (see
176 Materials and Methods). PCA shows that gene expression is very similar in the susceptible and
177 resistant interactions early during infection (1 and 3 DPI) (Fig. 1.). Most replicate samples are
178 well clustered, indicating limited biological variation within replicate time points. At 6 DPI, gene
179 expression in the susceptible and resistant interactions begins to diverge, and at 10 DPI, the sus-
180 ceptible interaction is distinctly separated from the resistant interactions, primarily along princi-
181 pal component 2, while gene expression in the samples from both resistant interactions at 10 DPI
182 remains similar to that at 6 DPI.

183 A similar pattern is observed at 17 and 23 DPI (Fig. 2), where the susceptible interaction
184 forms a separate cluster from the resistant interactions. In both susceptible and resistant interac-
185 tions, the 17 and 23 DPI points cluster together for each wheat variety, suggesting that there is
186 little change in gene expression from 17 to 23 DPI, although the susceptible and resistant interac-
187 tions remain clearly distinguished. The replicate points for the resistant interactions show consid-
188 erable variability due to the low number of read counts obtained at late infection stages in the re-
189 sistant interactions, but the trend is clear.

190 The highest number of DEGs in *Z. tritici* was observed at 10 DPI when comparing the
191 susceptible interaction on the cultivar Taichung 29 with both resistant interactions on the *Stb2*-
192 carrying cultivar Veranopolis (601 DEGs) and on the *Stb3*-carrying cultivar Israel 493 (587
193 DEGs) (Table 2). A total of 275 and 226 genes in *Z. tritici* was found to be up-regulated at 10
194 DPI during the susceptible interaction compared to the resistant *Stb2* and *Stb3* interactions, re-
195 spectively. The rapid and pronounced activation of a large number of DEGs in *Z. tritici* at 10
196 DPI in the susceptible interaction corresponds with the first visible symptoms on the leaves of
197 the susceptible cultivar Taichung 29 (Supplementary Fig. S1) and marks the transition from the
198 biotrophic to the necrotrophic stage. Interestingly, a total of 326 and 361 genes in *Z. tritici* were
199 identified as down-regulated in the susceptible interaction at 10 DPI when compared to the re-
200 sistant interactions with Veranopolis and Israel 493, respectively. Since the resistant interactions
201 were used as the baseline for these comparisons, this means that these same genes were up-regu-
202 lated in the resistant interactions relative to the susceptible interaction. This suggests that during
203 the resistant interactions, *Z. tritici* activates a larger set of genes, potentially as part of a counter-
204 active response to the defense mechanisms deployed by the resistant cultivars at 10 DPI.

205 We determined the number of up-regulated genes in *Z. tritici* that were in common
206 among the comparisons between the susceptible interaction and both resistant interactions. The
207 Venn diagram (Fig. 3A) represents the two sets of up-regulated genes. The intersection of these
208 two sets includes 183 (57.5%) genes that are up-regulated in both comparisons. These genes are
209 likely part of core mechanisms of interaction with a susceptible host at 10 DPI, independent of
210 which resistant interaction is used as the control. This suggests that these genes are likely in-
211 volved in the common molecular mechanisms or pathways in the pathogen that are triggered dur-
212 ing the susceptible interaction at 10 DPI. In addition to their potential role in mediating the tran-
213 sition to the necrotrophic stage of infection, the fungal genes that are upregulated in susceptible
214 compared to both resistant interactions may also represent targets of host-mediated suppression.
215 Their reduced expression in the interaction with resistant cultivars provides evidence of the di-
216 rect and indirect effects of the presence of the resistance genes in those cultivars. Similarly, in
217 the Venn diagram (Fig. 3B), the intersection includes 234 genes that are down-regulated (51.7%)
218 in the susceptible interaction compared to both resistant interactions at 10 DPI. Since the re-
219 sistant interactions serve as the baseline, these same genes are up-regulated in both resistant in-
220 teractions relative to the susceptible interaction. This shared gene set likely represents a core
221 transcriptional response in *Z. tritici* to counteract the defense mechanisms activated by resistant
222 cultivars, suggesting a common response against a resistant cultivar regardless of the specific
223 composition of the resistant genotype.

224 We identified genes that were exclusively expressed at certain time points in the suscepti-
225 ble interaction compared to the resistant interactions on cultivars Veranopolis and Israel 493. Re-
226 markably, 249 up-regulated DEGs were uniquely expressed at 10 DPI in the susceptible interac-
227 tion compared to the resistant interaction with Veranopolis (Fig. 4A). The same pattern of

228 uniquely differentially expressed genes was observed at 10 DPI in the comparison of *Z. tritici*
229 grown on the susceptible cultivar Taichung 29 compared to the resistant cultivar Israel 493 (Fig.
230 4B). These results demonstrate that the number of DEGs that are exclusively activated in *Z. trit-*
231 *ici* at 10 DPI is remarkably high compared to other time points, which indicates that a defined
232 reprogramming in gene expression occurs at this stage.

233 To identify differences in pathogen gene expression in the two resistant interactions, we
234 determined DEGs in *Z. tritici* during the resistant interaction with Veranopolis compared to the
235 resistant interaction with Israel 493. Only 1 DEG was up-regulated in *Z. tritici* inoculated on the
236 Veranopolis cultivar compared to Israel 493 at 6 DPI. In total 12, 14 and 3 genes were found to
237 be differentially expressed at 10, 17 and 23 DPI (Table 2), respectively. No DEGs were identi-
238 fied when comparing the two resistant interactions at 1 and 3 DPI. This shows that *Z. tritici* fol-
239 lows a nearly identical pattern of gene expression during its interaction with both resistant wheat
240 cultivars.

241

242 **Gene Ontology and enrichment analysis during host interactions**

243 *Zymoseptoria tritici* DEGs were grouped according to their putative roles in biological
244 processes (BP), molecular functions (MF) and cellular components (CC) as established by the
245 Gene Ontology Consortium (http://www.geneontology.org/). The enriched GO terms in the up-
246 regulated genes in *Z. tritici* at 10 DPI (Fig. 5) collectively indicate that the pathogen is actively
247 metabolizing and synthesizing key macromolecules, such as proteins, nucleic acids, and nitroge-
248 nous compounds. This is suggested by the enrichment of GO terms associated with macromolec-
249 ular metabolic and biosynthetic processes at 10 DPI (Fig. 5) including organonitrogen compound

250 metabolic process (GO:1901564), ribonucleoprotein complex biogenesis (GO:0022613), and py-
251 rimidine-containing compound biosynthetic process (GO:0072528). Numerous GO terms related
252 to ribosomal components are enriched at 10 DPI in the susceptible interaction compared to the
253 resistant interactions, suggesting that the pathogen is actively ramping up protein synthesis. This
254 is likely to support the pathogen's metabolic needs as it establishes a necrotrophic infection. The
255 enrichment of GO terms in the categories nucleic acid binding (GO:0003676) and rRNA binding
256 (GO:0019843) points to upregulation of processes related to RNA processing and stability,
257 which may further support the pathogen's increased need for protein synthesis and efficient gene
258 expression. At 17 DPI, the enrichment of GO categories related to transport activities (Fig. 5),
259 suggests that the pathogen is likely focusing on regulating the ion homeostasis and controlling
260 the cellular uptake and efflux of ions. These processes are likely linked to nutrient acquisition, as
261 ion transporters are essential for maintaining osmotic balance, acquiring nutrients, and detoxify-
262 ing the pathogen's environment (Barata-Antunes et al., 2021). Such activities might be crucial as
263 the pathogen progresses into later stages of infection, facilitating its adaptation and survival. It
264 might also suggest that *Z. tritici* is switching from internal synthesis to importing metabolites
265 from the breakdown of host cells.

266 The KEGG pathway enrichment analysis showed that 13 pathways were significantly en-
267 riched in the up-regulated genes at 10 DPI during the susceptible interaction compared to both
268 resistant interactions. The top five enriched pathways were carbon metabolism, biosynthesis of
269 antibiotics, biosynthesis of secondary metabolites, glycolysis and gluconeogenesis. In contrast, at
270 23 DPI only 3 pathways were enriched among the up-regulated genes in the susceptible interac-
271 tion compared to the resistant interactions including carbon metabolism, biosynthesis of antibiot-
272 ics, and glycolysis and gluconeogenesis.

273 In the susceptible interaction compared to the resistant interactions, we observed a signif-
274 icant up-regulation of genes at 10 DPI that encode carbohydrate-active enzymes (CAZymes).
275 Among these, we identified eight glycoside hydrolases (GHs) and one carbohydrate esterase
276 (CE), all of which are cell wall-degrading enzymes (CWDEs). Additionally, our analysis re-
277 vealed 10 glycosyltransferases (GTs) and 10 enzymes with auxiliary activity (AA) among the
278 up-regulated genes (Supplementary Fig. S2). Families of AA enzymes involved in oxidation of
279 aromatic compounds and fungal growth such as the multicopper oxidase family (AA1), and the
280 alcohol oxidase subfamily (AA3_3) were up-regulated at 10 DPI in both comparisons between
281 the susceptible interaction and the two resistant interactions.

282 Interestingly, among the down-regulated genes at 10 DPI in the susceptible interaction
283 using the resistant interactions as baseline, we also identified 12 GHs, 8 GTs, and 11 enzymes in
284 the AA category. Families of AA enzymes involved in detoxification, oxidation of compounds,
285 and fungal growth such as the benzoquinone reductase family (AA6), the alcohol dehydrogenase
286 subfamily (AA3_2) and the alcohol oxidase subfamily (AA3_3) were down-regulated in the sus-
287 ceptible interaction compared to both resistant interactions. This means that these families of en-
288 zymes were up-regulated in both resistant interactions. This observation indicates the likely pro-
289 duction of CAZymes in the pathogen at the transition stage during a resistant interaction, possi-
290 bly to counteract resistant responses in the wheat cultivars. For instance, the CWDEs secreted by
291 different plant pathogens can act as effectors, and they can inhibit or elicit plant immunity (Gu et
292 al., 2024; Gui et al., 2017; Zhang et al., 2021).

293 We identified predicted small, secreted proteins (SSPs) among DEGs at 10 DPI. Notably,
294 26 SSPs were down-regulated in the susceptible interaction compared to both resistant interac-

295 tions. Additionally, 22 SSPs were up-regulated in the susceptible interaction relative to the re-
296 sistant interaction on the cultivar Veranopolis, and 23 SSPs showed up-regulation in the suscepti-
297 ble interaction compared to the resistant interaction on the cultivar Israel 493.
298
299 **Gene expression during a non-host interaction**
300 Differential gene expression in *Z. tritici* was determined in three host interactions com-
301 pared to a non-host interaction with the barley cultivar Kindred (Table 1). Comparison of patho-
302 gen gene expression in the susceptible and resistant hosts, versus the non-host species, allows us
303 to identify genes involved in initial colonization and host recognition.
304 The percentage of reads mapped to the fungal genome during the non-host interaction re-
305 mained consistently low across all time points, showing no significant increase over time. It
306 never exceeded 0.2% and, in most replicates, ranged between 0.02% and 0.06% (Table 2). As a
307 result, only a limited set of genes could be detected in comparisons using the non-host interaction
308 as the baseline treatment.
309 In contrast to the comparison between the susceptible interaction and the resistant interac-
310 tions, the largest differences between the susceptible and the non-host interaction are seen at 3
311 DPI. There were 171 DEGs in *Z. tritici,* of which 124 were up-regulated and 47 were down-regu-
312 lated (Table 3) in the susceptible interaction compared to the non-host interaction with *H. vul-*
313 *gare* used as the baseline. The genes that are up-regulated in the susceptible interaction com-
314 pared to the non-host interaction may play a role in initially colonizing the susceptible host.
315 There were 154 DEGs in the resistant interaction between *Z. tritici* and the Veranopolis (*Stb2*)
316 resistant cultivar compared to the non-host interaction (Table 3). This is similar to the 160 DEGs

317 in *Z. tritici* in the resistant interaction between *Z. tritici* and the Israel 493 (*Stb3*) cultivar com-
318 pared to the non-host interaction used as the baseline (Table 3).

319 The numbers of up-regulated DEGs at 10 DPI show a slight increase in contrast to the
320 previous time point at 6 DPI when comparing both the susceptible and resistant interactions
321 against the non-host interaction. At 17 and 23 DPI, for the genes for which we were able to re-
322 trieve measurable counts, we observed higher numbers of DEGs in the susceptible interaction
323 than the numbers of DEGs at 17 and 23 DPI in the resistant interactions compared to the non-
324 host interaction. The fact that we were able to identify very little fungal RNA originating from
325 the *Z. tritici* genome at 17 and 23 DPI, in both resistant and non-host interactions, also reveals
326 that there is a significant reduction in the fungal biomass compared to 1 to 10 DPI in these inter-
327 actions and compared to the susceptible interaction. This also could mean that the fungus is not
328 transcriptionally active at 17 and 23 DPI in resistant and non-host interactions.

329 We determined the number of up-regulated genes in *Z. tritici* that were in common in the
330 three comparisons between the susceptible and the two resistant host interactions compared to
331 the non-host interaction. The Venn diagram (Fig. 6A) illustrates the three sets of up-regulated
332 genes, with an intersection of 98 genes (74.8%) that are consistently up-regulated in the pathogen
333 in the comparisons of susceptible versus non-host, resistant (Veranopolis) versus non-host, and
334 resistant (Israel 493) versus non-host. These genes likely have a role in core mechanisms in-
335 volved in host interaction at 3 DPI, irrespective of whether the host is susceptible or resistant,
336 i.e., genes that are important for the initial biotrophic growth phase. This suggests that these
337 genes are part of fundamental host recognition pathways shared between both susceptible and
338 resistant interactions at this early stage.

339 Similarly, for the down-regulated genes, the Venn diagram (Fig. 6B) shows an intersec-
340 tion of 40 genes (66.7%) shared across the three host interactions compared to the non-host inter-
341 action at 3 DPI. This indicates a common response to the interaction with barley, the non-host
342 species, regardless of whether the control host interaction is susceptible or resistant. These com-
343 mon down-regulated genes reflect differences in the interaction and growth of *Z. tritici* on a non
344 host at the early infection stages.

345 To find unique up-regulated DEGs that are activated at certain time points during the sus-
346 ceptible and resistant interactions compared to the non-host interaction and differentiate them
347 from those that were expressed steadily, we determined unique and shared up-regulated DEGs
348 between the sampling days. In the susceptible interaction compared to the non-host interaction,
349 there were 52 up-regulated DEGs that were unique at 3 DPI, followed by 50 up-regulated DEGs
350 shared at 1 and 3 DPI (Fig. 7A). There were 45 unique DEGs in *Z. tritici* at 3 DPI, followed by
351 45 DEGs at both 1 and 3 DPI when comparing the resistant interaction on Veranopolis (*Stb2*)
352 with the non-host interaction (Fig. 7B). The combined number of up-regulated DEGs at 1 and 3
353 DPI is much higher than the unique genes at other time points, which indicates that the main dif-
354 ference in the pattern of gene activation between the resistant interaction and the non-host inter-
355 action occurs at the beginning of the infection process.

356 We also wanted to determine the unique and shared up-regulated DEGs at different sam-
357 pling days during the resistant interaction on Israel 493 (*Stb3*) versus the non-host interaction on
358 barley. In total, 46 up-regulated DEGs were exclusively observed at 3 DPI, followed by 43 up-
359 regulated DEGs shared at 1 and 3 DPI (Fig. 7C). The peak of up-regulated genes at 3 DPI, dur-
360 ing the early stage of infection, represents a higher number of up-regulated DEGs than those up-
361 regulated at 10 DPI (Fig. 7C). This supports the idea of an early recognition of the host species

362 from 1 to 3 DPI in the resistant interactions, and the subsequent activation of a large number of
363 genes at 3 DPI. Presumably, the fungus recognizes the host species and activates a similar gene
364 expression program during the first three days after inoculation on both susceptible and resistant
365 hosts to initiate colonization of the plant leaves.
366

367 **Gene Ontology and enrichment analyses during the non-host interaction on barley**

368 The significantly enriched GO categories among the down-regulated genes at 1 and 3
369 DPI in the comparisons of both susceptible and resistant interactions against the non-host inter-
370 action reveal some insights into the early response of the pathogen during the interaction on the
371 non-host species. The enriched GO terms include those involved in the unfolded protein response
372 (UPR) in fungi including unfolded protein binding (GO:0051082), and protein folding chaperone
373 (GO:0044183) (Fig. 8). UPR is a stress-adaptive pathway that is activated under adverse envi-
374 ronmental conditions and is involved in regulation of virulence traits in fungi (Guirao-Abad et
375 al., 2022; Weichert et al., 2020).

376 Additionally, the down-regulated genes in *Z. tritici* at 10 DPI in the comparison between
377 the susceptible interaction and the non-host interaction were significantly enriched in GO catego-
378 ries including vacuolar acidification (GO:0007035), intracellular pH reduction (GO:0051452),
379 regulation of intracellular pH (GO:0051453), vacuolar proton transporting (GO:0000221), ubiq-
380 uitin ligase complex (GO:0019005) and nuclear ubiquitin ligase complex (GO:0043224) (Fig. 8).

381 The KEGG pathway enrichment analysis showed that 5 pathways were significantly en-
382 riched among the up-regulated genes at 1 DPI during the susceptible interaction compared to the
383 non-host interaction. These were glycolysis/gluconeogenesis, carbon metabolism, biosynthesis of
384 secondary metabolites, biosynthesis of antibiotics and fructose and mannose metabolism. At 3

385 DPI three pathways were enriched, which include pyruvate metabolism, carbon metabolism and
386 glycolysis and gluconeogenesis.

387 Three glycoside hydrolases (GHs) were significantly up-regulated at 1 DPI, and 6 CA-
388 Zymes were up-regulated at 3 DPI, including 1 glycosyl transferase (GT), 4 GHs and 1 carbohy-
389 drate-binding molecule (CBM). At 6 and 10 DPI, 3 GHs, 5 GTs and 1 CBM were up-regulated
390 (Supplementary Fig. S3). Also at 1 and 3 DPI, we were able to detect 7 and 9 SSPs that were up-
391 regulated in the susceptible versus the non-host interaction.

392

393 **Expression of *Z. tritici* candidate effectors during early disease development**

394 To gain further insight into *Z. tritici* pathogenicity, we used a set of established programs
395 for effector identification (Hallgren et al., 2022; Sperschneider & Dodds, 2022; Teufel et al.,
396 2022) using the predicted *Z. tritici* secretome, and selected thirty-one candidates with increased
397 transcript abundance during the early stages of infection (1 and 3 DPI) in the susceptible interac-
398 tion compared to the non-host interaction. The thirty-one selected effector candidates range in
399 size from 68 to 554 amino acids (Table 4). Although the majority of the putative effectors do not
400 contain subcellular-targeting peptide sequences, several encode predicted nuclear localization
401 signals (NLS), chloroplast transit peptides (cTPs), or mitochondrial-targeting sequences (Table
402 4). One putative effector, Mycgr394290, includes multiple predicted subcellular localization sig-
403 nals including a cTP, mitochondrial targeting sequence, and a NLS (Table 4). Further examina-
404 tion of the candidate effectors revealed that two proteins, Mycgr3101991 and Mycgr3102792,
405 contain predicted NLS, and one, Mycgr3106456, encoded a predicted cTP. Although most of the
406 candidate effectors are annotated as uncharacterized, two are annotated as having peptidoglycan-
407 binding LysM domains. Furthermore, two effector candidates encode Hce2-like domains, named

408 after the homologs of *Cladosporium fulvum* Ecp2 (Stergiopoulos et al., 2012). Ecp2 is a secreted
409 protein initially identified as a virulence factor in *C. fulvum* that belongs to a widely distributed
410 superfamily of putative fungal effectors (Stergiopoulos et al., 2012). Another effector candidate
411 is annotated as an allergen V5/Tpx-1-related protein, another as a heat shock protein, and one as
412 a cerato-platanin protein. The putative function of members of these families as fungal effectors
413 is described below.

414 Some of the effector candidates with annotations have been predicted to function as ef-
415 fectors or toxic compounds in other fungal plant pathogens, and some have been observed to be
416 differentially expressed in previous transcriptome studies on *Z. tritici* (Mirzadi Gohari et al.,
417 2015; Rudd et al., 2015; Yang et al., 2013). For example, five Hce2 domain-containing effectors
418 have been identified in *Valsa mali*, the causal agent of Valsa canker in apple. One of these effec-
419 tors induced cell death when transiently expressed in *N. benthamiana* (Zhang et al., 2019). In the
420 genome of the wheat pathogen *Fusarium graminearum*, there are two genes that encode putative
421 cerato-platanin proteins, which function as elicitors of defense responses on *Arabidopsis* leaves
422 (Quarantin et al., 2019). A novel cerato-platanin-like effector protein from *Fusarium oxysporum*
423 f. sp *cubense* triggers a hypersensitive response and systemic acquired resistance in tobacco (Li
424 et al., 2019). Additionally, a *Sclerotinia sclerotiorum* cerato-platanin induces cell death in *N.*
425 *benthamiana* and interacts with a PR-1 protein in the apoplast to facilitate infection (Yang et al.,
426 2018). Finally, LysM domain-containing effectors from *Z. tritici* and *C. fulvum* have been previ-
427 ously characterized and shown to suppress chitin-induced plant immunity and to protect fungal
428 hyphae from plant chitinase activity (Marshall et al., 2011; Sánchez-Vallet et al., 2013, 2020;
429 Tian et al., 2021). Overall, the evidence from other fungal pathogens suggests that the candidate

430 effectors identified in the present study could have a functional role at the early stages of infec-
431 tion.

432 The gene expression profiles of the thirty-one selected effector candidates were compared
433 across all time points using the log-transformed normalized counts of each gene in the individual
434 samples of the susceptible interaction. Our analyses reveal three clusters of candidate effector
435 genes based on similarities in their gene expression patterns (Fig. 9). Each cluster contains candi-
436 date effector genes that are commonly regulated at specific time points. We found a cluster con-
437 sisting of 10 candidate effectors that were commonly up-regulated at 1 and 3 DPI compared to
438 the average relative expression of the 31 selected candidate effector genes. A second cluster,
439 containing 10 commonly up-regulated genes, was identified at 10 and 17 DPI, and a third cluster
440 of 11 genes was identified at 23 DPI (Fig. 9).

441

442 **Subcellular localization patterns of *Z. tritici* candidate effector-fluorescent protein fusions**

443 Since several candidate effector proteins encode predicted subcellular-targeting se-
444 quences, we investigated the localization of six of these putative effectors to plant cellular com-
445 partments. These effectors were chosen based on their gene expression profiles (Fig. 9), with
446 three (Mycgr3109710, Mycgr394290, Mycgr3106502) exhibiting higher expression at either 1 or
447 3 DPI, and the other three (Mycgr3107904, Mycgr3104794, Mycgr3111221) showing increased
448 expression after 10 DPI. The localization of specific proteins can be determined by creating fluo-
449 rescent protein (FP) fusion constructs (Berg & Beachy, 2008), where an FP is attached to the
450 protein of interest, enabling visualization within intact tissues (Tanz et al., 2013). This approach
451 has been applied to study viral and fungal proteins, allowing researchers to examine their interac-

452 tions with plant organelles (Helm et al., 2022; Li et al., 2020; Petre et al., 2016). To test the lo-
453 calization of the six putative effectors, we fused super Yellow Fluorescent Protein (sYFP) to the
454 C-terminus of candidate effector sequences, with and without their predicted signal peptides. We
455 also examined the subcellular localization of the remaining 21 putative effectors using their ma-
456 ture protein sequences (lacking predicted signal peptides) and include the results in the supple-
457 mentary data. These constructs were transiently expressed in *Nicotiana benthamiana* using *Agro-*
458 *bacterium*-mediated transformation (agroinfiltration), and their localization patterns were exam-
459 ined using laser-scanning confocal microscopy (Helm et al., 2022; Jaiswal et al., 2023; Rogers et
460 al., 2024). We used free sYFP as a negative control to establish a baseline for comparison, as it is
461 a derivative of green fluorescent protein (GFP) and is used commonly to assess protein localiza-
462 tion in plant cells (Berg & Beachy, 2008; Tanz et al., 2013). Due to their small size, FPs localize
463 to both the cytoplasm and nucleus, providing a reference for identifying specific protein localiza-
464 tion (Tanz et al., 2013).

465 In our analysis, if the fluorescence signal from an effector-sYFP fusion is observed in
466 both the nucleus and cytosol, we consider the localization non-informative, as it matches the dis-
467 tribution of free sYFP. This suggests that the effector lacks a location-specific signal sequence to
468 direct the fusion protein to a particular compartment. However, if the fluorescence signal is de-
469 tected in a distinct organelle rather than both the nucleus and cytosol, so it is distinguishable
470 from the localization of free sYFP, it indicates that the effector likely contains a targeting se-
471 quence that directs the sYFP to a specific subcellular compartment, confirming its potential lo-
472 calization.

473 Additionally, one challenge of using FPs in plants is the natural autofluorescence of cel-
474 lular components such as cell walls and plastids, which can overlap with FP signals (Tanz et al.,

475 2013). However, modern confocal microscopes can largely account for this background auto-
476 fluorescence (Tanz et al., 2013). To further rule out autofluorescence, we examined *N. bentham-*
477 *iana* leaves infiltrated with *Agrobacterium* expressing a protein construct tagged with hemagglu-
478 tinin (HA) instead of sYFP (Supplementary Fig. S5) and also imaged an uninfiltrated leaf at the
479 sYFP excitation wavelength under the confocal microscope (Supplementary Fig. S6). In both
480 cases we did not observe autofluorescence.

481 Live-cell imaging of *N. benthamiana* epidermal cells revealed that fluorescence signals
482 from Mycgr3111221, Mycgr3106502, and Mycgr3104794, when expressed without their signal
483 peptides, were indistinguishable from those of the free sYFP controls and were thus considered
484 to have a non-informative localization (Fig. 10A). The fluorescence signal from My-
485 cgr3107904:sYFP without its signal peptide was predominantly observed in the cytosol (Fig.
486 10A), suggesting that Mycgr3107904 may be cytosolic. However, it also could be associated
487 with the plasma membrane or the apoplastic space, and further analyses will be required to con-
488 firm its precise localization. Intriguingly, Mycgr3109710:sYFP and Mycgr394290:sYFP, when
489 expressed without their signal peptides, labeled what appear to be cytosolic bodies or punctuate
490 structures, and these punctuate structures appear to be mobile for Mycgr3109710:sYFP (Fig. 12,
491 Supplementary video 1).

492 When expressed with their native signal peptides, Mycgr3106502, Mycgr3104794, My-
493 cgr3109710, and Mycgr394290 predominantly localized to the cytosol, with no detectable fluo-
494 rescence in the nucleus (Fig. 10B). This distinct pattern, compared to the nucleus-cytosol locali-
495 zation of the free sYFP control, suggests that these effectors may be cytosolic. However, further
496 observations including co-localization markers and plasmolysis are required to exclude the po-
497 tential localization of these effectors to the plasma membrane or the apoplastic space. In contrast,

498 Mycgr3111221, when expressed with its signal peptide, labeled both the cytosol and nucleus, re-
499 sulting in a non-informative localization pattern indistinguishable from that of free sYFP. My-
500 cgr3107904 did not show a fluorescent signal at 48 hours post infiltration, likely indicating pro-
501 tein degradation or rapid delivery into the apoplast (Fig. 10B).

502 Immunoblot analyses were used to confirm the expression and integrity of the *Z. tritici*
503 effector–fluorescent protein fusions in *N. benthamiana*. This assay revealed that, of the twenty-
504 seven candidate effectors screened, twenty-six accumulated at detectable levels when transiently
505 expressed without their predicted signal peptides (Supplementary Fig. S8). When expressed with
506 their signal peptides, five of six predicted effectors showed detectable accumulation (Supplemen-
507 tary Fig. S9). While Mycgr3104794 accumulated at a low level, Mycgr3107904 did not produce
508 an observable band in the immunoblot assay (Supplementary Fig. S9). Notably, for several effec-
509 tors expressed with or without their signal peptides, we observed multiple bands in the im-
510 munoblots, often with one band corresponding to the expected size and additional bands of lower
511 molecular weight (Supplementary Figs. S8 and S9). This pattern suggests possible post-transla-
512 tional cleavage, partial degradation, or the presence of processing intermediates, which may af-
513 fect the stability or integrity of the effector fusions. In some cases, the lower-molecular-weight
514 bands were approximately the size of free sYFP, raising the possibility that the fluorescence ob-
515 served in both the cytosol and nucleus for some effectors may be due to free sYFP rather than the
516 intact fusion protein.

517

518 **Discussion**

519

520 Comparative RNAseq analysis clearly shows that different suites of genes are expressed
521 by *Z. tritici* during its biotrophic and necrotrophic infection stages. The comparison of the infec-
522 tion time course in the susceptible host and the two resistant hosts, allows us to identify genes
523 that are necessary for or participate in the transition from the biotrophic to the necrotrophic
524 growth stages. The sudden increase in the number of differentially expressed genes at 10 days
525 post inoculation coincides with the onset of visible lesions on the leaves (Supplementary Fig.
526 S1). This aligns with expectations, as previous studies have demonstrated that *Z. tritici* under-
527 goes significant transcriptomic reprogramming during the transition to its necrotrophic phase
528 (Kellner et al., 2014; Palma-Guerrero et al., 2017; Rudd et al., 2015; Yang et al., 2013) prior to
529 the exponential growth in fungal biomass that occurs in susceptible cultivars beginning 18-20
530 DPI (Adhikari et al., 2025). Our results provide the first confirmation that the main difference in
531 the pathogen gene expression in a susceptible compared to a resistant interaction occurs at the
532 transition stage rather than during the early infection stage (1-6 DPI), consistent with the low lev-
533 els of fungal biomass reported in both resistant and susceptible interactions before 10 DPI (Adhi-
534 kari et al., 2025). These results also reveal that *Z. tritici* deploys a similar gene activation pattern
535 and comparable molecular mechanisms during the symptomless early stage of the disease in a
536 susceptible interaction and in resistant host interactions.

537 In previous comparisons of host and non-host interactions, investigators found that when
538 other grass species, such as *Brachypodium distachyon* or *Agropyron repens* are inoculated with
539 *Z. tritici*, the pathogen penetrates the leaf surface through stomata, but the infection is halted in
540 the substomatal cavity (Kellner et al., 2014). This suggests an early recognition and interaction
541 between the host and pathogen, during which *Z. tritici* can escape detection or manipulate host

542 defenses in susceptible wheat lines to penetrate the leaves, colonize the plant, and initiate the
543 symptomless phase (Kellner et al., 2014).

544 Comparison of gene expression in susceptible and resistant wheat cultivars to gene ex-
545 pression in a non-host allows us to examine genes involved in initiating/supporting host coloni-
546 zation and avoiding pathogen recognition. We suggest that some of these genes may play a role
547 in early epiphytic growth, stomatal detection and penetration by *Z. tritici* during its biotrophic
548 phase. Previous research shows that while *Z. tritici* can colonize epiphytically in susceptible, re-
549 sistant, and some non-host species, its penetration attempt efficiency is significantly lower in
550 barley accessions (about 10% less) compared to near-isogenic wheat lines (NILs) containing *Stb*
551 resistance genes (Battache et al., 2024). This difference may help explain the variation in early-
552 stage transcriptomic responses in host and non-host interactions. It is possible that *Z. tritici* pos-
553 sesses a more efficient mechanism for stomatal recognition and penetration of its host species,
554 which could influence gene expression, survival, and pathogenicity.

555 Battache et al. (2024) found no difference in penetration attempt efficiency and a similar
556 percentage of reached stomata, in susceptible and resistant interactions in NILs. Additionally, *Z.*
557 *tritici* can undergo both asexual and sexual reproduction during its phase of epiphytic growth,
558 even on resistant wheat cultivars (Fones et al., 2023). This is supported by the similar expression
559 profiles that we observe in susceptible and resistant interactions from 1 to 6 DPI. This is particu-
560 larly interesting, as previous research also has shown that *Z. tritici* can grow epiphytically for up
561 to 10 days on both wheat and non-host species like barley (Battache et al., 2024; Fones et al.,
562 2017). However, the efficiency of preventing stomatal penetration by *Z. tritici* varies according
563 to the resistance types, with *Stb6*-mediated and barley non-host resistance being the most effec-
564 tive among those tested (Battache et al., 2024). Understanding the expression profile of *Z. tritici*

565 associated with its extended epiphytic growth is an important area for future research which
566 could provide valuable insights into the symptomless infection phase and help inform early-stage
567 disease management strategies.

568 Because we noticed similar expression profiles in *Z. tritici* during both susceptible and
569 resistant interactions at early time points, and given the resistance response in cultivars carrying
570 *Stb6***,** we became interested in the expression dynamics of *AvrStb6*, the apoplastic effector of *Z.*
571 *tritici* that is recognized by Stb6. To explore this, we re-analyzed our RNAseq data (see Supple-
572 mentary Excel material). Given that *AvrStb6* was not predicted in the JGI annotation (Goodwin
573 et al., 2011) originally used for our analysis, we mapped the reads against a recently released *Z.*
574 *tritici* genome annotation that correctly includes this gene (Lapalu et al., 2025). At 1 DPI,
575 *AvrStb6* showed high expression in all host interactions (susceptible and resistant) compared to
576 the non-host, where no transcripts were detected. Notably, expression was strongest in the re-
577 sistant interaction with Israel493, while levels in the susceptible interaction and in Veranopolis
578 were lower. At 3 DPI, *AvrStb6* expression decreased in all host interactions and remained absent
579 in the non-host. By 10 DPI, expression was strongly upregulated in the susceptible interaction,
580 coinciding with the appearance of the first visible disease symptoms. In contrast, both resistant
581 interactions showed only low transcript counts at this stage, which likely reflects reduced fungal
582 biomass in resistant plants. Across these time points, *AvrStb6* was never detected in the non-host
583 interaction. These results suggest that *AvrStb6* is transiently expressed early during infection and
584 peaks later in the susceptible interaction, supporting a role in virulence, while its recognition by
585 *Stb6* explains its avirulence function in resistant cultivars.

586 Our results confirm that the transcriptomic response in *Z. tritici* is significantly different
587 during the early infection stage in both susceptible and resistant interactions on the host species

588 compared to the non-host interaction with barley. *Z. tritici* activates a different gene expression
589 program, implying that it uses different molecular mechanisms at 1 and 3 DPI when interacting
590 with susceptible or resistant wheat cultivars, compared to its program when interacting with a
591 non-host species. This suggests that non-host species may recognize and neutralize *Z. tritici* at a
592 very early stage, preventing the implementation in the pathogen of its normal biotrophic growth
593 program. Future research on the mechanisms of host recognition through the analysis of non-host
594 interactions should incorporate transcriptomic data with increased sequencing depth to capture
595 low-abundance transcripts, especially during the early stages of disease and in non-host interac-
596 tions where there is limited fungal growth. This deeper analysis should be complemented by ad-
597 ditional experiments that accurately monitor fungal growth, development and plant colonization
598 during non-host interactions. Such an integrated approach could provide insights into the mecha-
599 nisms of host recognition by the pathogen and inform strategies for developing wheat cultivars
600 with broad-spectrum resistance.

601 The highest number of DEGs in *Z. tritici* when comparing the susceptible interaction on
602 the cultivar Taichung 29 with both resistant interactions on Veranopolis and Israel 493 is seen at
603 10 DPI. Interestingly, based on a previous principal component analysis (PCA), Yang et al.
604 (2013) identified 13 DPI as the point with the greatest difference in transcription in a susceptible
605 interaction with the wheat cultivar Sevin. However, inspection of their Figure 3 shows that the
606 10 DPI and 13 DPI samples are very similar and that the largest change is actually between 4
607 DPI and 10 DPI. This supports our finding that the most important transcriptome reprogramming
608 in the pathogen, in a susceptible compared to a resistant interaction, occurs during the bio-
609 trophic/necrotrophic transition stage (10 DPI) rather than during the necrotrophic phase (13
610 DPI), revealing molecular mechanisms in *Z. tritici* that are activated at 10 DPI and determine the

611 outcome of the infection in each type of interaction. Rudd et al. (2015) found that, in a suscepti-
612 ble interaction compared to growth in Czapek-Dox broth culture medium, the highest number of
613 up-regulated genes in *Z. tritici* was observed during the transition to the necrotrophic stage (9
614 DPI), while in our study, it occurred at 10 DPI. Rudd et al. (2015) identified 1,389 DEGs at 9
615 DPI, while we found 601 and 587 total DEGs in the susceptible interaction compared to the re-
616 sistant *Stb2*-gene and *Stb3*-gene interactions, respectively. Again, these findings indicate that sig-
617 nificant transcriptional reprogramming in *Z. tritici* occurs during the transition stage, around 9-13
618 dpi, in a susceptible interaction compared to fungal growth in culture media or to infection of a
619 resistant host.

620 Yang et al. (2013) demonstrated distinct transcriptional responses during different phases
621 of the infection. Their PCA showed separation between the 4-day, 10-day, and 13-day infected
622 samples, representing the asymptomatic phase, the intermediate transition stage, and the necrot-
623 rophic phase, respectively. In our analyses, PCA identified four clusters for the replicates of the
624 susceptible interaction (C1: 1 and 3 DPI, indicated by the red circles and diamonds on Fig. 1; C2:
625 6 DPI, denoted by the red triangles on Fig. 1; C3: 10 DPI, red squares; C4: 17 and 23 DPI, red
626 circles and diamonds on Fig. 2). C1 contains all the replicates from both susceptible and resistant
627 host interactions, revealing a similar gene activation in the fungus at 1 and 3 DPI. From 6 DPI,
628 we observe the beginning of a change in transcriptional response in the susceptible and resistant
629 interactions according to PC2 of the PCA (Fig. 1). This time point marks the separation of repli-
630 cates from the susceptible interaction into their own cluster. In C3 and C4 gene expression pat-
631 terns in the susceptible interactions are clearly separated from all replicates of the resistant inter-
632 actions (Figs. 1 and 2). This finding strongly suggests the existence of defining molecular pro-
633 cesses in the pathogen that govern or result from the successful switch from the biotrophic phase

634 to the necrotrophic stage at 10 DPI, ultimately determining whether the interaction is susceptible
635 or resistant. In our analyses, 1,504 genes at 1, 3, 6, and 10 DPI and 222 genes at 17 and 23 DPI
636 were detectable and passed the normalization and filtering criteria for the comparison of the sus-
637 ceptible and resistant interactions. It is worth noting that DEGs identified at 10 DPI account for
638 approximately 40% of the normalized read counts, highlighting that expression of a large frac-
639 tion of all genes is reprogrammed during the transition to the necrotrophic stage in the suscepti-
640 ble interaction. These genes are likely involved in molecular pathways that determine the ability
641 of the pathogen to overcome the plant defense response and induce symptoms at around 10 DPI
642 in a susceptible interaction. Adhikari et al. (2025) showed that fungal biomass in two susceptible
643 interactions begins to increase exponentially after 18 DPI. The transcriptional changes indicated
644 by the clear separation of C4 in Fig. 2 reflects and supports this exponential growth of fungal bi-
645 omass. Interestingly, as demonstrated by previous research, changes in gene expression of the
646 pathogen are mirrored by those in the host at early and late points in the infection process (Adhi-
647 kari et al., 2007). The host responds during early detection of the pathogen and then again when
648 the pathogen transitions from biotrophic to necrotrophic growth (Adhikari et al., 2007).

649 KEGG analysis identified biosynthesis of antibiotics and biosynthesis of secondary me-
650 tabolites as significantly enriched pathways in the susceptible interaction compared with both re-
651 sistant interactions at 10 DPI. Similarly, in a study conducted on *Bipolaris maydis* on resistant
652 and susceptible non-CMS (cytoplasmic male sterile) maize genotypes, these same biosynthetic
653 pathways were exclusively enriched in susceptible interactions (Meshram et al., 2022). The au-
654 thors concluded that the successful pathogenicity of *B. maydis* depends on pathogen genes such
655 as toxin-related effector molecules, cell wall degradation of the host, detoxification, and host de-

656 fense evasion (Meshram et al., 2022). These findings agree with our observation that *Z. tritici* ac-
657 tivates an arsenal of biosynthetic pathways, CAZymes including CWDEs, and SSPs during the
658 transition to the necrotrophic stage in the compatible interaction. However, among the down-reg-
659 ulated genes, although we could not find significantly enriched pathways due to the low number
660 of genes that were annotated, we identified down-regulated CAZymes and SSPs at 10 DPI, such
661 as the alcohol dehydrogenase CAZyme family (AA3_2). This group includes enzymes with im-
662 portant roles in the fungal life cycle and colonization of the host (Gutiérrez-Corona et al., 2023).
663 In *B. cinerea,* an alcohol dehydrogenase regulates fungal development, environmental adaptation
664 and pathogenicity as observed in the morphology and virulence of knock-out mutants (DafaAlla
665 et al., 2022). The benzoquinone reductase family (AA6) also was down-regulated, which con-
666 tains intracellular enzymes involved in the biodegradation of aromatic compounds and in the
667 protection of fungal cells from reactive quinone compounds (Levasseur et al., 2013).

668 In the comparison of the susceptible and the resistant interactions to the non-host interac-
669 tion with barley, the main difference in the *Z. tritici* transcriptional responses occurs at 1 and 3
670 DPI in all the comparisons evaluated. We identified 285, 261 and 269 DEGs at 1 and 3 DPI in
671 the comparisons of the susceptible, the resistant *Stb2*-gene, and the resistant *Stb3*-gene interac-
672 tions with the non-host interaction, respectively. At 3 DPI the numbers of DEGs were always
673 higher than those at 10 DPI for the three comparisons, which reveals that the main difference in
674 the pattern of gene expression in the fungus during a host interaction compared to a non-host in-
675 teraction occurs at the early stage of infection rather than during the transition stage. We detected
676 352 genes with measurable counts at 10 DPI, indicating that the pathogen is able to grow and
677 colonize to a certain extent in the non-host species. In a previous report (Kellner et al., 2014), the
678 patterns of transcription in *Z. tritici* during infection in the susceptible wheat cultivar Obelisk and

679 in the non-host grass species *B. distachyon* were evaluated after 4 DPI. They found that genes
680 encoding proteins with putative secretion signals were enriched among those up-regulated during
681 infection of wheat and genes with plant-specific expression patterns. In our analysis, we observe
682 a higher proportion of small, secreted proteins (SSPs) in the up-regulated sets of genes at 1 and 3
683 DPI compared to the down-regulated sets.

684 Down-regulated genes at 1 and 3 DPI in the host interactions, compared to the non-host
685 interaction, were enriched in GO terms linked to the unfolded protein response (UPR). UPR is a
686 stress-adaptive pathway that modulates the accumulation of misfolded proteins in the endoplas-
687 mic reticulum (ER), typically activated when the pathogen faces an increased demand for protein
688 secretion (Weichert et al., 2020). It also helps pathogenic fungi survive under adverse environ-
689 mental conditions, such as the stress of infection (Guirao-Abad et al., 2022). Notably, plant-path-
690 ogenic fungi can exploit UPR to regulate virulence traits like thermotolerance, nutrient acquisi-
691 tion, effector secretion, and resistance to antimicrobial peptides (Weichert et al., 2020). In *Z. trit-*
692 *ici*, the need to deploy more secreted proteins for effective epiphytic colonization, combined with
693 a potential early resistance response from the non-host interaction, may create stress that triggers
694 UPR activation to meet the demands for survival in such a challenging environment. Interest-
695 ingly, at 10 DPI, genes down-regulated in the host interaction compared to the non-host were en-
696 riched for GO terms related to intracellular pH regulation and vacuolar acidification. Although
697 intracellular pH in fungi is typically stable, it can shift rapidly in response to environmental
698 stress, such as changes in extracellular pH or nutrient availability (Fernandes et al., 2017). In *As-*
699 *pergillus niger*, extracellular acidification induces a transient drop in cytosolic pH. Similar re-
700 sponses in *Fusarium oxysporum* and *Saccharomyces cerevisiae* lead to MAPK reprogramming,

701 suggesting a conserved role for pH-dependent signaling in morphogenesis and invasion (Fer-
702 nandes et al., 2017; 2023). Acid stress has also been shown to promote fungal survival by trig-
703 gering growth arrest (Lucena et al., 2020), while heat shock and cell wall stress cause transient
704 intracellular acidification that enhances stress tolerance (Triandafillou et al., 2020; Garcia et al.,
705 2017). The upregulation of genes involved in vacuolar acidification and pH regulation during the
706 non-host interaction suggests that *Z. tritici* may be activating adaptive mechanisms to counteract
707 stress, maintain pH homeostasis, and enable survival under unfavorable conditions.

708 Among the 31 selected effector candidates, an interesting finding is that effector candi-
709 date Mycgr3109710 localized to mobile cytosolic bodies near the cell periphery when expressed
710 without its signal peptide in *N. benthamiana*, whereas with its signal peptide, it was restricted to
711 the cytosol. Immunoblot analysis showed a clear band corresponding to the expected size of the
712 fusion protein in both cases, along with a lower band corresponding to free sYFP, suggesting
713 some degree of degradation or cleavage (Supplementary Fig. S8). However, the observed fluo-
714 rescence signal did not follow the typical diffuse nucleus-cytosol pattern associated with free
715 sYFP, indicating that the effector is likely localizing to specific compartments. This effector is
716 annotated as part of the Allergen V5/Tpx-1-related group, containing CAP/SCP domains charac-
717 teristic of the PR-1-like superfamily (Wangorsch et al., 2022). BLAST analysis confirmed ho-
718 mology with PR-1-like proteins from *Zymoseptoria brevis* and *Aureobasidium* sp. While PR-1-
719 like proteins are well studied in plants and animals, few studies exist in filamentous ascomycetes.
720 Notably, in *Fusarium graminearum*, deletion of a PR-1-like gene reduced virulence (Lu & Ed-
721 wards, 2018), and in *Moniliophthora* species, these genes are upregulated during biotrophic
722 stages (Teixeira et al., 2012). Mycgr3109710 also shows early infection expression (1 and 3

723 DPI), supporting its potential role in host–pathogen interactions. We hypothesize that My-
724 cgr3109710 targets the plant vesicle-trafficking system, given its localization to mobile punctate
725 structures resembling the multivesicular body localization reported for PR-1 variants from *Ara-*
726 *bidopsis thaliana* when expressed in *N. benthamiana* (Pečenková et al., 2022). To further con-
727 firm the localization of Mycgr3109710 to mobile cytosolic bodies in *N. benthamiana*, we rec-
728 orded a time-lapse series capturing the localization of the effector. This analysis revealed the dy-
729 namic motility of the observed cytosolic elements (Supplementary video 1).

730 Similarly, Mycgr394290, when expressed without its signal peptide, localizes to the nu-
731 cleus and labels cytosolic punctate structures with less mobility than those labeled by My-
732 cgr3109710. When expressed with its signal peptide, Mycgr394290 localizes predominantly to
733 the cytosol. We suggest that Mycgr394290, without its signal peptide, may target organelles in-
734 volved in sorting and trafficking of molecules. An example of a fungal effector with similar lo-
735 calization is Foa3 from *Fusarium oxysporum*, which functions within the plant cell to suppress
736 host defenses. Foa3 showed a weak signal in the cytosol but was strongly detected in punctate
737 structures when a secretory signal peptide was included (Tintor et al., 2022), opposite to what we
738 observed for Mycgr394290. However, their study demonstrates that Foa3 suppresses pattern-trig-
739 gered defense responses to the same extent regardless of whether the protein carries the signal
740 peptide (Tintor et al., 2022). Regarding the identity of the punctuate structures, Tintor et al.
741 (2022) proposed that the labeled structures may represent vesicles containing proteins targeted
742 for secretion. This is intriguing because Mycgr394290 encodes predicted mitochondrial, chloro-
743 plast, and nuclear localization signals according to LOCALIZER (Table 4). Although the exact
744 identity of the punctate subcellular structures labeled by Mycgr394290:sYFP is uncertain, it is

745 plausible that this protein acts to suppress the defense mechanisms of the plant in the same way
746 as Foa3, which is known to suppress the plant immune response.

747 Another candidate effector, Mycgr3107904, was mainly localized to the cytosol only
748 when expressed without its signal peptide. Interestingly, no fluorescent signal was detected when
749 the effector was expressed with its signal peptide, likely suggesting degradation or rapid translo-
750 cation into the apoplastic space. This effector is annotated as a Hce2 domain-containing protein.
751 Hce2 (named from **h**omologs of ***C***. *fulvum* **E**cp2 effector) is a domain that causes plant cell
752 death, and is widely conserved in the fungal kingdom (Laugé et al., 1997; Zhang et al., 2019).
753 There are three predicted Hce2-containing effectors in the genome of *Z. tritici*: MgEcp2 (My-
754 cgr3104404); MgEcp2-2 (Mycgr3107904); and MgEcp2-3 (Mycgr3111636) (Stergiopoulos et
755 al., 2010, 2012). In addition, a fourth homolog of Ecp2 was found to be up-regulated in *Z. tritici*
756 at 8 DPI and then down-regulated at 12 DPI. This effector candidate induces necrosis in wheat in
757 a cultivar-dependent manner (Ben M'barek et al., 2015). In another study (Mirzadi Gohari et al.,
758 2015), Mycgr3104404, Mycgr3107904 and Mycgr3111636 were up-regulated during the transi-
759 tion to necrotrophy, and in the necrotrophic stage at 8 and at 12 DPI. In our study, My-
760 cgr3111636 was up-regulated at 1 DPI and at 10 DPI but we were unable to transform this effec-
761 tor candidate into *Agrobacterium*, suggesting a possible toxic effect on *Agrobacterium* cells. We
762 transformed Mycgr3107904, which was up-regulated at 10 DPI, and we found that the fluores-
763 cence signal was mainly localized to the cytosol. This is very interesting as the Ecp effector of *C.*
764 *fulvum* is one of the few proteins that can induce necrosis in tomato and tobacco plants irrespec-
765 tive of the signal peptide, which indicates that its host target is intracellular (Ben M'barek et al.,
766 2015). We did not observe fluorescence in a specific intracellular compartment, but the protein is
767 localized within the cytosol, which suggests a plausible intracellular target protein in the plant.

768 In our analysis, Mycgr3111221, which is a Lysin (LysM) domain-containing effector,
769 was up-regulated at the early stage of infection in the susceptible compared to the non-host inter-
770 action. There are three LysM effector genes identified and characterized in the *Z. tritici* genome
771 (Marshall et al., 2011; Sánchez-Vallet et al., 2020; Tian et al., 2021). Two of them, My-
772 cgr3111221 and Mycgr3105487, were previously shown to be up-regulated during the asympto-
773 matic phase (Marshall et al., 2011; Tian et al., 2021). Interestingly, Mycgr3111221 suppresses
774 chitin-induced plant immunity and protects fungal hyphae against plant chitinase activity (Mar-
775 shall et al., 2011). Mycgr3111221 is a homolog of Ecp6 effectors in *C. fulvum,* which are se-
776 creted directly into the apoplastic space where they perform their chitin-binding function
777 (Sánchez-Vallet et al., 2020). However, in our analysis, Mycgr3111221 shows a non-informative
778 localization in both the nucleus and cytosol, which is indistinguishable from the localization of
779 the free sYFP control. This occurs irrespective of the presence or absence of the putative signal
780 peptide.

781 Our findings also underscore the limitations of using sYFP fusions to assess effector sub-
782 cellular localization. While our localization assays provide some insight into the potential intra-
783 cellular compartments targeted by *Z. tritici* candidate effectors, several caveats must be consid-
784 ered. Fusion of sYFP to the C-terminus may interfere with proper protein folding, stability, traf-
785 ficking, or function, potentially resulting in mislocalization or loss of activity (Tian et al., 2004;
786 Snapp, 2005). In addition, fluorescent proteins like sYFP contain protease-sensitive regions that
787 may be cleaved during expression in plant cells, releasing the free fluorophore and producing
788 misleading localization signals unrelated to the effector itself (Chen et al., 2013).

789 These limitations are supported by our immunoblot results, which reveal degradation
790 products for several constructs. This is particularly evident for the candidate effectors expressed

791 with their native signal peptides (Supplementary Fig. S9). The inclusion of the fungal signal pep-
792 tide likely directs the protein into the plant secretory pathway, targeting it for secretion into the
793 apoplast or extracellular space (Petre & Kamoun, 2014). Within this pathway, the fusion protein
794 may undergo post-translational processing, including signal peptide removal or additional prote-
795 olytic cleavage at internal processing sites, as well as misfolding or degradation, especially in the
796 endoplasmic reticulum or apoplast. Such proteolytic processing can result in activation, inactiva-
797 tion, and completely altered protein function (Rogers and Overall, 2013). These cleavage events
798 could generate truncated protein fragments that are still detected by immunoblot but would not
799 necessarily retain the fluorescent tag, potentially leading to misleading or incomplete localization
800 patterns.

801 One type of cleavage site that could influence post processing is KEX2. Bioinformatics
802 identification of KEX2 cleavage sites in secreted proteins from *Z. tritici* could provide insights
803 into the proteolytic processing that some candidate effectors undergo within the secretory path-
804 way, but so far this has not been performed. The KEX2 cleavage site is highly conserved among
805 fungi and its characteristic motifs are recognized by Kex2 proteases involved in protein pro-
806 cessing (Ding et al., 2016; Le Marquer et al., 2019). Studies on KEX2-processed repeat proteins
807 (KEPs) in fungal secretomes revealed that plant pathogens displayed a larger number of KEPs
808 than animal pathogens or saprotrophs (Le Marquer et al., 2019). They also found that, among
809 fungal species with the largest numbers of KEPs, twelve of them interacted with plants either as
810 symbionts, endophytes or pathogens, suggesting that KEPs may play a role in the diversity of
811 mechanisms deployed by fungi to interact with their plant hosts (Le Marquer et al., 2019).
812 Whether KEPs are important for *Z. tritici* is not known but their identification and analysis could
813 be a subject for future research.

814 Additionally, because candidate effectors are secreted, they may not be present in the to-
815 tal intracellular protein extract, resulting in weak or undetectable signal in standard immunoblot
816 analyses. Therefore, observed localization patterns should be interpreted with caution and ideally
817 validated through complementary approaches, such as apoplastic fluid extraction, plasmolysis,
818 confocal imaging with co-localization markers, or ER retention constructs. In this context, the
819 immunoblot analyses presented in Supplementary Figs. 8-9 provide evidence of post-transla-
820 tional cleavage and degradation, and should be considered a primary line of support for the limi-
821 tations of the localization experiments.

822 Future studies also should assess the biological relevance of these effectors by evaluating
823 their potential roles in suppressing plant immunity through functional assays, including ROS
824 burst suppression, necrosis induction, and inhibition of NLR-triggered responses. Further func-
825 tional characterization of the effectors with their signal peptides is particularly important because
826 many cloned resistance proteins in wheat that recognize *Z. tritici* effectors are localized in the
827 plasma membrane. For example, Stb6 is a wall-associated kinase (WAK) with an extracellular
828 domain that recognizes the apoplastic AvrStb6 effector (Brown et al., 2015; Saintenac et al.,
829 2018; Zhong et al., 2017). Similarly, *Stb16q* encodes a cysteine-rich, wall-associated-like recep-
830 tor kinase that likely interacts with a fungal carbohydrate to trigger resistance (Saintenac et al.,
831 2021), and *Stb15* encodes a G-type lectin receptor-like kinase (LecRK) with extracellular do-
832 mains that mediate recognition (Hafeez et al., 2025). Therefore, assessing the activity and locali-
833 zation of effectors with their signal peptides will provide a more comprehensive understanding
834 of their roles in pathogen-host interactions.

835 In summary, we have characterized the *Z. tritici* transcriptome during susceptible, re-
836 sistant, and non-host interactions and identified key temporal shifts in gene expression dynamics.

837 A central finding of this work is that the most significant divergence in fungal transcriptional
838 profiles between susceptible and resistant wheat cultivars occurs during the transition to necrot-
839 rophy around 10 DPI, whereas early infection stages (1 and 3 DPI) show highly similar expres-
840 sion patterns. In addition, comparison with the non-host interaction on barley reveals that major
841 differences in gene expression emerge early, suggesting that non-host resistance acts during the
842 initial stages of infection. These findings provide new insights into how *Z. tritici* tailors its tran-
843 scriptional programs in response to different host environments. Pathway and gene function en-
844 richment analyses of each interaction type identified 31 effector candidates that are upregulated
845 early during susceptible interactions. This early induction highlights their potential roles in host
846 colonization and immune modulation. Together, our results advance our understanding of tem-
847 poral and interaction-specific transcriptional reprogramming in *Z. tritici.* Future investigations
848 will address whether the effector candidates identified in our study have a functional role in fun-
849 gal pathogenicity as well as suppress immune responses in wheat.
850

851 **Materials and Methods**

852

853 **Plant material and inoculum preparation**

854 Highly susceptible wheat cultivar Taichung 29, R-gene resistant cultivars Veranopolis
855 (*Stb2* resistance gene) and Israel 493 (*Stb3*), and the non-host barley cultivar Kindred were
856 grown in a greenhouse in Metro-mix 500 series potting soil (SunGro Horticulture, Bellevue,
857 WA), with a constant 16-h light and 8-h dark cycle for 2-3.5 weeks. Wheat and barley were
858 planted in three biological replicates consisting of 3 plants per 4-inch pot. A 1 cm^2 piece of ly-
859 ophilized filter paper stock (stored at -80°C) of isolate IPO323 of *Z. tritici* was placed into 100

860 ml of yeast-sucrose broth with 100 µl of kanamycin sulfate (25 mg/ml). The flask was placed on
861 a shaker at 25ºC for 3 days. The inoculum concentration was adjusted to 1.0×10^6 conidia/ml,
862 and 1 µl of Tween 20 (polysorbate 20) was added per 100 ml of inoculum. The inoculum was
863 evenly hand sprayed over 14-days-old (2nd-3rd leaf stage) wheat and barley plants. Inoculated
864 plants were enclosed in a humidity chamber draped in plastic and muslin for 72 h, then removed
865 to normal growth chamber conditions for the duration of the experiment. Emerging leaves of
866 wheat and barley were trimmed every 2-3 days to ensure that the inoculated leaves remained
867 "healthy" and that only inoculated tissue was harvested.
868 *Nicotiana benthamiana* was grown in Berger Seed Germination and Propagation Mix
869 supplemented with Osmocote slow-release fertilizer (14-14-14). Plants were maintained in a
870 growth chamber with a 16h:8h light:dark photoperiod at 24°C with light and 22°C in the dark
871 and 60% humidity with average light intensities at plant height of 130 µmols/m^2/s.
872
873 **RNA extraction and sequencing**
874 Wheat and barley leaf tissue was harvested by clipping 2 leaves per plant per replicate
875 and bulking 3 plants per replicate. Leaf tissue was harvested at 1, 3, 6, 10, 17 and 23 days post
876 inoculation (DPI). All harvested leaf material was immediately frozen in liquid nitrogen. RNA
877 was extracted using the RNeasy Plant Mini kit (Qiagen). For each replicate, 1 µg of total RNA
878 was used to produce cDNA libraries (Purdue Genomics Core Facility, West Lafayette, IN) for
879 RNA sequencing. The sequencing was done using Illumina HiSeq producing 100-base, paired-
880 end (PE) reads. Read quality was checked with FastQC (Andrews, 2010) before and after trim-
881 ming to remove low-quality and residual adapter sequences (Trimmomatic v.0.36). All reads

882 were mapped to the reference genome of the *Z. tritici* IPO323 strain (*M. graminicola* v.2.0) re-
883 trieved from the Joint Genome Institute (JGI) (Goodwin et al., 2011) using BBMap **(**v 35.85;
884 Bushnell B., sourceforge.net/projects/bbmap/). Reads mapped to the reference genome were
885 counted using HTSeq (Anders et al., 2015). Fewer fungal reads were detected in all the samples
886 of the non-host interaction, and in the samples of the resistant interactions at 17 and 23 DPI com-
887 pared to the samples of the susceptible interaction, due to reduced fungal growth in the resistant
888 wheat cultivars at the late stage and in the non-host species barley. As a result, for the compari-
889 sons of susceptible versus resistant interactions, and susceptible versus non-host interactions, we
890 removed from the whole dataset the genes that did not have any measurable counts in the repli-
891 cates of the resistant and non-host interactions at specific time points. This allowed us to improve
892 the normalization of the counts and the consistency between replicates. This approach reduced
893 the total number of DEGs that we were able to quantify at each time point, but we could accu-
894 rately detect significant differences in the highly expressed genes in the samples and reduce the
895 false positives. We encountered limitations in the analysis due to the low read counts obtained in
896 the replicates of the resistant interactions and non-host interaction. These limitations include re-
897 duced sensitivity in detecting low-abundance transcripts or lower-expressed genes in the patho-
898 gen, and difficulty in assigning functional annotations or representative GO terms for some sets
899 of DEGs.

900 Data were normalized and filtered using the R package DESeq2 v.4.0.3 (Love et al.,
901 2014), which uses the median of ratios method to determine the size factors and shrinkage for
902 variance estimation. The normalization for the comparison of susceptible versus resistant interac-
903 tions was conducted on two groups of samples. One group contains the samples at 1, 3, 6 and 10
904 DPI, and the other group contains the samples at 17 and 23 DPI. We used this approach because

905 very few reads were detected in the samples of the resistant interactions at 17 and 23 DPI, result-
906 ing in many genes without measurable expression. Similarly, in the comparison of susceptible
907 and resistant interactions versus the non-host interaction, the normalization was conducted on
908 one group that contains the samples from 1 and 3 DPI, a second group of samples from 6 and 10
909 DPI, and a third group that contains the samples at 17 and 23 DPI. Differential gene expression
910 analysis for the pathogen between inoculation treatment samples within each 6-point time course
911 was completed using DESeq2 v.4.0.3 (Love et al., 2014). Significant DEGs were determined at
912 FDR = 5% and using a cutoff of 1-fold change in expression between comparisons.
913

914 **GO and KEGG pathway enrichment analyses**

915 Differentially expressed genes (DEGs) were subjected to Gene Ontology (GO) enrich-
916 ment analysis using gProfiler (Raudvere et al., 2019). *Mycosphaerella graminicola* v.2.0 genes
917 with detectable counts in our analysis were used as the background reference for *Z. tritici*. The
918 significance threshold was determined by the default gProfiler method, the g:SCS method, which
919 corresponds to an experiment-wide threshold of $\alpha = 0.05$ (Raudvere et al., 2019). KOBAS v.3.0.
920 (Bu et al., 2021) supports *Z. tritici* and was used to calculate KEGG pathway enrichment
921 (Kanehisa et al., 2017) of the significantly expressed genes; significance was determined by
922 Fisher's exact test (Fisher, 1925) using the Benjamini and Hochberg method to correct for multi-
923 ple testing (Benjamini and Hochberg 1995).
924

925 **Selection of candidate effectors from *Z. tritici***

926 Effector predictions were performed as described previously by Helm et al. (2022) with
927 modifications. We used SignalP (v6.0) (Teufel et al., 2022) and Phobius (v1.01) to predict signal

928 peptide sequences and we applied a probability threshold of 0.9. The absence of transmembrane
929 domains was predicted using Phobius (v1.01) (Käll et al., 2004) and DeepTMHMM (v1.0.24**)**
930 (Hallgren et al., 2022). EffectorP (v.3.0) (Sperschneider & Dodds, 2022) was used to select *Z.*
931 *tritici* proteins that contained effector-like sequence characteristics. LOCALIZER (v.1.0.4)
932 (Sperschneider et al., 2017) and ApoplastP (v.1.0) (Sperschneider et al., 2018) were used to pre-
933 dict the possible localization of the candidate effectors. The list of *Z. tritici* putative effectors is
934 shown in Table 4.
935
936 **Generation of plant expression constructs**
937 Constructs were generated using a modified multisite Gateway cloning (Invitrogen) strat-
938 egy (Helm et al., 2022; Qi et al., 2012). The 3xHA:sYFP (free super yellow fluorescent protein)
939 construct has been described previously (Helm et al., 2022; Jaiswal et al., 2023).
940 The attL1 and attL4 Gateway recombination sequences were fused to the 5' and 3' ends
941 of the open reading frames (ORFs) of each *Z. tritici* candidate effector, thereby generating Gate-
942 way-compatible donor clones. A commercial gene synthesis company (Azenta Life Sciences)
943 was used to synthesize 31 candidate effector genes without predicted signal peptides and six of
944 the candidate effector genes with their predicted signal peptides. The sequences were inserted
945 into the pUC57 plasmid by the service provider and designated pDONR(L1-L4):ZtEC.
946 To generate the ZtEC:sYFP protein fusions, the pDONR(L1-L4):ZtEC constructs were
947 mixed with pBSDONR(L4r-L2):sYFP (Helm et al., 2022; Qi et al., 2012) and recombined into
948 the plant expression plasmid pEG100 (Earley et al., 2006) using LR Clonase II (Invitrogen) fol-
949 lowing the manufacturer's instructions. The resulting constructs were verified by sequencing and
950 subsequently used for transient expression assays.
951

952 ***Agrobacterium*-mediated transient protein expression in *N. benthamiana***

953 *Agrobacterium*-mediated transient expression was performed as described previously
954 (Helm et al., 2022) with modifications. The constructs described above were mobilized into *Ag-*
955 *robacterium tumefaciens* strain GV3101 (pMP90) and grown in Luria-Bertani (LB) broth supple-
956 mented with 25 µg of gentamicin sulfate and 50 µg of kanamycin per milliliter at 30°C for two
957 days. Transformants were inoculated into 10 mL of liquid LB containing the appropriate antibi-
958 otics and were shaken overnight at 30°C at 250 rpm. Following overnight incubation, the cells
959 were pelleted by centrifuging at 3,800 rpm for 3 minutes and resuspended in 10 mM $MgCl_2$. The
960 bacterial suspensions were adjusted to an optical density at 600 nm (OD_{600}) of 0.5 and incubated
961 with 100 µM acetosyringone for 3-4 hours at room temperature prior to agroinfiltration. Bacte-
962 rial suspensions were infiltrated into the abaxial surface of 3- to 4-week-old *N. benthamiana*
963 leaves with a needleless syringe.

964

965 **Laser scanning confocal microscopy**

966 Live-cell imaging of *N. benthamiana* epidermal cells was performed forty-eight hours
967 post agroinfiltration using a Zeiss LSM880 Axio Examiner upright confocal microscope
968 equipped with a Plan Apochromat 20×/0.8 objective (pinhole 1.0 AU). The sYFP-tagged fusion
969 proteins were excited using a 514-nm argon laser, and fluorescence signals were detected be-
970 tween 517 nm and 562 nm. All confocal micrographs were processed using the Zeiss Zen Blue
971 Lite program. Image analysis was performed using the Fiji plugin of Image J 2.0.0
972 (http://fiji.sc/Fiji).

973

974 **Immunoblot analyses**

975

976 Immunoblot analyses were performed as described previously with slight modifications
977 (Helm et al., 2022; Jaiswal et al., 2023). Nine leaf discs of *N. benthamiana* (0.15 g per sample)
978 were collected at 48 hours after agroinfiltration and flash frozen in liquid nitrogen. Frozen tissue
979 was homogenized with 2 volumes of protein extraction buffer (150 mM NaCl, 50 mM Tris [pH
980 7.5], 0.1% Nonidet P-40 [Sigma-Aldrich], 1% plant protease inhibitor cocktail [Sigma-Aldrich],
981 and 1% 2,2'-dipyridyl disulfide) using a cold ceramic mortar and pestle. The solution was centri-
982 fuged at 13,000 × g for 15 minutes at 4°C. Seventy-five microliters of the collected supernatants
983 were combined with 25 µL of 4× Laemmli Buffer (BioRad) supplemented with beta-mercap-
984 toethanol. Total protein samples were separated on a 4-20% Tris-glycine stain-free polyacryla-
985 mide gel (BioRad) at 180 V for 1 hour in 1× Tris/glycine/SDS running buffer. Total proteins
986 were transferred to a nitrocellulose membrane and subsequently blocked in 5% skim milk for 1
987 hour at room temperature. Horseradish peroxidase-conjugated anti-GFP antibody (1:5,000) (Mil-
988 tenyi Biotec) was used to detect sYFP-tagged recombinant proteins. Immunoblots were incu-
989 bated for 5 minutes at room temperature with Supersignal West Femto maximum sensitivity sub-
990 strates (Thermo Scientific) and developed using an ImageQuant 500 CCD imaging system
991 (Cytiva).
992

993 **Acknowledgments**

994 The authors thank Drs. Terri Cameron and Ian Thompson (USDA-ARS, Crop Production
995 and Pest Control Research Unit) for technical assistance and the Purdue University Imaging Fa-
996 cility for access to the Zeiss LSM880 Axio Examiner upright confocal microscope. Two anony-
997 mous reviewers provided helpful comments for improving previous drafts of the manuscript. The

funding body had no role in designing the experiments, collecting the data, or writing the manuscript. All opinions expressed in this paper are the authors' and do not necessarily reflect the policies and views of USDA. USDA is an equal opportunity provider and employer.

Funding

This research was funded by the United States Department of Agriculture, Agricultural Research Service (USDA-ARS) research project 5020-21220-014-00D.

Literature Cited

Adhikari, T. B., Balaji, B., Breeden, J. D. and Goodwin, S.B. 2007. Resistance of wheat to *Mycosphaerella graminicola* involves early and late peaks of gene expression. Physiol. Mol. Plant Pathol. 71: 55–68.

Adhikari, T. B., Balaji, B. and Goodwin, S. B. 2025. Real-time quantitative PCR method for assessing wheat cultivars for resistance to *Zymoseptoria tritici*. Front. Plant Sci. 16:1605156. doi: 10.3389/fpls.2025.1605156.

Alassimone, J., Praz, C., Lorrain, C., De Francesco, A., Carrasco-López, C., Faino, L., Shen, Z., Meile, L., and Sánchez-Vallet, A. 2024. The *Zymoseptoria tritici* avirulence factor AvrStb6 accumulates in hyphae close to stomata and triggers a wheat defense response hindering fungal penetration. Molecular Plant-Microbe Interactions 37: 432–444. https://doi.org/10.1094/MPMI-11-23-0181-R.

Amezrou, R., Audéon, C., Compain, J., Gélisse, S., Ducasse, A., Saintenac, C., Lapalu, N., Louet, C., Orford, S., Croll, D., Amselem, J., Fillinger, S., and Marcel, T. C. 2023. A secreted protease-like protein in *Zymoseptoria tritici* is responsible for avirulence on *Stb9*

1021 resistance gene in wheat. PLOS Pathogens 19: e1011376. https://doi.org/10.1371/jour-
1022 nal.ppat.1011376.

1023 Anders, S., Pyl, P. T., and Huber, W. (2015). HTSeq—A Python framework to work with high-
1024 throughput sequencing data. Bioinformatics 31: 166–169. https://doi.org/10.1093/bioin-
1025 formatics/btu638.

1026 Andrews, S. 2010. FastQC: A quality control tool for high throughput sequence
1027 data. https://www.bioinformatics.babraham.ac.uk/projects/fastqc/.

1028 Ayliffe, M. and Sørensen, C.K. 2019. Plant nonhost resistance: paradigms and new environ-
1029 ments. Curr. Opin. Plant Biol. 50:104–113. https://doi.org/10.1016/j.pbi.2019.03.011.

1030 Barata-Antunes, C., Alves, R., Talaia, G., Casal, M., Gerós, H., Mans, R., and Paiva, S. 2021.
1031 Endocytosis of nutrient transporters in fungi: The ART of connecting signaling and traf-
1032 ficking. Computational and Structural Biotechnology Journal 19: 1713–1737.
1033 https://doi.org/10.1016/j.csbj.2021.03.013.

1034 Battache, M., Suarez-Fernandez, M., Klooster, M. V., Cambon, F., Sánchez-Vallet, A., Lebrun,
1035 M.-H., Langin, T., and Saintenac, C. 2024. Stomatal penetration: The cornerstone of
1036 plant resistance to the fungal pathogen *Zymoseptor*ia tritici. BMC Plant Biology 24: 736.
1037 https://doi.org/10.1186/s12870-024-05426-5.

1038 Ben M'barek, S., Cordewener, J. H. G., Tabib, S. M., Lee, T. A. J. V. D., Liu, Z., Mirzadi, A.,
1039 Mehrabi, R., America, A. H. P., Robert, O., Friesen, T. L., Hamza, S., Stergiopoulos, I.,
1040 Wit, P. J. G. M. D., and Kema, G. H. J. 2015. FPLC and liquid-chromatography mass
1041 spectrometry identify candidate necrosis-inducing proteins from culture filtrates of the

1042 fungal wheat pathogen *Zymoseptoria tritici*. Fungal Genetics and Biology 79: 54–62.
1043 https://doi.org/10.1016/j.fgb.2015.03.015.

1044 Benjamini, Y. and Hochberg, Y. 1995. Controlling the false discovery rate: a practical and pow-
1045 erful approach to multiple testing. J. R. Stat. Soc. Ser. B 57:289–300.
1046 https://doi.org/10.1111/j.2517-6161.1995.tb02031.x.

1047 Berg, R. H., and Beachy, R. N. 2008. Fluorescent protein applications in plants. In *Methods in*
1048 *Cell Biology* (Vol. 85, pp. 153–177). Academic Press. https://doi.org/10.1016/S0091-
1049 679X(08)85008-X.

1050 Brown, J. K. M., Chartrain, L., Lasserre-Zuber, P., and Saintenac, C. 2015. Genetics of re-
1051 sistance to Zymoseptoria tritici and applications to wheat breeding. Fungal Genetics and
1052 Biology 79: 33–41. https://doi.org/10.1016/j.fgb.2015.04.017.

1053 Bu, D., Luo, H., Huo, P., Wang, Z., Zhang, S., He, Z., Wu, Y., Zhao, L., Liu, J., Guo, J., Fang,
1054 S., Cao, W., Yi, L., Zhao, Y., and Kong, L. 2021. KOBAS-i: Intelligent prioritization and
1055 exploratory visualization of biological functions for gene enrichment analysis. Nucleic
1056 Acids Research 49(W1): W317–W325. https://doi.org/10.1093/nar/gkab447.

1057 Chen, X., Zaro, J., and Shen, W.-C., 2013. Fusion protein linkers: property, design and function-
1058 ality. Adv. Drug Deliv. Rev. 65: 1357–1369. https://doi.org/10.1016/j.addr.2012.09.039.
1059 DafaAlla, T. E. I. M., Abdalla, M., El-Arabey, A. A., Eltayb, W. A., and Mohapatra, R. K. 2022.
1060 *Botrytis cinerea* alcohol dehydrogenase mediates fungal development, environmental ad-
1061 aptation and pathogenicity. Journal of Biomolecular Structure and Dynamics 40: 12426–
1062 12438. https://doi.org/10.1080/07391102.2021.1971112.

1063 Ding W, Liu W-Q, Jia Y, Li Y, van der Donk WA, and Zhang Q. 2016. Biosynthetic investiga-
1064 tion of phomopsins reveals a widespread pathway for ribosomal natural products in asco-
1065 mycetes. Proc. Natl. Acad. Sci. U.S.A., 113:3521–
1066 6. https://doi.org/10.1073/pnas.1522907113.
1067 Earley, K.W., Haag, J.R., Pontes, O., Opper, K., Juehne, T., Song, K. and Pikaard, C.S. 2006.
1068 Gateway-compatible vectors for plant functional genomics and proteomics. Plant J,
1069 45:616–629. https://doi.org/10.1111/j.1365-313X.2005.02617.x.
1070 Fernandes, T., Segorbe, D., Prusky, D., and Di Pietro, A. 2017. How alkalinization drives fungal
1071 pathogenicity. PLoS Pathog. 13:e1006621. doi: 10.1371/journal.ppat.1006621.
1072 Fernandes, T., Mariscal, M., Serrano, A., Segorbe, D., Fernández-Acero, T., Martín, H., Turrà,
1073 D., and Di Pietro, A. 2023. Cytosolic pH controls fungal MAPK signaling and patho-
1074 genicity. mBio 14:e0028523. doi: 10.1128/mbio.00285-23.
1075 Feurtey, A., Lorrain, C., Croll, D., Eschenbrenner, C., Freitag, M., Habig, M., Haueisen, J., Möl-
1076 ler, M., Schotanus, K., and Stukenbrock, E. H. 2020. Genome compartmentalization pre-
1077 dates species divergence in the plant pathogen genus *Zymoseptoria*. BMC Genomics 21:
1078 588. https://doi.org/10.1186/s12864-020-06871-w.
1079 Fisher, R.A. 1925. Statistical methods for research workers. Edinburgh: Oliver and Boyd.
1080
1081 Fones, H. N., Eyles, C. J., Kay, W., Cowper, J., and Gurr, S. J. 2017. A role for random, humid-
1082 ity-dependent epiphytic growth prior to invasion of wheat by *Zymoseptoria tritici*. Fungal
1083 Genetics and Biology 106: 51–60. https://doi.org/10.1016/j.fgb.2017.07.002.
1084 Fones, H. N., Soanes, D., and Gurr, S. J. 2023. Epiphytic proliferation of *Zymoseptoria tritici*
1085 isolates on resistant wheat leaves. Fungal Genetics and Biology 168: 103822.
1086 https://doi.org/10.1016/j.fgb.2023.103822.

1087 Francisco, C.S., Ma, X., Zwyssig, M.M., McDonald, B.A. and Palma-Guerrero, J. 2019. Mor-
1088 phological changes in response to environmental stresses in the fungal plant pathogen *Zy-*
1089 *moseptoria tritici*. Sci. Rep. 9:9642. https://doi.org/10.1038/s41598-019-45994-3.
1090 García, R., Bravo, E., Diez-Muñiz, S., Nombela, C., Rodríguez-Peña, J., and Arroyo, J. 2017. A
1091 novel connection between the cell wall integrity and the PKA pathways regulates cell
1092 wall stress response in yeast. Sci. Rep. 7:5703. doi: 10.1038/s41598-017-06001-9.
1093 Gill, U.S., Lee, S. and Mysore, K.S. 2015. Host versus nonhost resistance: distinct wars with
1094 similar arsenals. Phytopathology 105:580–587. https://doi.org/10.1094/PHYTO-11-14-
1095 0298-RVW.

1096 Goodwin, S. B., Ben M'barek, S. B., Dhillon, B., Wittenberg, A. H. J., Crane, C. F., Hane, J. K.,
1097 Foster, A. J., van der Lee, T. A. J., Grimwood, J., Aerts, A., Antoniw, J., Bailey, A.,
1098 Bluhm, B., Bowler, J., Bristow, J., van der Burgt, A., Canto-Canché, B., Churchill, A. C.
1099 L., Conde-Ferràez, L., … and Kema, G. H. J. 2011. Finished genome of the fungal wheat
1100 pathogen *Mycosphaerella graminicola* reveals dispensome structure, chromosome plas-
1101 ticity, and stealth pathogenesis. PLoS Genetics 7: 1002070. https://doi.org/10.1371/jour-
1102 nal.pgen.1002070.

1103 Goodwin, S. B., and Zismann, V. L. 2001. Phylogenetic analyses of the ITS region of ribosomal
1104 DNA reveal that *Septoria passerinii* from barley is closely related to the wheat pathogen
1105 *Mycosphaerella graminicola*. Mycologia 93: 934-946.

1106 Gu, X., Cao, Z., Li, Z., Yu, H., and Liu, W. 2024. Plant immunity suppression by an β-1,3-glu-
1107 canase of the maize anthracnose pathogen *Colletotrichum graminicola*. BMC Plant Biol-
1108 ogy 24: 339. https://doi.org/10.1186/s12870-024-05053-0.

1109 Gui, Y.-J., Chen, J.-Y., Zhang, D.-D., Li, N.-Y., Li, T.-G., Zhang, W.-Q., Wang, X.-Y., Short, D.
1110 P. G., Li, L., Guo, W., Kong, Z.-Q., Bao, Y.-M., Subbarao, K. V., and Dai, X.-F. 2017.
1111 *Verticillium dahliae* manipulates plant immunity by glycoside hydrolase 12 proteins in
1112 conjunction with carbohydrate-binding module 1. Environmental Microbiology 19:
1113 1914–1932. https://doi.org/10.1111/1462-2920.13695.
1114 Guirao-Abad, J. P., Weichert, M., and Askew, D. S. 2022. Cell death induction in *Aspergillus fu-*
1115 *migatus*: Accentuating drug toxicity through inhibition of the unfolded protein response
1116 (UPR). Current Research in Microbial Sciences 3: 100119.
1117 https://doi.org/10.1016/j.crmicr.2022.100119.
1118 Gutiérrez-Corona, J. F., González-Hernández, G. A., Padilla-Guerrero, I. E., Olmedo-Monfil, V.,
1119 Martínez-Rocha, A. L., Patiño-Medina, J. A., Meza-Carmen, V., and Torres-Guzmán, J.
1120 C. 2023. Fungal alcohol dehydrogenases: physiological function, molecular properties,
1121 regulation of their production, and biotechnological potential. Cells 2023 12: 2239.
1122 https://doi.org/10.3390/cells12182239.

1123 Hafeez, A. N., Chartrain, L., Feng, C., Cambon, F., Clarke, M., Griffiths, S., Hayta, S., Jiang,
1124 M., Keller, B., Kirby, R., Kolodziej, M. C., Powell, O. R., Smedley, M., Steuernagel, B.,
1125 Xian, W., Wingen, L. U., Cheng, S., Saintenac, C., Wulff, B. B. H., and Brown, J. K. M.
1126 2025. Septoria tritici blotch resistance gene *Stb15* encodes a lectin receptor-like kinase.
1127 Nat. Plants 11: 410–420 (2025). https://doi.org/10.1038/s41477-025-01920-2.

1128 Hallgren, J., Tsirigos, K. D., Pedersen, M. D., Armenteros, J. J. A., Marcatili, P., Nielsen, H.,
1129 Krogh, A., and Winther, O. 2022. DeepTMHMM predicts alpha and beta transmembrane
1130 proteins using deep neural networks. bioRxiv.
1131 https://doi.org/10.1101/2022.04.08.487609.

1132 Helm, M., Singh, R., Hiles, R., Jaiswal, N., Myers, A., Iyer-Pascuzzi, A. S., and Goodwin, S. B.
1133 2022. Candidate effector proteins from the maize tar spot pathogen *Phyllachora maydis*
1134 localize to diverse plant cell compartments. Phytopathology 112: 2538–2548.
1135 https://doi.org/10.1094/PHYTO-05-22-0181-R.
1136 Jaiswal, N., Myers, A., Weese, T. L., Carter, M. E., Scofield, S. R., and Helm, M. 2023. Analysis
1137 of cell death induction by the barley NLR immune receptor PBR1. PhytoFrontiers 3:
1138 663–678. https://doi.org/10.1094/PHYTOFR-01-23-0005-R.

1139 Käll, L., Krogh, A., and Sonnhammer, E. L. L. 2004. A combined transmembrane topology and
1140 signal peptide prediction method. Journal of Molecular Biology 338: 1027–1036.
1141 https://doi.org/10.1016/j.jmb.2004.03.016.

1142 Kanehisa, M., Furumichi, M., Tanabe, M., Sato, Y., and Morishima, K. 2017. KEGG: New per-
1143 spectives on genomes, pathways, diseases and drugs. Nucleic Acids Research 45: D353–
1144 D361. https://doi.org/10.1093/nar/gkw1092.

1145 Karki, S. J., Reilly, A., Zhou, B., Mascarello, M., Burke, J., Doohan, F., Douchkov, D., and
1146 Schweizer, P. 2021. A small secreted protein from *Zymoseptoria tritici* interacts with a
1147 wheat E3 ubiquitin ligase to promote disease. Journal of Experimental Botany 72: 733–
1148 746. https://doi.org/10.1093/jxb/eraa489.

1149 Kellner, R., Bhattacharyya, A., Poppe, S., Hsu, T. Y., Brem, R. B., and Stukenbrock, E. H. 2014.
1150 Expression profiling of the wheat pathogen Zymoseptoria tritici reveals genomic patterns
1151 of transcription and host-specific regulatory programs. Genome Biology and Evolution 6:
1152 1353–1365. https://doi.org/10.1093/gbe/evu101.

1153 Kettles, G.J. and Kanyuka, K. 2016. Dissecting the molecular interactions between wheat and the
1154 fungal pathogen *Zymoseptoria tritici*. Front. Plant Sci. 7:508.
1155 https://doi.org/10.3389/fpls.2016.00508.

1156 Lapalu, N., Lamothe, L., Petit, Y., Genissel, A., Delude, C., Feurtey, A., Abraham, L.N., Smith,
1157 D., King, R., Renwick, A., Appertet, M., Sucher, J., Steindorff, A.S., Goodwin, S.B.,
1158 Kema, G.H.J., Grigoriev, I.V., Hane, J., Rudd, J., Stukenbrock, E., Croll, D., Scalliet, G.,
1159 and Lebrun, M.-H. 2025. Improved gene annotation of the fungal wheat pathogen *Zy-*
1160 *moseptoria tritici* based on combined Iso-Seq and RNA-Seq evidence. Molecular Plant-
1161 Microbe Interactions (in press).

1162 Laugé, R., Joosten, M. H. A. J., Van den Ackerveken, G. F. J. M., Van den Broek, H. W. J., and
1163 De Wit, P. J. G. M. 1997. The in planta-produced extracellular proteins ECP1 and ECP2
1164 of *Cladosporium fulvum* are virulence factors. Molecular Plant-Microbe Interactions 10:
1165 725–734. https://doi.org/10.1094/MPMI.1997.10.6.725.

1166 Le Marquer, M., San Clemente, H., Roux, C. Savelli, B., and Frei dit Frey, N. 2019. Identifica-
1167 tion of new signalling peptides through a genome-wide survey of 250 fungal secretomes.
1168 BMC Genomics 20: 64. https://doi.org/10.1186/s12864-018-5414-2.

1169 Levasseur, A., Drula, E., Lombard, V., Coutinho, P. M., and Henrissat, B. 2013. Expansion of
1170 the enzymatic repertoire of the CAZy database to integrate auxiliary redox enzymes. Bio-
1171 technology for Biofuels 6: 41. https://doi.org/10.1186/1754-6834-6-41.

1172 Li, S., Dong, Y., Li, L., Zhang, Y., Yang, X., Zeng, H., Shi, M., Pei, X., Qiu, D., and Yuan, Q.
1173 2019. The novel cerato-platanin-like protein FocCP1 from *Fusarium oxysporum* triggers

1174 an immune response in plants. International Journal of Molecular Sciences 20: 2849.
1175 https://doi.org/10.3390/ijms20112849.
1176 Li, S., Su, X., Luo, X., Zhang, Y., Zhang, D., Du, J., Zhang, Z., OuYang, X., Zhang, S., and Liu,
1177 Y. 2020. First evidence showing that *Pepper vein yellows virus* P4 protein is a movement
1178 protein. BMC Microbiology 20: 72. https://doi.org/10.1186/s12866-020-01758-y.

1179 Love, M. I., Huber, W., and Anders, S. 2014. Moderated estimation of fold change and disper-
1180 sion for RNA-seq data with DESeq2. Genome Biology 15: 550.
1181 https://doi.org/10.1186/s13059-014-0550-8.

1182 Lu, S., and Edwards, M. C. 2018. Molecular characterization and functional analysis of PR-1-
1183 like proteins identified from the wheat head blight fungus *Fusarium graminearum*. Phy-
1184 topathology 108: 510–520. https://doi.org/10.1094/PHYTO-08-17-0268-R.

1185 Lucena, R., Dolz-Edo, L., Brul, S., de Morais, M., and Smits, G. 2020. Extreme low cytosolic
1186 pH is a signal for cell survival in acid stressed yeast. Genes 11: 656. doi:
1187 10.3390/genes11060656.

1188 Marshall, R., Kombrink, A., Motteram, J., Loza-reyes, E., Lucas, J., Hammond-kosack, K. E.,
1189 Thomma, B. P. H. J., and Rudd, J. J. 2011. Analysis of two in planta expressed LysM ef-
1190 fector homologs from the fungus *Mycosphaerella graminicola* reveals novel functional
1191 properties and varying contributions to virulence on wheat. Plant Physiology 156: 756–
1192 769. https://doi.org/10.1104/pp.111.176347.
1193 Meile, L., Garrido-Arandia, M., Bernasconi, Z., Peter, J., Schneller, A., Bernasconi, A., Alas-
1194 simone, J., McDonald, B. A., and Sánchez-Vallet, A. 2023. Natural variation in Avr3D1

1195 from *Zymoseptoria* sp. contributes to quantitative gene-for-gene resistance and to host
1196 specificity. New Phytologist (2023) 238: 1562–1577. https://doi.org/10.1111/nph.18690.
1197 Mekonnen, T., Haileselassie, T., Goodwin, S.B. and Tesfaye, K. 2020. Genetic diversity and
1198 population structure of *Zymoseptoria tritici* in Ethiopia as revealed by microsatellite
1199 markers. Fungal Genet. Biol. 141:103413. https://doi.org/10.1016/j.fgb.2020.103413.

1200 Meshram, S., Gogoi, R., Bashyal, B. M., Kumar, A., Mandal, P. K., and Hossain, F. 2022. Com-
1201 parative transcriptome analysis of fungal pathogen Bipolaris maydis to understand patho-
1202 genicity behavior on resistant and susceptible non-CMS maize genotypes. Frontiers in
1203 Microbiology 13: 837056. https://doi.org/10.3389/fmicb.2022.837056.

1204 Mirzadi Gohari, A., Ware, S. B., Wittenberg, A. H. J., Mehrabi, R., Ben M'Barek, S., Verstap-
1205 pen, E. C. P., van der Lee, T. A. J., Robert, O., Schouten, H. J., de Wit, P. P. J. G. M., and
1206 Kema, G. H. J. 2015. Effector discovery in the fungal wheat pathogen *Zymoseptoria trit-*
1207 *ici*. Molecular Plant Pathology 16: 931–945. https://doi.org/10.1111/mpp.12251.
1208 Motteram, J., Küfner, I., Deller, S., Brunner, F., Hammond-Kosack, K.E., Nürnberger, T. and
1209 Rudd, J.J. 2009. Molecular characterization and functional analysis of MgNLP, the sole
1210 NPP1 domain-containing protein, from the fungal wheat leaf pathogen *Mycosphaerella*
1211 *graminicola*. Mol. Plant Microbe Interact. 22:790–799. https://doi.org/10.1094/MPMI-
1212 22-7-0790.
1213 Orton, E.S., Rudd, J.J. and Brown, J.K.M. 2017. Early molecular signatures of responses of
1214 wheat to *Zymoseptoria tritici* in compatible and incompatible interactions. Plant
1215 Pathoogy 66:450–459. https://doi.org/10.1111/ppa.12633.

1216 Palma-Guerrero, J., Ma, X., Torriani, S. F. F., Zala, M., Francisco, C. S., Hartmann, F. E., Croll,
1217 D., and McDonald, B. A. 2017. Comparative transcriptome analyses in *Zymoseptoria trit-*
1218 *ici* reveal significant differences in gene expression among strains during plant infection.
1219 Molecular Plant-Microbe Interactions 30: 231–244. https://doi.org/10.1094/MPMI-07-16-
1220 0146-R.
1221 Panstruga, R. and Moscou, M.J. 2020. What is the molecular basis of nonhost resistance? Mol.
1222 Plant-Microbe Interact. 33:1253–1264. https://doi.org/10.1094/MPMI-06-20-0161-CR.

1223 Pečenková, T., Pejchar, P., Moravec, T., Drs, M., Haluška, S., Šantrůček, J., Potocká, A., Žárský,
1224 V., and Potocký, M. 2022. Immunity functions of *Arabidopsis* pathogenesis-related 1 are
1225 coupled but not confined to its C-terminus processing and trafficking. Molecular Plant
1226 Pathology 23: 664–678. https://doi.org/10.1111/mpp.13187.

1227 Petit-Houdenot, Y. and Fudal, I. 2017. Complex interactions between fungal avirulence genes
1228 and their corresponding plant resistance genes and consequences for disease resistance
1229 management. Front. Plant Sci. 8:1072. https://doi.org/10.3389/fpls.2017.01072.
1230 Petre, B., and Kamoun, S. 2014. How do filamentous pathogens deliver effector proteins into
1231 plant cells? PLOS Biology 12: e1001801. https://doi.org/10.1371/journal.pbio.1001801.
1232 Petre, B., Saunders, D. G. O., Sklenar, J., Lorrain, C., Krasileva, K. V., Win, J., Duplessis, S.,
1233 and Kamoun, S. (2016). Heterologous expression screens in *Nicotiana benthamiana* iden-
1234 tify a candidate effector of the wheat yellow rust pathogen that associates with processing
1235 bodies. PLOS ONE 11: e0149035. https://doi.org/10.1371/journal.pone.0149035.
1236 Ponomarenko, A., Goodwin, S.B. and Kema, G.H.J. 2011. Septoria tritici blotch (STB) of wheat.
1237 Plant Health Instructor. https://doi.org/10.1094/PHI-I-2011-0407-01.
1238

1239 Qi, D., DeYoung, B.J. and Innes, R.W. 2012. Structure-function analysis of the coiled-coil and
1240 leucine-rich repeat domains of the RPS5 disease resistance protein. Plant Physiol,
1241 158:1819–1832. https://doi.org/10.1104/pp.112.194035.
1242 Quarantin, A., Castiglioni, C., Schäfer, W., Favaron, F., and Sella, L. 2019. The *Fusarium gra-*
1243 *minearum* cerato-platanins loosen cellulose substrates enhancing fungal cellulase activity
1244 as expansin-like proteins. Plant Physiology and Biochemistry 139: 229–238.
1245 https://doi.org/10.1016/j.plaphy.2019.03.025.

1246 Raudvere, U., Kolberg, L., Kuzmin, I., Arak, T., Adler, P., Peterson, H., and Vilo, J. 2019. g:Pro-
1247 filer: A web server for functional enrichment analysis and conversions of gene lists (2019
1248 update). Nucleic Acids Research 47(W1): W191–W198.
1249 https://doi.org/10.1093/nar/gkz369.

1250 Reilly, A., Karki, S.J., Twamley, A., Tiley, A.M.M., Kildea, S. and Feechan, A. 2021. Isolate-
1251 specific responses of the nonhost grass *Brachypodium distachyon* to the fungal pathogen
1252 *Zymoseptoria tritici* compared with wheat. Phytopathology 111:356–368.
1253 https://doi.org/10.1094/PHYTO-02-20-0041-R.
1254 Rogers, A., Jaiswal, N., Roggenkamp, E., Kim, H.-S., MacCready, J. S., Chilvers, M. I., Sco-
1255 field, S. R., Iyer-Pascuzzi, A. S., and Helm, M. 2024. Genome-informed trophic classifi-
1256 cation and functional characterization of virulence proteins from the maize tar spot patho-
1257 gen *Phyllachora maydis*. Phytopathology 114: 1940–1949.
1258 https://doi.org/10.1094/PHYTO-01-24-0037-R.
1259 Rogers, L., and Overall C. 2013. Proteolytic post-translational modification of proteins: proteo-
1260 mic tools and methodology. Molecular Cell Proteomics 12:3532-42.
1261 https://doi.org/10.1074/mcp.M113.031310.

1262 Rudd, J. J., Kanyuka, K., Hassani-Pak, K., Derbyshire, M., Andongabo, A., Devonshire, J., Ly-
1263 senko, A., Saqi, M., Desai, N. M., Powers, S. J., Hooper, J., Ambroso, L., Bharti, A.,
1264 Farmer, A., Hammond-Kosack, K. E., Dietrich, R. A., and Courbot, M. 2015. Transcrip-
1265 tome and metabolite profiling of the infection cycle of *Zymoseptoria tritici* on wheat re-
1266 veals a biphasic interaction with plant immunity involving differential pathogen chromo-
1267 somal contributions and a variation on the hemibiotrophic lifestyle definition. Plant Phys-
1268 iology 167: 1158–1185. https://doi.org/10.1104/pp.114.255927.

1269 Saintenac, C., Cambon, F., Aouini, L., Verstappen, E., Ghaffary, S. M. T., Poucet, T., Marande,
1270 W., Berges, H., Xu, S., Jaouannet, M., Favery, B., Alassimone, J., Sánchez-Vallet, A.,
1271 Faris, J., Kema, G., Robert, O., and Langin, T. 2021. A wheat cysteine-rich receptor-like
1272 kinase confers broad-spectrum resistance against Septoria tritici blotch. Nature Commu-
1273 nications 12: 433. https://doi.org/10.1038/s41467-020-20685-0.

1274 Saintenac, C., Lee, W.-S., Cambon, F., Rudd, J. J., King, R. C., Marande, W., Powers, S. J., Ber-
1275 gès, H., Phillips, A. L., Uauy, C., Hammond-Kosack, K. E., Langin, T., and Kanyuka, K.
1276 2018. Wheat receptor-kinase-like protein Stb6 controls gene-for-gene resistance to fungal
1277 pathogen *Zymosept*oria tritici. Nature Genetics 50: 368–374.
1278 https://doi.org/10.1038/s41588-018-0051-x.

1279 Sánchez-Vallet, A., Saleem-Batcha, R., Kombrink, A., Hansen, G., Valkenburg, D.-J., Thomma,
1280 B. P., and Mesters, J. R. 2013. Fungal effector Ecp6 outcompetes host immune receptor
1281 for chitin binding through intrachain LysM dimerization. eLife 2: e00790.
1282 https://doi.org/10.7554/eLife.00790.

1283 Sánchez-Vallet, A., Tian, H., Rodriguez-Moreno, L., Valkenburg, D.-J., Saleem-Batcha, R.,
1284 Wawra, S., Kombrink, A., Verhage, L., de Jonge, R., van Esse, H. P., Zuccaro, A., Croll,

1285 D., Mesters, J. R., and Thomma, B. P. H. J. 2020. A secreted LysM effector protects fun-
1286 gal hyphae through chitin-dependent homodimer polymerization. PLoS Pathogens 16:
1287 e1008652. https://doi.org/10.1371/journal.ppat.1008652.

1288 Selin, C., de Kievit, T.R., Belmonte, M.F., and Fernando, W.G.D. (2016. Elucidating the role of
1289 effectors in plant-fungal interactions: progress and challenges. Front. Microbiol. 7:600.
1290 doi: 10.3389/fmicb.2016.00600.

1291 Singh P and Zimmerli L. 2013. Lectin receptor kinases in plant innate immunity. Front. Plant
1292 Sci. 4:124. https://doi.org/10.3389/fpls.2013.00124.

1293 Snapp, E., 2005. Design and use of fluorescent fusion proteins in cell biology. Current Protocols
1294 in Cell Biology 27: 21.4.1-21.4.13. https://doi.org/10.1002/0471143030.cb2104s27.

1295 Sperschneider, J., Catanzariti, A.-M., DeBoer, K., Petre, B., Gardiner, D. M., Singh, K. B.,
1296 Dodds, P. N., and Taylor, J. M. 2017. LOCALIZER: Subcellular localization prediction
1297 of both plant and effector proteins in the plant cell. Sci. Rep. **7**: 44598.
1298 https://doi.org/10.1038/srep44598.

1299 Sperschneider, J., and Dodds, P. N. 2022. EffectorP 3.0: Prediction of apoplastic and cytoplas-
1300 mic effectors in fungi and Oomycetes. Molecular Plant-Microbe Interactions 35: 146–
1301 156. https://doi.org/10.1094/MPMI-08-21-0201-R.

1302 Sperschneider, J., Dodds, P. N., Singh, K. B., and Taylor, J. M. 2018. ApoplastP: Prediction of
1303 effectors and plant proteins in the apoplast using machine learning. New Phytologist 217:
1304 1764–1778. https://doi.org/10.1111/nph.14946.

1305 Steinberg, G. 2015. Cell biology of *Zymoseptoria tritici*: pathogen cell organization and wheat
1306 infection. Fungal Genet. Biol. 79:17–23. https://doi.org/10.1016/j.fgb.2015.04.002.

1307 Stergiopoulos, I., Burg, H. A. V. D., Ökmen, B., Beenen, H. G., Liere, S. V., and Kema, G. H. J.
1308 2010. Tomato Cf resistance proteins mediate recognition of cognate homologous effec-
1309 tors from fungi pathogenic on dicots and monocots. Proceedings of the National Acad-
1310 emy of Sciences, USA 107: 7610–7615. https://doi.org/10.1073/pnas.1002910107.

1311 Stergiopoulos, I., Kourmpetis, Y. A. I., Slot, J. C., Bakker, F. T., Wit, P. J. G. M. D., and Rokas,
1312 A. 2012. In silico characterization and molecular evolutionary analysis of a novel super-
1313 family of fungal effector proteins. Molecular Biology and Evolution 29: 3371–3384.
1314 https://doi.org/10.1093/molbev/mss143.

1315 Tanz, S. K., Castleden, I., Small, I. D., and Millar, A. H. 2013. Fluorescent protein tagging as a
1316 tool to define the subcellular distribution of proteins in plants. Frontiers in Plant Science
1317 4 - 2013. https://doi.org/10.3389/fpls.2013.00214.

1318 Teixeira, P. J. P. L., Thomazella, D. P. T., Vidal, R. O., Prado, P. F. V. do, Reis, O., Baroni, R.
1319 M., Franco, S. F., Mieczkowski, P., Pereira, G. A. G., and Mondego, J. M. C. 2012. The
1320 fungal pathogen *Moniliophthora perniciosa* has genes similar to plant PR-1 that are
1321 highly expressed during its interaction with cacao. PLOS One 7: e45929.
1322 https://doi.org/10.1371/journal.pone.0045929.

1323 Teufel, F., Almagro Armenteros, J. J., Johansen, A. R., Gíslason, M. H., Pihl, S. I., Tsirigos, K.
1324 D., Winther, O., Brunak, S., von Heijne, G., and Nielsen, H. 2022. SignalP 6.0 predicts
1325 all five types of signal peptides using protein language models. Nature Biotechnology 40:
1326 1023–1025. https://doi.org/10.1038/s41587-021-01156-3.

1327 Thynne, E., Ali, H., Seong, K., Abukhalaf, M., Guerreiro, M.A., Flores-Nunez, V.M., Hansen,
1328 R., Bergues, A., Salman, M.J., Rudd, J.J., Kanyuka, K., Tholey, A., Krasileva, K.V., Ket-
1329 tles, G.J., and Stukenbrock, E.H. 2024. An array of *Zymoseptoria tritici* effectors sup-
1330 press plant immune responses. Molecular Plant Pathology 25: e13500.
1331 https://doi.org/10.1111/mpp.13500.

1332 Tian, H., MacKenzie, C. I., Rodriguez-Moreno, L., van den Berg, G. C. M., Chen, H., Rudd, J.
1333 J., Mesters, J. R., and Thomma, B. P. H. J. 2021. Three LysM effectors of *Zymoseptoria*
1334 *tritici* collectively disarm chitin-triggered plant immunity. Molecular Plant Pathology 22:
1335 683–693. https://doi.org/10.1111/mpp.13055.

1336 Tian, G.-W., Mohanty, A., Chary, S.N., Li, S., Paap, B., Drakakaki, G., Kopec, C.D., Li, J.,
1337 Ehrhardt, D., Jackson, D., Rhee, S.Y., Raikhel, N.V., and Citovsky, V. 2004. High-
1338 throughput fluorescent tagging of full-length Arabidopsis gene products in planta. Plant
1339 Physiol. 135: 25–38. https://doi.org/10.1104/pp.104.040139.

1340 Tintor, N., Nieuweboer, G. A. M., Bakker, I. A. W., and Takken, F. L. W. 2022. The intracellu-
1341 larly acting effector Foa3 suppresses defense responses when infiltrated into the apoplast.
1342 Frontiers in Plant Science 13: 813181. ttps://doi.org/10.3389/fpls.2022.813181.

1343 Triandafillou, C., Katanski, C., Dinner, A., and Drummond, D. 2020. Transient intracellular
1344 acidification regulates the core transcriptional heat shock response. Elife 9:e54880. doi:
1345 10.7554/eLife.54880.

1346 Wangorsch, A., Scheurer, S., Blanca, M., Blanca-Lopez, N., Somoza, M. L., and Martín-
1347 Pedraza, L. 2022. Allergenic properties and molecular characteristics of PR-1 proteins.
1348 Frontiers in Allergy 3: 824717. https://doi.org/10.3389/falgy.2022.824717.

1349 Weichert, M., Guirao-Abad, J., Aimanianda, V., Krishnan, K., Grisham, C., Snyder, P., Sheehan,
1350 A., Abbu, R. R., Liu, H., Filler, S. G., Gruenstein, E. I., Latgé, J.-P., and Askew, D. S.
1351 2020. Functional coupling between the unfolded protein response and endoplasmic retic-
1352 ulum/golgi Ca2+-ATPases promotes stress tolerance, cell wall biosynthesis, and viru-
1353 lence of *Aspergillus fumigatus*. mBio 11: e01060-20.
1354 https://doi.org/10.1128/mBio.01060-20.

1355 Yang, F., Li, W., and Jørgensen, H. J. L. 2013. Transcriptional reprogramming of wheat and the
1356 hemibiotrophic pathogen *Septoria tritici* during two phases of the compatible interaction.
1357 PLoS One 8: 1–15. https://doi.org/10.1371/journal.pone.0081606.

1358 Yang, N, Ovenden, B, Baxter, B, McDonald, MC, Solomon, PS, and Milgate, A. 2022. Multi-
1359 stage resistance to *Zymoseptoria tritici* revealed by GWAS in an Australian bread wheat
1360 diversity panel. Front. Plant Sci.13:990915. https://doi.org/10.3389/fpls.2022.990915.

1361 Yang, G., Tang, L., Gong, Y., Xie, J., Fu, Y., Jiang, D., Li, G., Collinge, D. B., Chen, W., and
1362 Cheng, J. 2018. A cerato-platanin protein SsCP1 targets plant PR1 and contributes to vir-
1363 ulence of *Sclerotinia sclerotiorum*. New Phytologist 217: 739–755.
1364 https://doi.org/10.1111/nph.14842.

1365 Zhang, L., Yan, J., Fu, Z., Shi, W., Ninkuu, V., Li, G., Yang, X., and Zeng, H. 2021. FoEG1, a
1366 secreted glycoside hydrolase family 12 protein from *Fusarium oxysporum*, triggers cell
1367 death and modulates plant immunity. Molecular Plant Pathology 22: 522–538.
1368 https://doi.org/10.1111/mpp.13041.

Zhang, M., Xie, S., Zhao, L., Meng, X., Song, L., Feng, H., &and Huang, L. 2019. Hce2 domain-containing effectors contribute to the full virulence of Valsa mali in a redundant manner. Molecular Plant Pathology 20: 843-856. https://doi.org/10.1111/mpp.12796.

Zhong, Z., Marcel, T. C., Hartmann, F. E., Ma, X., Plissonneau, C., Zala, M., Ducasse, A., Confais, J., Compain, J., Lapalu, N., Amselem, J., McDonald, B. A., Croll, D., and Palma-Guerrero, J. 2017. A small secreted protein in *Zymoseptoria tritici* is responsible for avirulence on wheat cultivars carrying the *Stb6* resistance gene. New Phytologist 214: 619–631. https://doi.org/10.1111/nph.14434.

1378 **Table 1.** Comparisons of gene expression by the wheat pathogen *Zymoseptoria tritici* during sus-
1379 ceptible and resistant interactions on wheat and its non-host interaction on barley

Host inoculated	Compared to	Type of comparison
Taichung 29 wheat	Veranopolis (*Stb2*) wheat	Susceptible vs. resistant
	Israel 493 (*Stb3*) wheat	Susceptible vs. resistant
	Kindred barley	Susceptible vs. Non host
Veranopolis (*Stb2*) wheat	Israel 493 (*Stb3*) wheat	Resistant vs. resistant
Kindred barley	Veranopolis (*Stb2*) wheat	Non host vs. resistant
	Israel 493 (*Stb3*) wheat	Non host vs. resistant

1380

1381

1382 **Table 2.** Differentially expressed genes (DEGs) of the wheat pathogen *Zymoseptoria tritici* when
1383 comparing three types of host interaction[a]

Comparison	Time point[b]	Up[c]	Down[c]	Total DEGs	Total detectable genes
Resistant (*Stb2*) – Resistant (*Stb3*)[d]	1	0	0	0	1,504
	3	0	0	0	
	6	1	0	1	
	10	1	11	12	
	17	13	1	14	222
	23	3	0	3	
Susceptible - Resistant (*Stb2*)[e]	1	0	0	0	1,504
	3	1	4	5	
	6	12	0	12	
	10	275	326	601	
	17	21	11	32	222
	23	33	23	56	
Susceptible - Resistant (*Stb3*)[f]	1	1	1	2	1,504
	3	0	4	4	
	6	21	0	21	
	10	226	361	587	
	17	34	13	47	222
	23	34	22	56	

1384
1385 [a] DEGs were identified for the first-listed condition in each comparison relative to the second-
1386 listed condition, which served as the baseline. Horizontal lines within each comparison indicate
1387 normalization groups. Gene counts for time points 1, 3, 6, and 10 DPI were normalized together,
1388 while counts for time points 17 and 23 DPI were normalized separately as a distinct group.
1389 [b] 6-point time course. Time points are measured in days after inoculation.
1390 [c] Significantly differentially expressed genes that are up- or down-regulated at a False Discovery
1391 Rate (FDR) of 5%.
1392 [d] Responses of *Z. tritici* isolate IPO323 when grown on *Stb2*-resistant plants of cultivar Veranop-
1393 olis compared to those on *Stb3*-resistant plants of cultivar Israel 493
1394 [e] Responses of *Z. tritici* isolate IPO323 when grown on susceptible cultivar Taichung 29 com-
1395 pared to those on *Stb2*-resistant plants of cultivar Veranopolis
1396 [f] Responses of *Z. tritici* isolate IPO323 when grown on susceptible cultivar Taichung 29 com-
1397 pared to those on *Stb3*-resistant plants of cultivar Israel 493
1398
1399
1400

1401 **Table 3.** Differentially expressed genes (DEGs) of the wheat pathogen *Zymoseptoria tritici* when
1402 comparing susceptible and resistant interactions versus a non-host interaction on barley[a]
1403

Comparison	Time point[b]	Up[c]	Down[c]	Total DEGs	Total detectable genes
Susceptible–non host[d]	1	74	40	114	284
	3	123	47	171	
	6	43	48	91	352
	10	94	52	146	
	17	57	14	71	107
	23	63	17	80	
Resistant (*Stb2*) – non host[e]	1	67	40	107	284
	3	107	47	154	
	6	40	44	84	352
	10	68	41	109	
	17	20	9	29	107
	23	30	27	57	
Resistant (*Stb3*) - non host[f]	1	68	41	109	284
	3	108	52	160	
	6	54	59	113	352
	10	70	39	109	
	17	9	9	18	107
	23	22	23	45	

1404
1405 [a] DEGs were identified for the first-listed condition in each comparison relative to the second-
1406 listed condition, which served as the baseline. Horizontal lines within each comparison indicate
1407 normalization groups. Gene counts for time points 1 and 3 DPI were normalized together, 6 and
1408 10 DPI were normalized as a separate group, and 17 and 23 DPI were normalized together as an-
1409 other distinct group.
1410 [b] 6-point time course. Time points are measured days after inoculation.
1411 [c] Significantly differential expressed genes that are up- or down-regulated at a False Discovery
1412 Rate (FDR) of 5%.
1413 [d] Responses of *Z. tritici* isolate IPO323 when grown on plants of susceptible wheat cultivar Tai-
1414 chung 29 compared to those on non-host barley plants
1415 [e] Responses of *Z. tritici* isolate IPO323 when grown on *Stb2*-resistant plants of cultivar Veranop-
1416 olis compared to those on non-host barley plants
1417 [f] Responses of *Z. tritici* isolate IPO323 when grown on *Stb3*-resistant plants of cultivar Israel 493
1418 compared to those on non-host barley plants
1419
1420
1421

1422 **Table 4.** Characteristics of the 31 *Zymoseptoria tritici* candidate effectors that were selected for
1423 further analysis based on differential expression at the early or transition stages of the infection
1424 process
1425

ID	Amino acids	Signal peptide	Protein size (kDa)	LOCALIZER prediction	Annotation
Mycgr394290	184	18-19	18.61	Chloroplast (95-118) Mitochondria (68-88) NLS	Uncharacterized
Mycgr3111221	232	16-17	22.43	—[a]	Peptidoglycan-binding LysM
Mycgr3106502	89	18-19	8.01	—	Uncharacterized
Mycgr3104794	157	20-21	15.15	—	Uncharacterized
Mycgr3109991	235	20-21	24.87	NLS	Uncharacterized
Mycgr3105487	97	18-19	8.7	—	Peptidoglycan-binding LysM
Mycgr3109710	200	26-27	18.8	—	Allergen V5/Tpx-1 related
Mycgr3106125	70	23-24	4.95	—	Uncharacterized
Mycgr3111223	554	18-19	58.81	—	Heat shock protein DnaJ, N-terminal
Mycgr3110220	131	19-20	12.88	—	Uncharacterized
Mycgr3107904	170	23-24	15.65	—	Hce2 domain-containing protein

Mycgr346866	427	22-23	41.15	—	Carbohydrate kinase, PfkB
Mycgr383064	75	18-19	6.15	—	Uncharacterized
Mycgr3102792	114	19-20	10.63	NLS	Uncharacterized
Mycgr379161	68	19-20	4.98	—	Uncharacterized
Mycgr3106106	140	20-21	14.44	—	Uncharacterized
Mycgr3111636	159	19-20	14.63	—	Hce2 domain-containing protein
Mycgr3109137	154	18-19	15.81	—	Uncharacterized
Mycgr3102996	163	23-24	15.12	—	Uncharacterized
Mycgr3110887	283	19-20	30.59	—	Uncharacterized
Mycgr3104009	483	25-26	51.39	—	Beta-Ig-H3/fasciclin
Mycgr339947	149	17-18	13.95	—	Cerato-platanin
Mycgr3105223	188	23-24	18.19	—	Uncharacterized
Mycgr3105182	143	18-19	13.88	—	Uncharacterized
Mycgr3104697	149	19-20	13.49	—	Uncharacterized
Mycgr3101652	77	21-22	6.06	—	Uncharacterized
Mycgr3106456	193	30-31	16.59	Chloroplast (27-65)	GPI-anchored domain-containing protein
Mycgr3106329	135	19-20	13.06	—	Uncharacterized

Mycgr382936	155	20-21	13.97	—	Plastocyanin-like
Mycgr399161	164	15-16	16.03	—	Uncharacterized
Mycgr3102849	285	20-21	27.95	—	Uncharacterized

1426 [a] No specific prediction made.

1427

1428

FIGURES

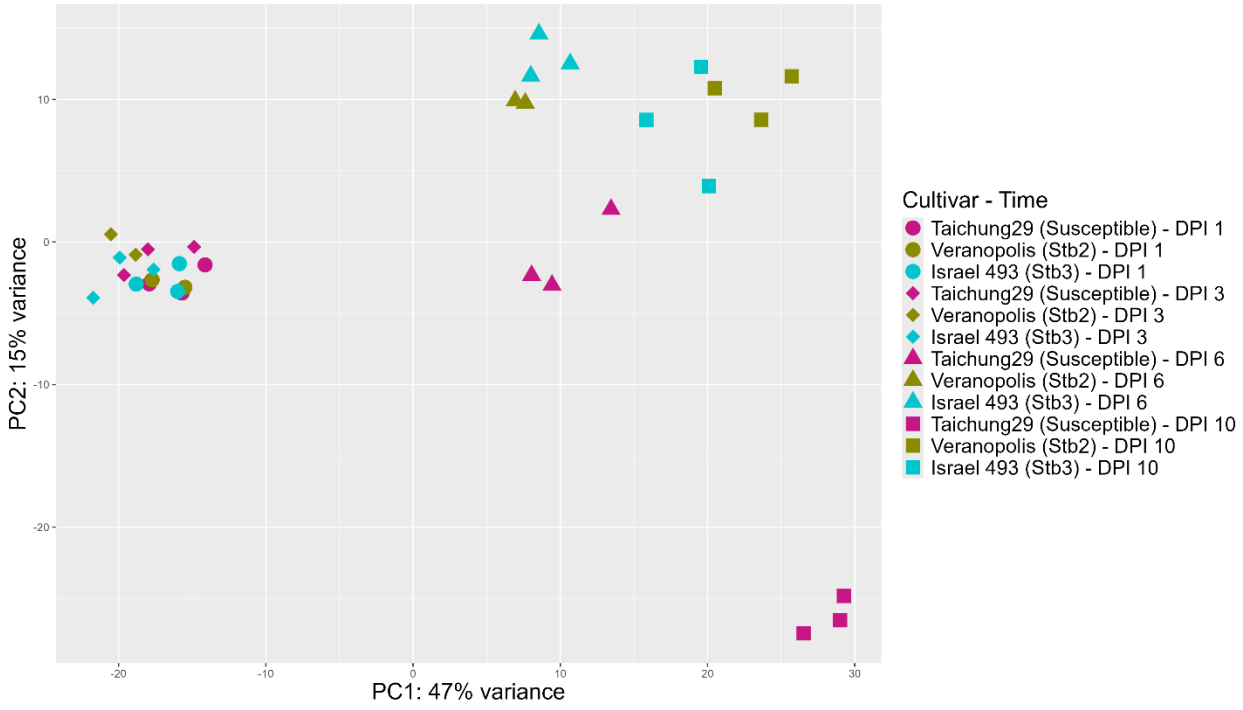

Fig. 1. Principal component analysis (PCA) of the normalized and filtered counts for RNA sequencing reads of *Zymoseptoria tritici* inoculated onto the highly susceptible wheat cultivar Taichung 29 (Susceptible) or the R-gene-containing resistant wheat cultivars Veranopolis (*Stb2* resistance gene) or Israel 493 (*Stb3*) at 1, 3, 6, and 10 days post inoculation (DPI).

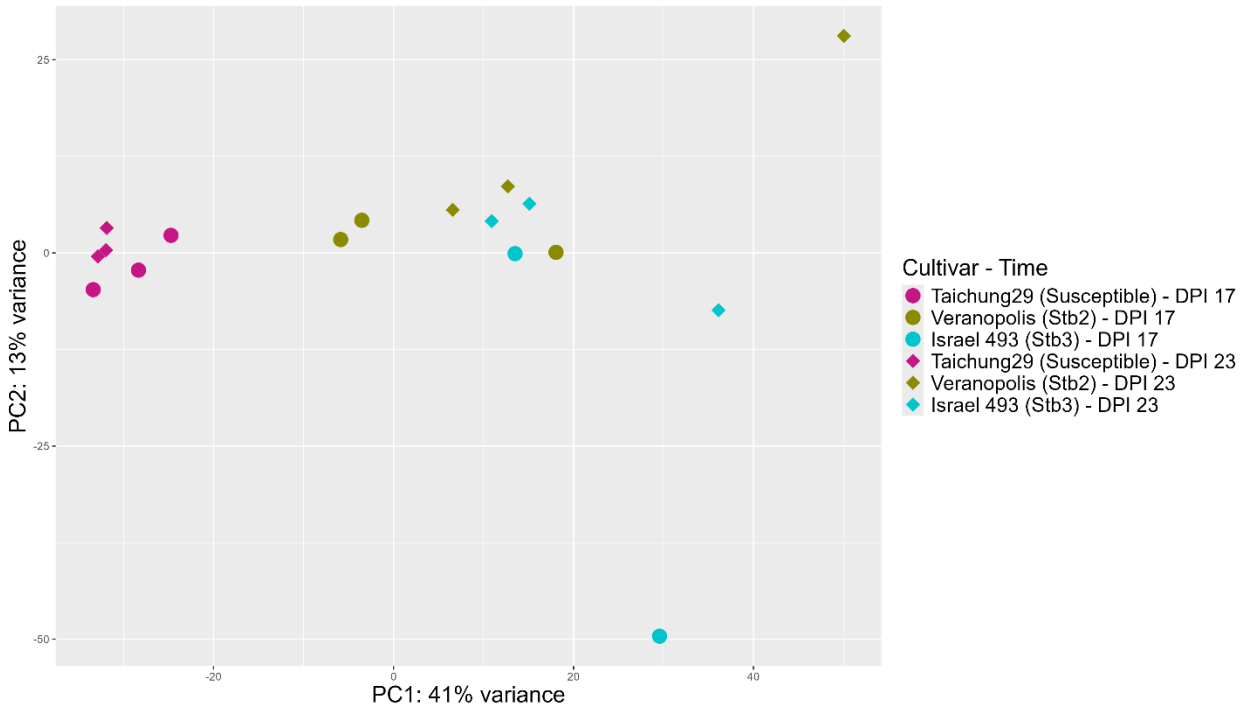

Fig. 2. Principal component analysis (PCA) of the normalized and filtered counts for RNA sequencing reads of *Zymoseptoria tritici* inoculated onto the highly susceptible wheat cultivar Taichung 29 (Susceptible) or the R-gene-containing resistant wheat cultivars Veranopolis (*Stb2* resistance gene) or Israel 493 (*Stb3*) at 17 and 23 days post inoculation (DPI).

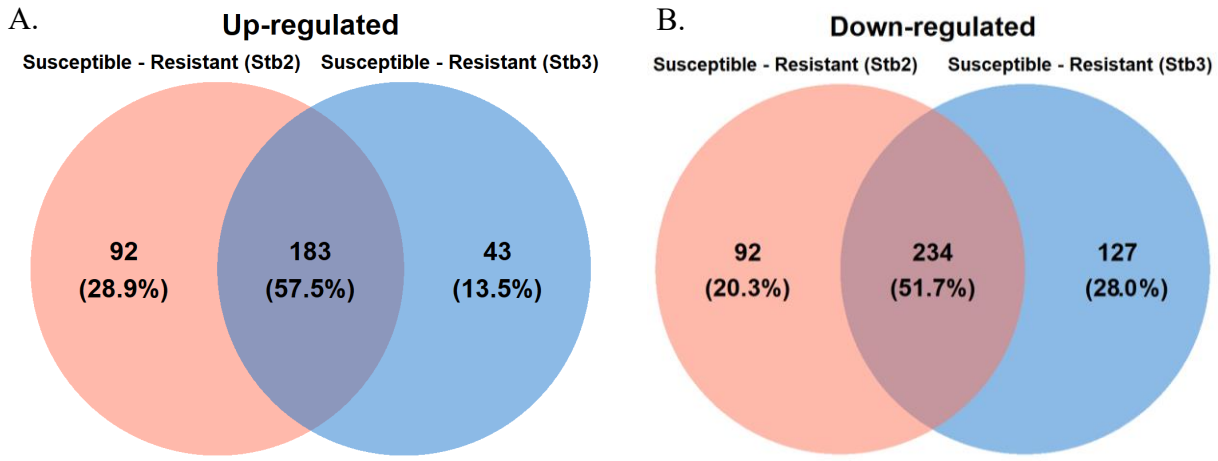

Fig. 3. Venn diagrams showing common and unique differentially expressed genes of *Zymoseptoria tritici* at 10 days post inoculation (DPI) in the susceptible interaction compared to the two

resistant interactions on wheat. (A) Up-regulated genes shared between the comparisons of the susceptible interaction versus the resistant interactions with cultivars Veranopolis (*Stb2*) and Israel 493 (*Stb3*). The intersection represents 183 (57.5%) genes that are up-regulated in the pathogen during the susceptible interaction relative to both resistant interactions. (B) Down-regulated genes shared between the comparisons of the susceptible interaction versus the resistant interactions with cultivars Veranopolis (*Stb2*) and Israel 493 (*Stb3*). The intersection represents 234 (51.7%) genes that are down-regulated in the pathogen during the susceptible interaction relative to both resistant interactions.

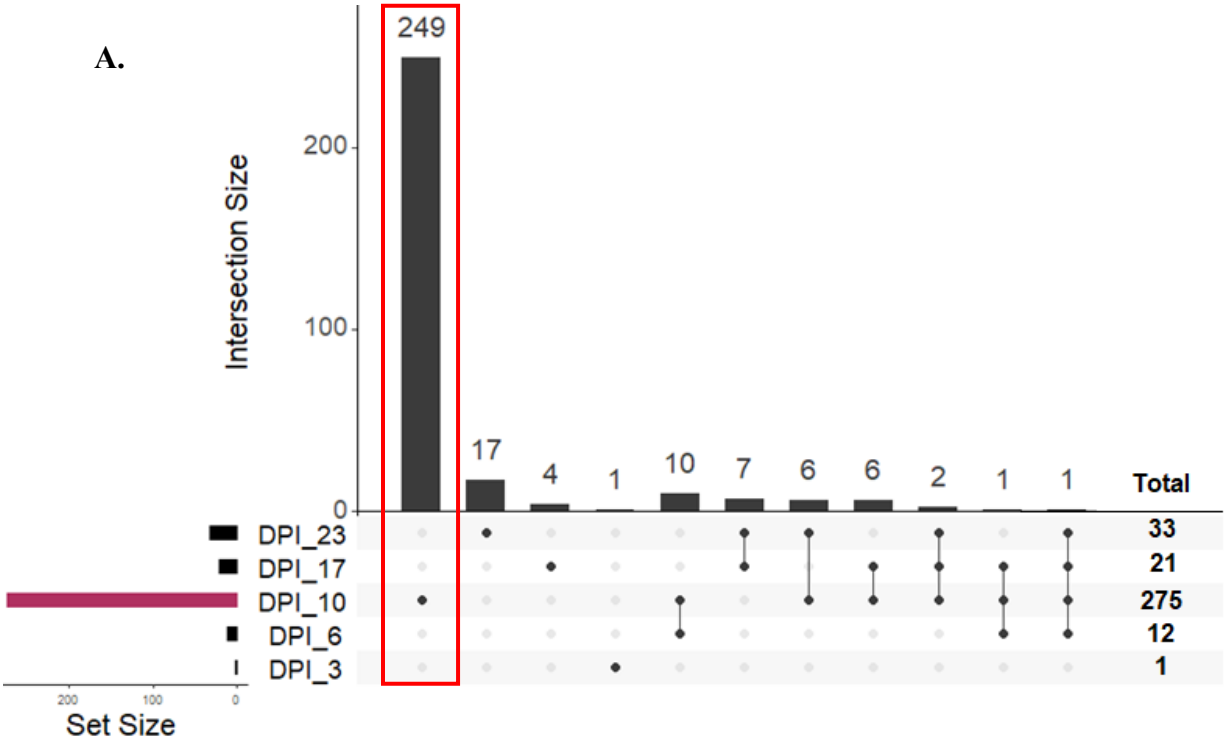

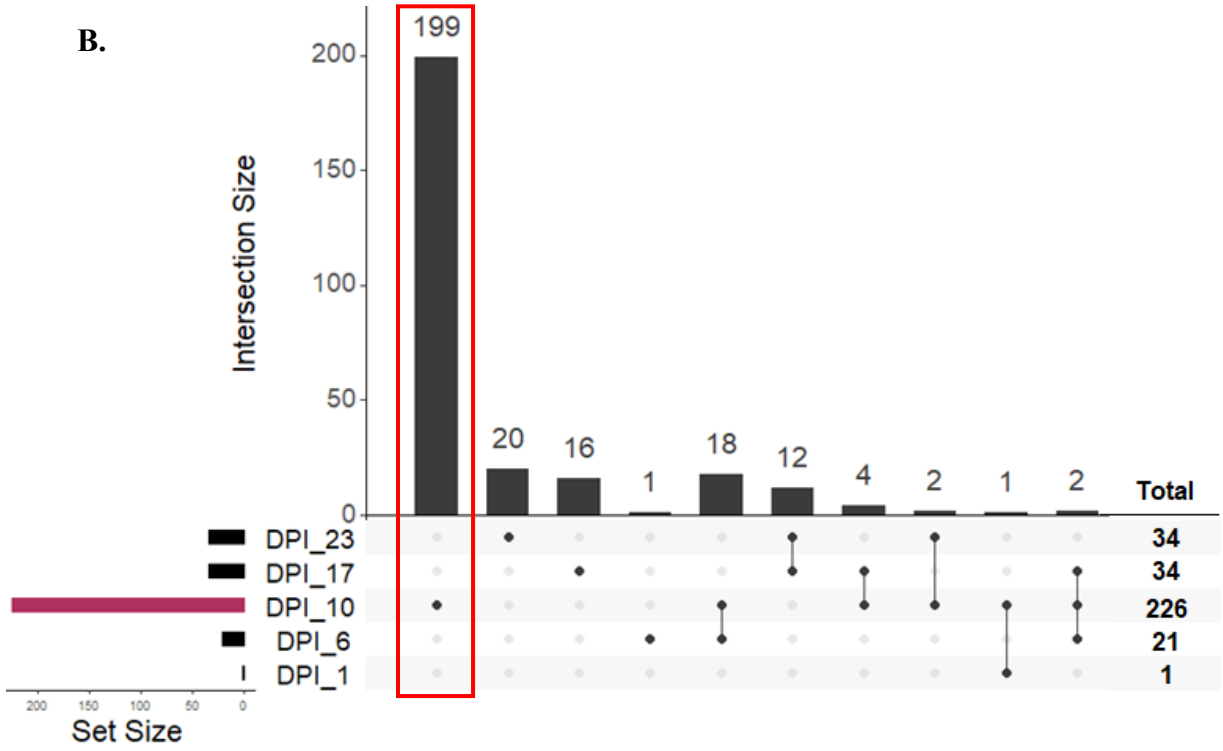

1453

1454 **Fig. 4.** Numbers of unique and shared up-regulated differentially expressed genes (DEGs) of the

1455 wheat pathogen *Zymoseptoria tritici* during the susceptible interaction on the cultivar Taichung

1456 29 compared to the resistant interaction on: A) the *Stb2*-carrying cultivar Veranopolis; and to the

1457 resistant interaction on B) the *Stb3*-carrying cultivar Israel 493; at 1, 3, 6, 10, 17 and 23 days post

1458 inoculation (DPI). The colored horizontal bar indicates the total number of up-regulated DEGs at

1459 the time point showing the highest number of uniquely up-regulated genes. The red rectangle

1460 highlights the number of genes that were exclusively differentially up-regulated at 10 DPI.

1461

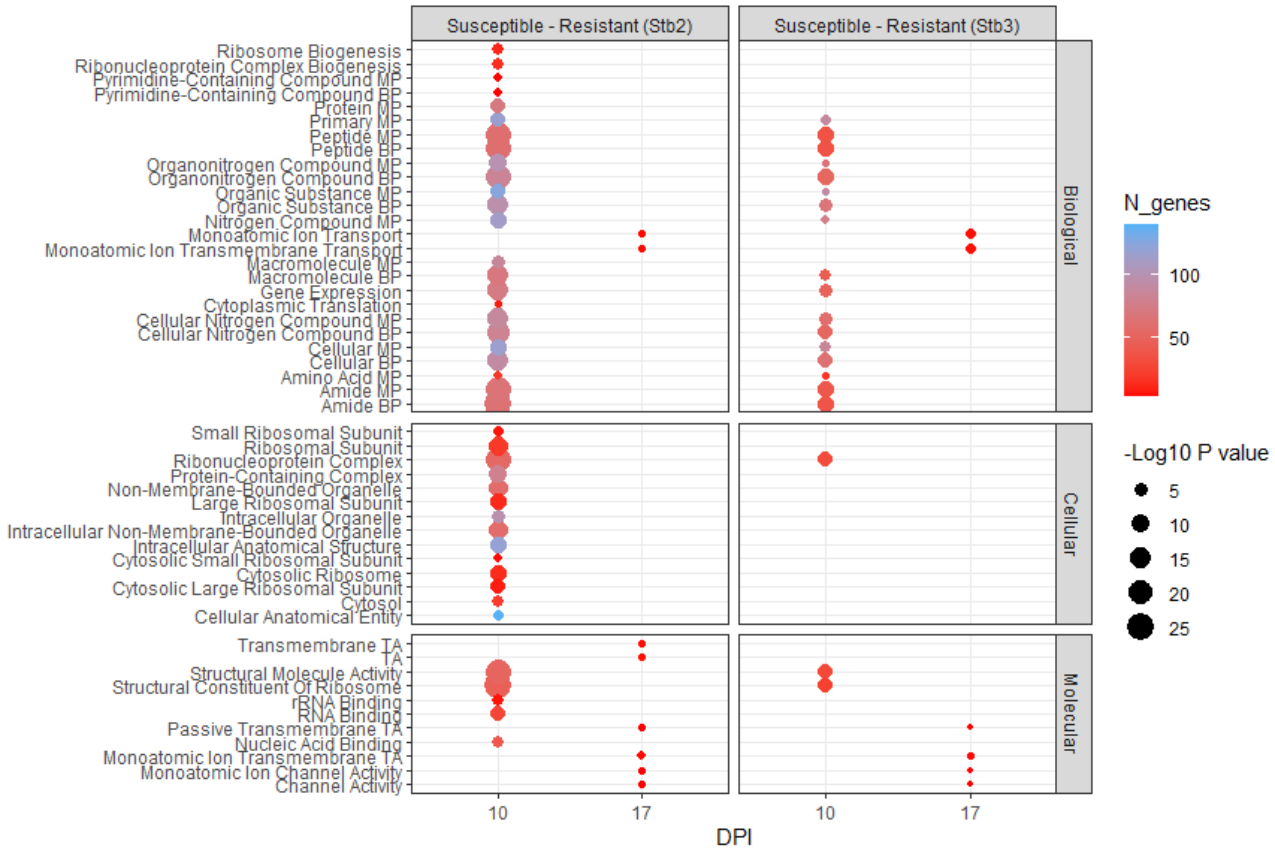

Fig. 5. Gene Ontology (GO) terms enriched at 10 and 17 days post inoculation (DPI) in the susceptible interaction compared to the resistant interactions on the *Stb2*-contining cultivar Veranopolis (left panel) and on the *Stb3*-containing cultivar Israel 493 (right panel) following inoculation with the wheat pathogen *Zymoseptoria tritici*. Only up-regulated genes were included in the GO analysis. The number of genes included in the GO analysis is 207 for the susceptible interaction compared to the resistant interaction on the *Stb2*-containing cultivar Veranopolis at 10 and 17 DPI, and 166 for the susceptible interaction compared to the resistant interaction on the *Stb3*-containing cultivar Israel 493 at 10 and 17 DPI. Metabolic process (MP), Biosynthetic process (BP), Transporter Activity (TA).

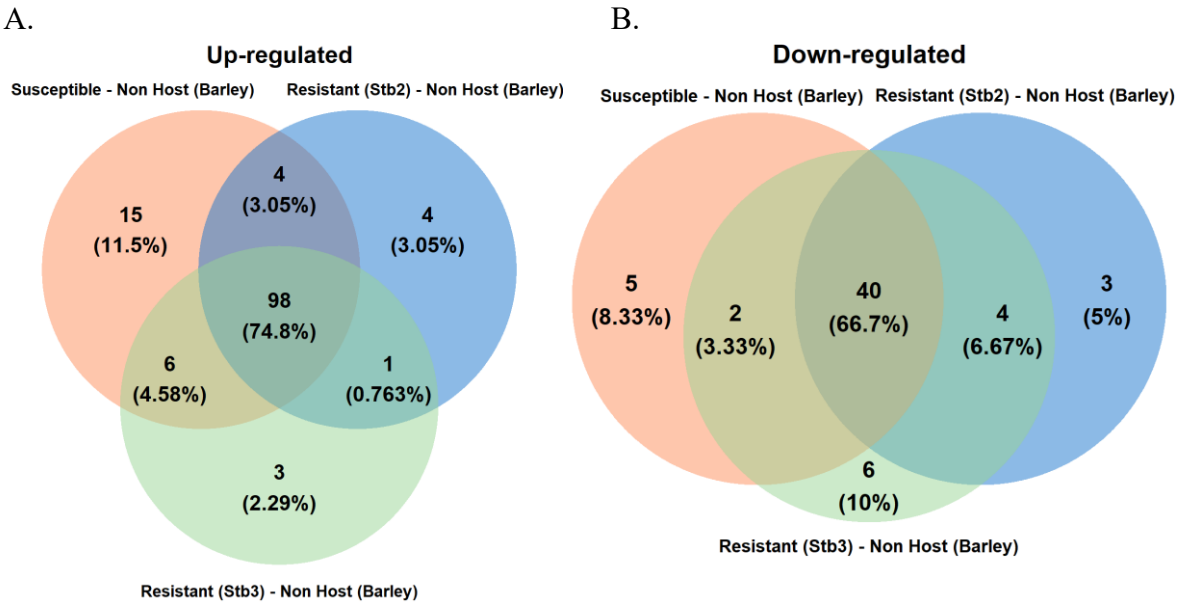

Fig. 6. Venn diagrams showing common and unique differentially expressed genes of *Zymoseptoria tritici* at 3 days post inoculation (DPI) in the susceptible and resistant interactions on wheat compared to the non-host interaction on barley. (A) Up-regulated genes shared between the comparisons of the susceptible interaction versus the non-host interaction, the resistant interaction with Veranopolis (*Stb2*) versus the non-host interaction, and the resistant interaction with Israel 493 (*Stb3*) versus the non-host interaction. The intersection represents 98 (74.8%) genes that were up-regulated in the pathogen during the susceptible and resistant interactions relative to the non-host interaction. (B) Down-regulated genes shared between the comparisons of the susceptible interaction versus the non-host interaction, the resistant interaction with Veranopolis (*Stb2*) versus the non-host interaction, and the resistant interaction with Israel 493 (*Stb3*) versus the non-host interaction. The intersection represents 40 (66.7%) genes that were down-regulated in the pathogen during the susceptible and resistant interactions relative to the non-host interaction.

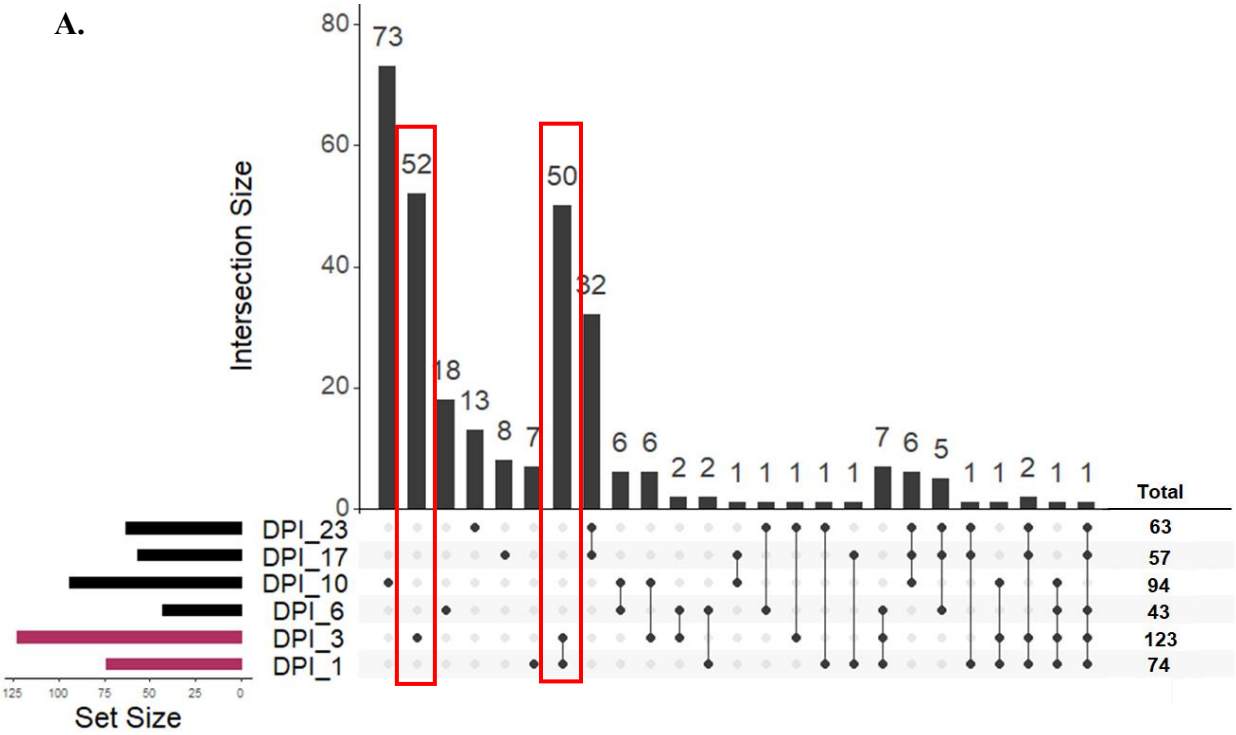
A.
Intersection Size
80
60
40
20
0
73
52
18
13
8
7
50
32
6
6
2
2
1
1
1
1
1
7
6
5
1
1
2
1
1
Total
DPI_23
DPI_17
DPI_10
DPI_6
DPI_3
DPI_1
63
57
94
43
123
74
125
100
75
50
25
0
Set Size

1486

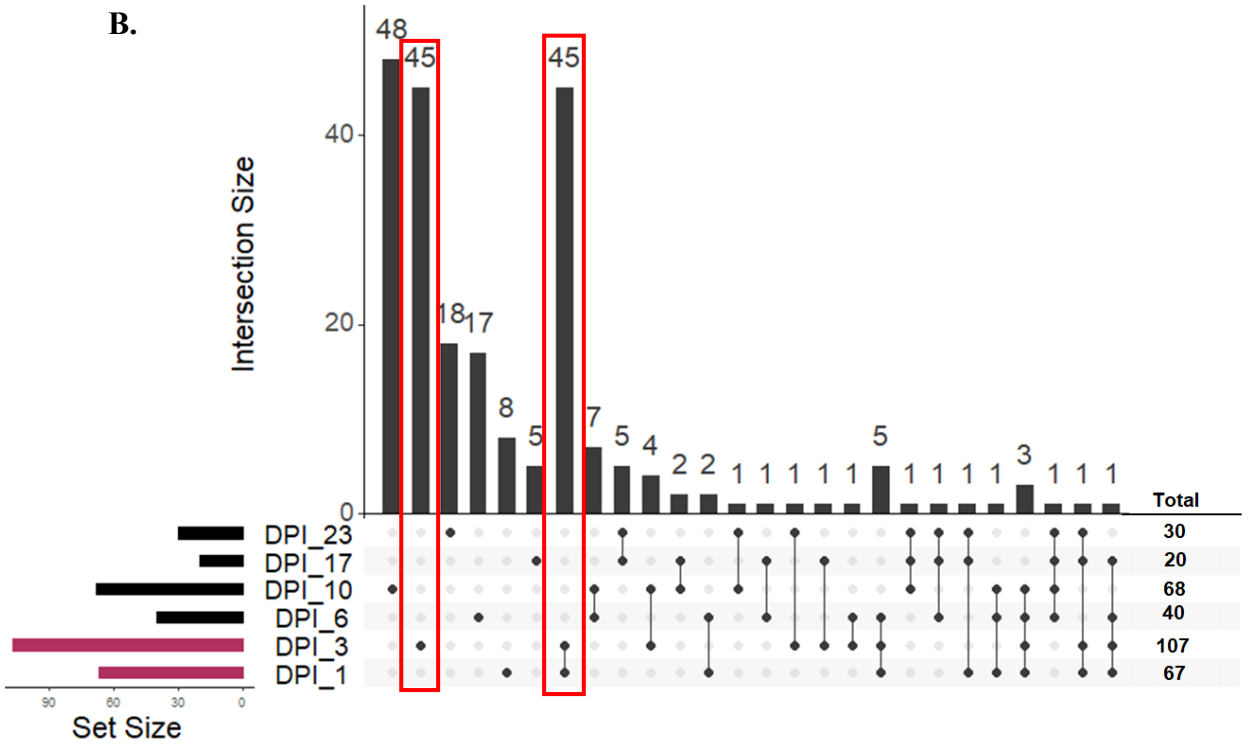

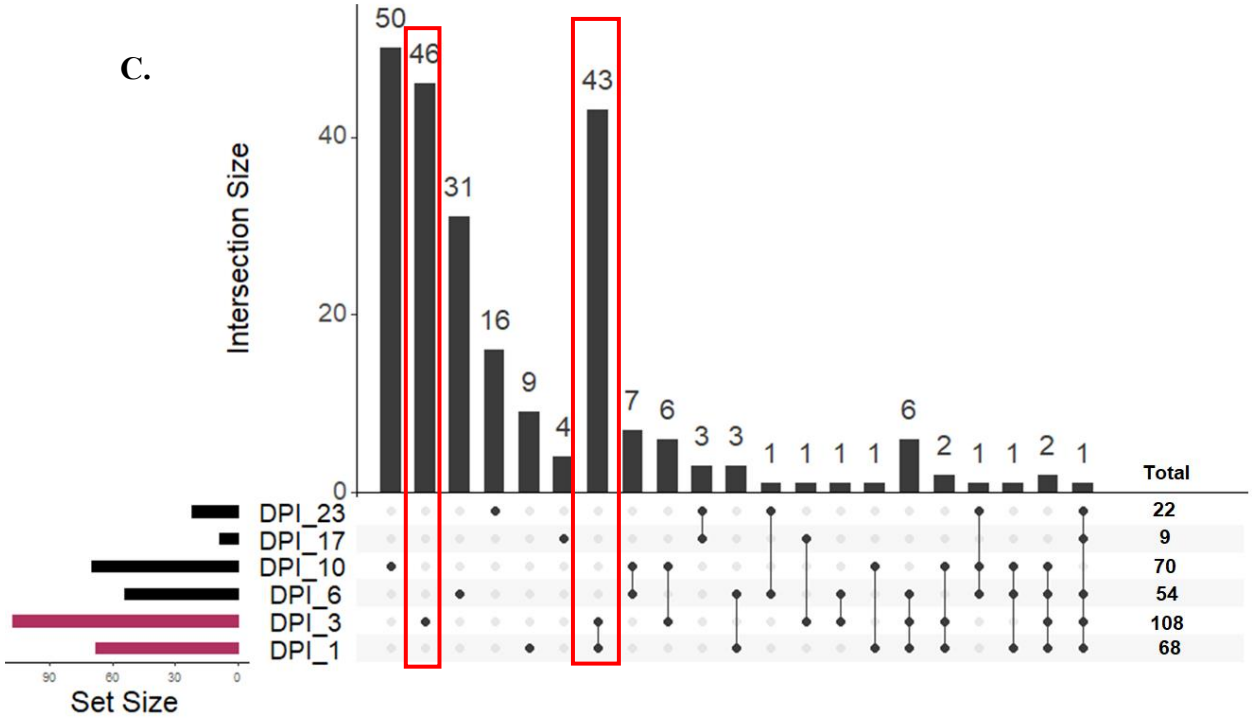

Fig. 7. Numbers of unique and shared up-regulated differentially expressed genes (DEGs) of the wheat pathogen *Zymoseptoria tritici* among six time points during the: A) susceptible interaction

on wheat cultivar Taichung 29; B) resistant interaction on the *Stb2*-carrying cultivar Veranopolis; and C) resistant interaction on the *Stb3*-carrying cultivar Israel 493compared to its non-host interaction on barley. The colored horizontal bars indicate the total number of up-regulated DEGs at the time points showing the highest number of uniquely up-regulated genes. The red rectangles highlight the numbers of genes that were exclusively differentially up-regulated at 1 DPI and at 1 and 3 DPI.

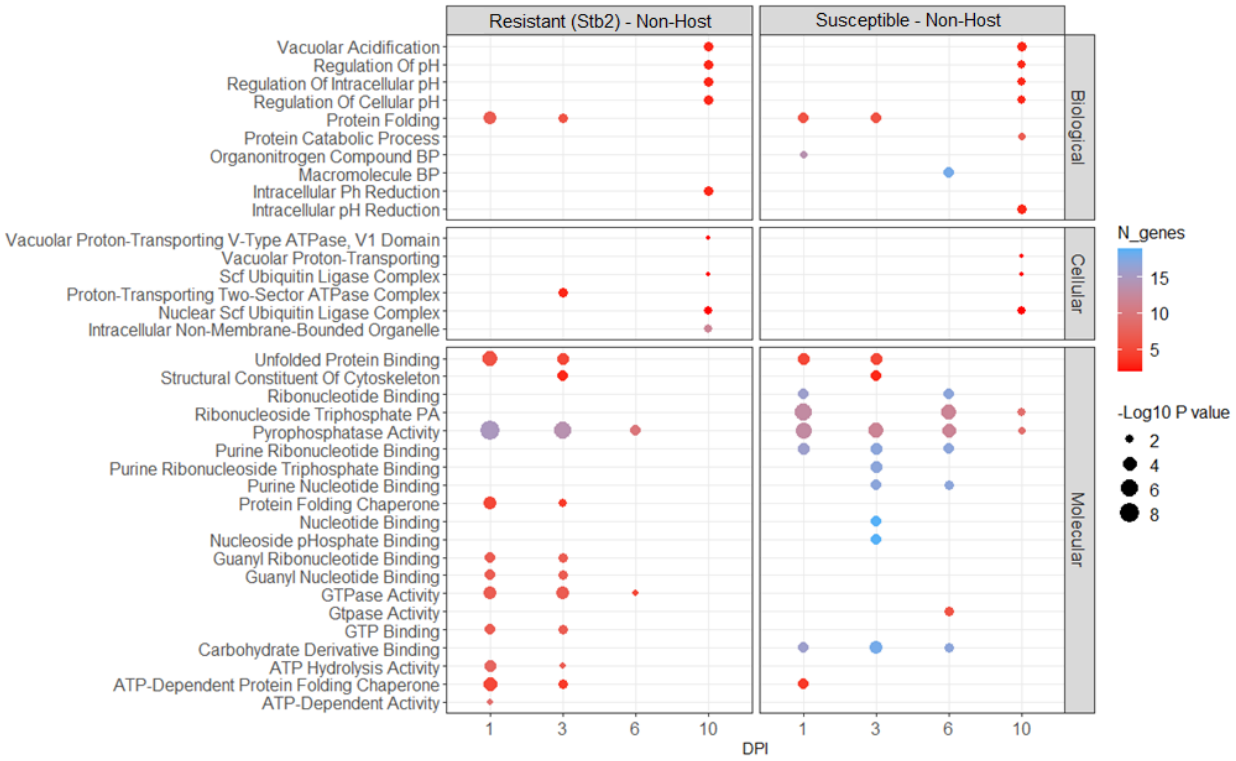

Fig. 8. Gene Ontology terms enriched at 1, 3, 6 and 10 days post inoculation (DPI) with the wheat pathogen *Zymoseptoria tritici* in the non-host interaction on barley compared to the resistant interaction on the *Stb2*-containing cultivar Veranopolis (left panel) and on the susceptible wheat cultivar Taichung 29 (right panel). Only down-regulated genes (with the non-host interaction as the baseline) were included in the GO analysis. The number of down-regulated genes included in the GO analysis is 148 for the resistant interaction on the *Stb2*-containing cultivar Veranopolis compared to the non-host interaction at 1, 3, 6 and 10 DPI, and 145 genes for the susceptible interaction compared to the non-host interaction at 1, 3, 6 and 10 DPI. BP: Biosynthetic process.

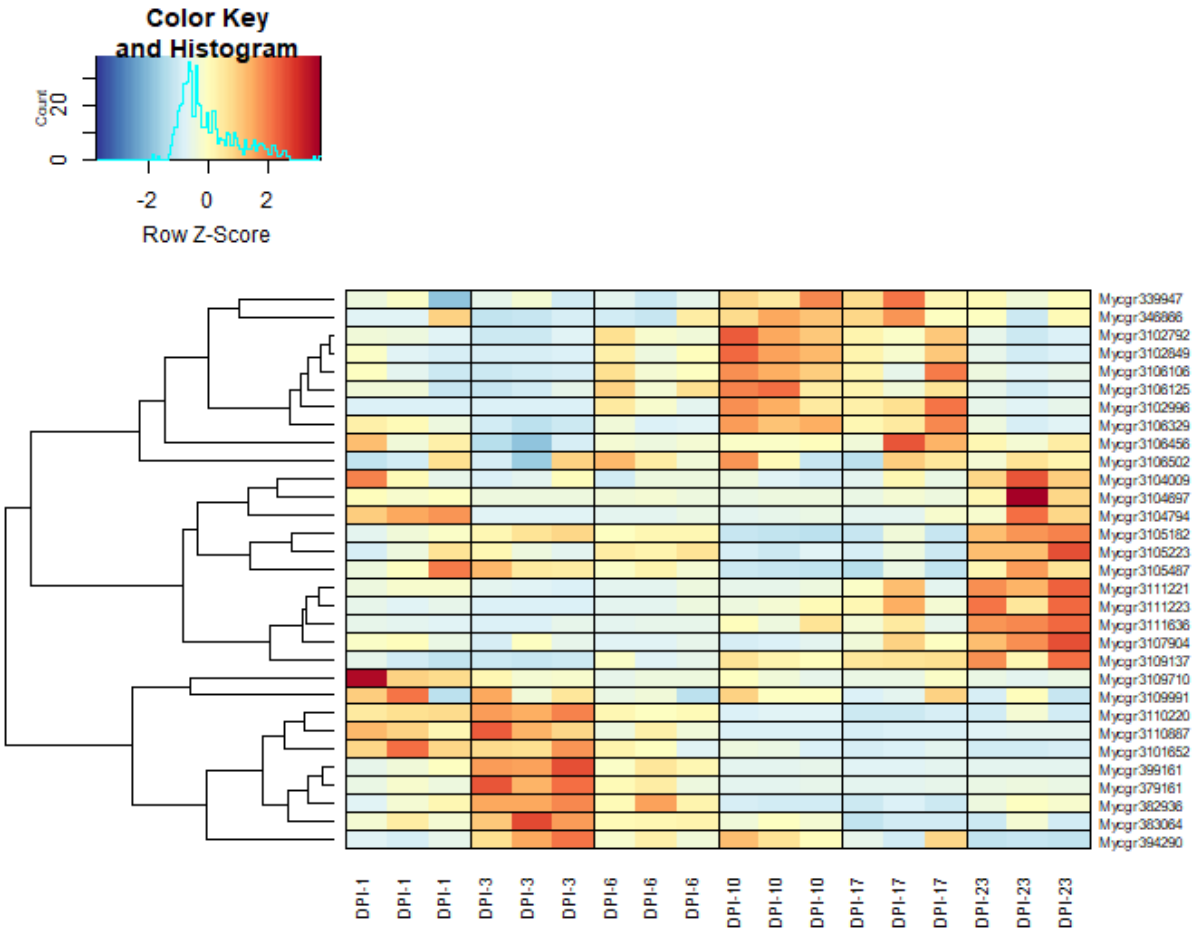

Fig. 9. Relative expression of 31 selected *Zymoseptoria tritici* effector candidates over a 23-day time course in the susceptible wheat cultivar cultivar Taichung 29. The heat map shows the normalized expression value of each effector candidate in the individual samples for each time point for the susceptible interaction on cultivar Taichung 29 and not relative to another interaction. The dendrogram on the left shows the clustering of the candidate effectors based on their relative expression calculated by the Pearson correlation. All of these 31 effectors were expressed early when compared to the non-host interaction.

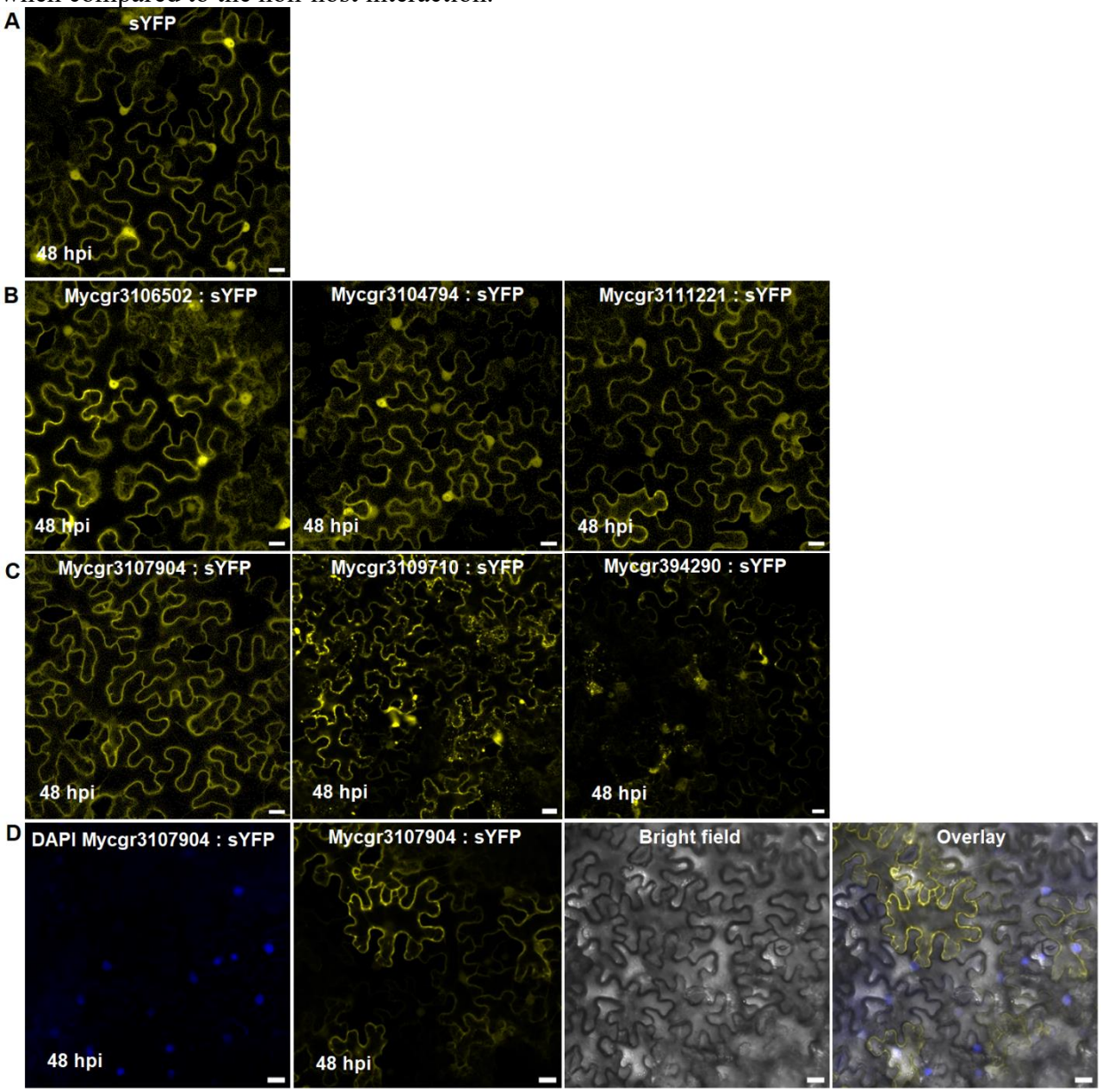

Fig. 10. Subcellular localization of six *Zymoseptoria tritici* effectors in *Nicotiana benthamiana* leaf cells expressed without their putative signal peptides. A) Free sYFP localizes to the nucleus and cytosol of the cell, and was included as a negative control to establish a baseline for comparison; B) *Zymoseptoria tritici* candidate effectors Mycgr3106502, Mycgr3104794 and Mycgr3111221 display a non-informative localization that is indistinguishable from the localization

of the negative control free sYFP; C) Mycgr3107904 localizes only to the cytosol and no localization signal is detected in the nucleus; Mycgr3109710- and Mycgr394290-fluorescent proteins accumulate in what appears to be mobile (Supplementary video) cytosolic elements in *N. benthamiana* cells. D) DAPI nucleus staining is shown as a nuclear marker for comparison using effector Mycgr3107904 that localizes predominantly to the cytosol. sYFP-tagged *Z. tritici* candidate effectors were transiently expressed without their putative signal peptides in *N. benthamiana* leaves using agroinfiltration. Confocal micrographs of leaf epidermal cells were captured 48 hours following agroinfiltration. The scale bars shown at the bottom right of each image represent 20 µm. All confocal micrographs are of single optical sections.

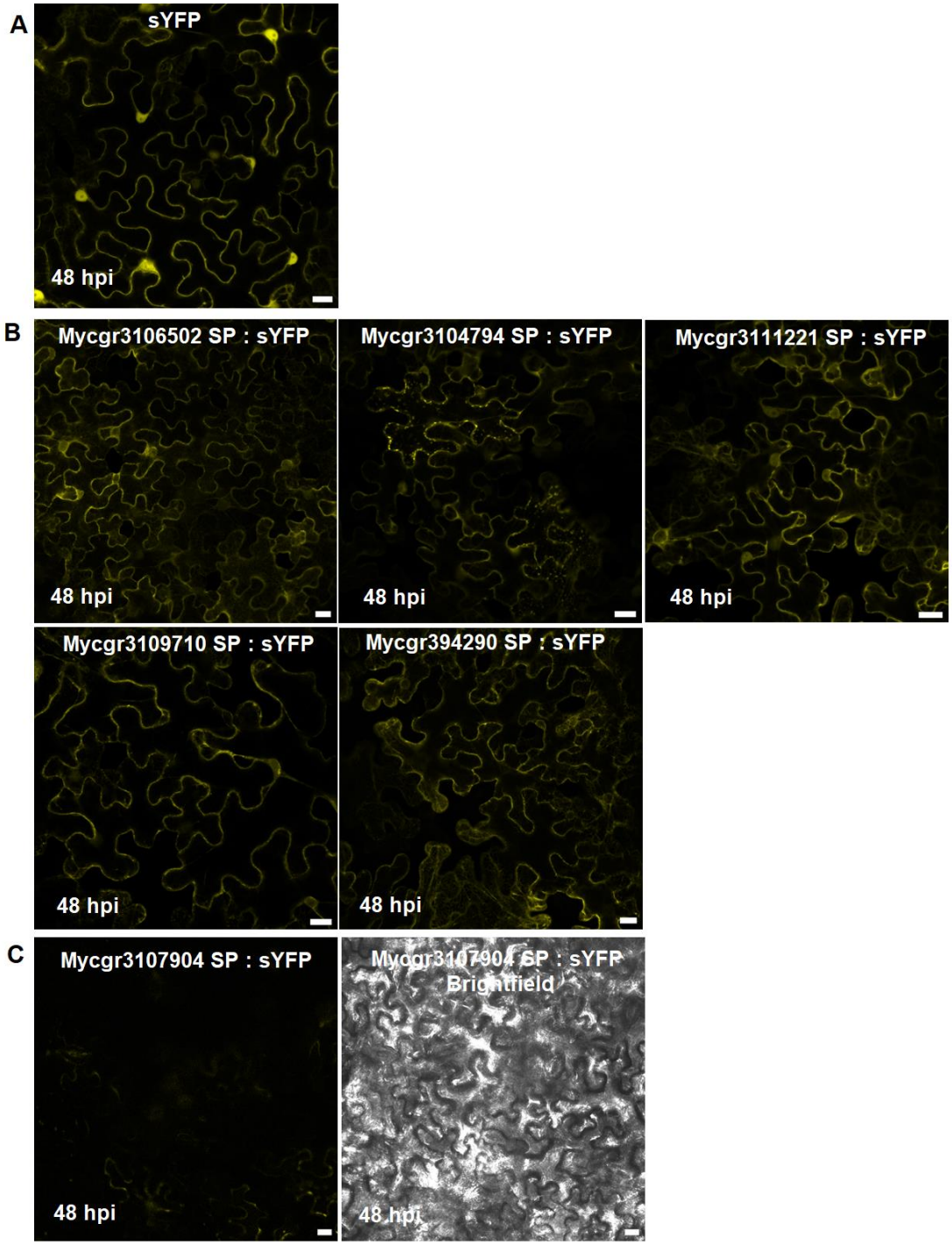

Fig. 11. Subcellular localization of six *Zymoseptoria tritici* effectors in *Nicotiana benthamiana* leaf cells expressed with their putative signal peptides. A) Free sYFP localizes to the nucleus and cytosol of the cell, and was included as a negative control to establish a baseline for comparison; B) *Zymoseptoria tritici* candidate effectors were expressed with their putative signal peptides. Mycgr3106502, Mycgr3104794, Mycgr3109710, and Mycgr394290 localize predominantly to the cytosol and no localization signal is detected in the nucleus. Mycgr3111221 localizes to both

1539 the cytosol and nucleus; C) No fluorescence signal was detected for Mycgr3107904. The bright-
1540 field section for this effector is included to show the absence of the fluorescence signal. sYFP-
1541 tagged *Z. tritici* candidate effectors were transiently expressed with their putative signal peptides
1542 in *N. benthamiana* leaves using agroinfiltration. Confocal micrographs of leaf epidermal cells
1543 were captured 48 hours following agroinfiltration. The scale bars shown at the bottom right of
1544 each image represent 20 µm. All confocal micrographs are of single optical sections.
1545

1546 **Supplementary Table 1.** RNAseq read counts and statistics of mapped reads to the *Zymosepto-*
1547 *ria tritici* genome

Treatment or interaction	Days after inoculation	Replicate	Total reads	Mapped to the *Z. tritici* genome	
				No.	Percentage
Susceptible (Taichung 29)	1	1	110453572	350676	0.32
		2	6537312	26747	0.41
		3	135784373	266323	0.20
	3	1	61526162	128868	0.21
		2	85685602	203046	0.24
		3	88708485	373321	0.42
	6	1	123384952	513906	0.42
		2	125288900	626416	0.50
		3	103978562	711360	0.68
	10	1	71214614	584716	0.82
		2	118542141	560482	0.47
		3	120641473	1380018	1.14
	17	1	118166646	9926081	8.40
		2	130632837	13405771	10.26
		3	126972350	17570113	13.84
	23	1	109832349	46219025	42.08
		2	108115959	50693615	46.89
		3	129487230	25332585	19.56
Resistant (Veranopolis)	1	1	95008077	378782	0.40
		2	80804231	178213	0.22
	3	1	83940937	405367	0.48
		2	103525342	293261	0.28
	6	1	116839693	406077	0.35
		2	119822495	385102	0.32
	10	1	119716902	853382	0.71

		2	129205510	911841	0.71
		3	81584036	289627	0.36
	17	1	85949935	122551	0.14
		2	85722745	205935	0.24
		3	119560704	71224	0.06
	23	1	114628505	145815	0.13
		2	109622307	139061	0.13
		3	119144665	115900	0.10
Resistant (Israel 493)	1	1	105033483	518963	0.49
		2	112367071	399980	0.36
		3	79757459	298668	0.37
	3	1	100632609	133408	0.13
		2	118171767	262615	0.22
		3	100294847	452927	0.45
	6	1	132467171	333932	0.25
		2	138203399	353806	0.26
		3	124662793	466263	0.37
	10	1	162835830	379145	0.23
		2	88109775	164831	0.19
		3	87081363	468964	0.54
	17	1	101648946	299357	0.29
		2	190074395	314572	0.17
		3	112094936	568115	0.51
	23	1	116023358	99876	0.09
		2	106154281	88367	0.08
		3	134635693	63029	0.05
Non-Host (Barley)	1	1	160104601	41053	0.03
		2	131020166	44453	0.03
		3	155134932	47347	0.03

3	1	82439473	35586	0.04
	2	186043912	80428	0.04
	3	206439750	238372	0.12
6	1	187850381	44492	0.02
	2	193811945	123686	0.06
	3	218025800	51888	0.02
10	1	103790478	31435	0.03
	2	108153121	42534	0.04
17	1	103402937	19967	0.02
	2	98934372	19957	0.02
	3	110655888	23280	0.02
23	1	114287194	33570	0.03
	2	112142224	21078	0.02
	3	106512151	24446	0.02

Supplementary Figures

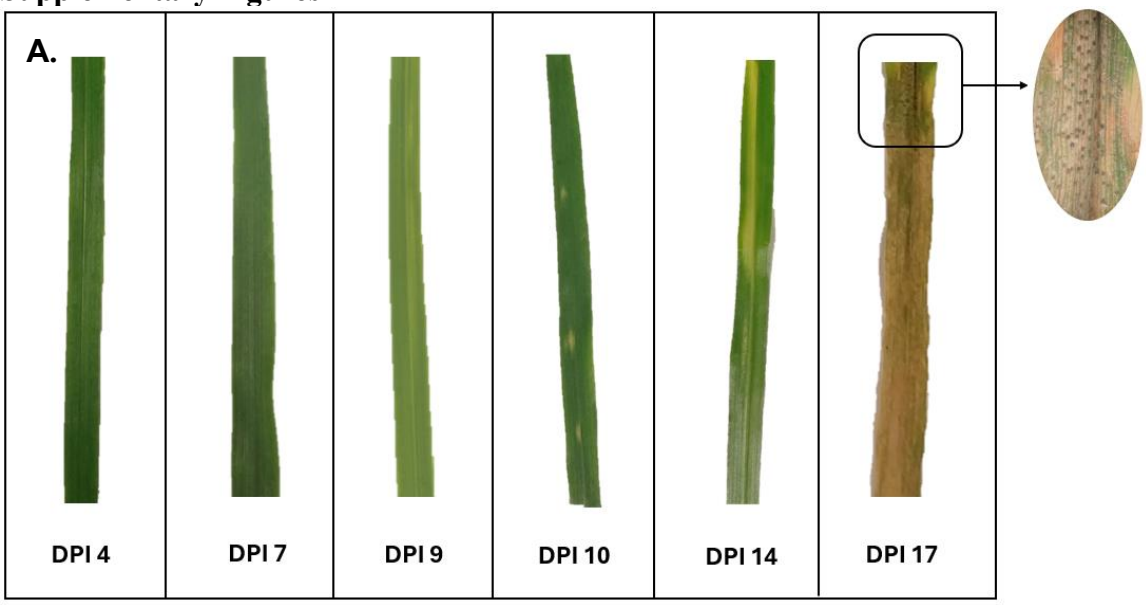

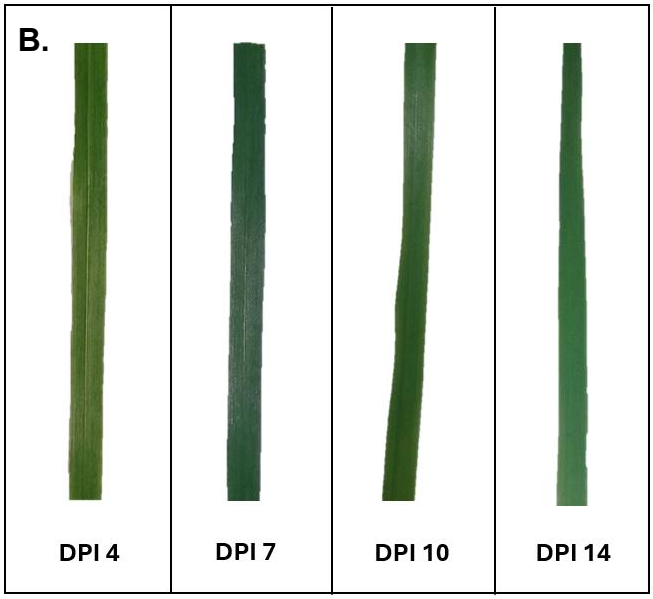

Supplementary Fig. S1. Disease establishment in the A) susceptible cultivar Taichung 29 of wheat and in the B) resistant cultivar Israel 493 at the indicated days post inoculation (DPI) with the wheat pathogen *Zymoseptoria tritici*. A closeup of the susceptible response at 17 DPI is shown in the expanded view at the upper right.

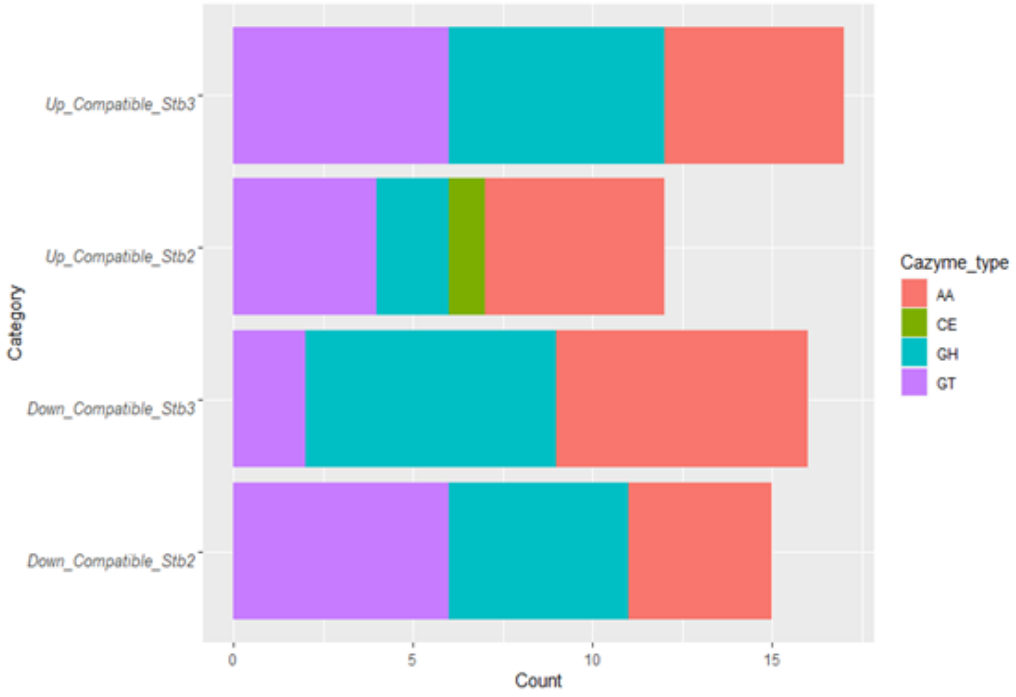

Supplementary Fig. S2. Carbohydrate-active enzymes of *Zymoseptoria tritici* identified at 10 days post inoculation in the comparison between susceptible and resistant interactions. Compatible = Susceptible.

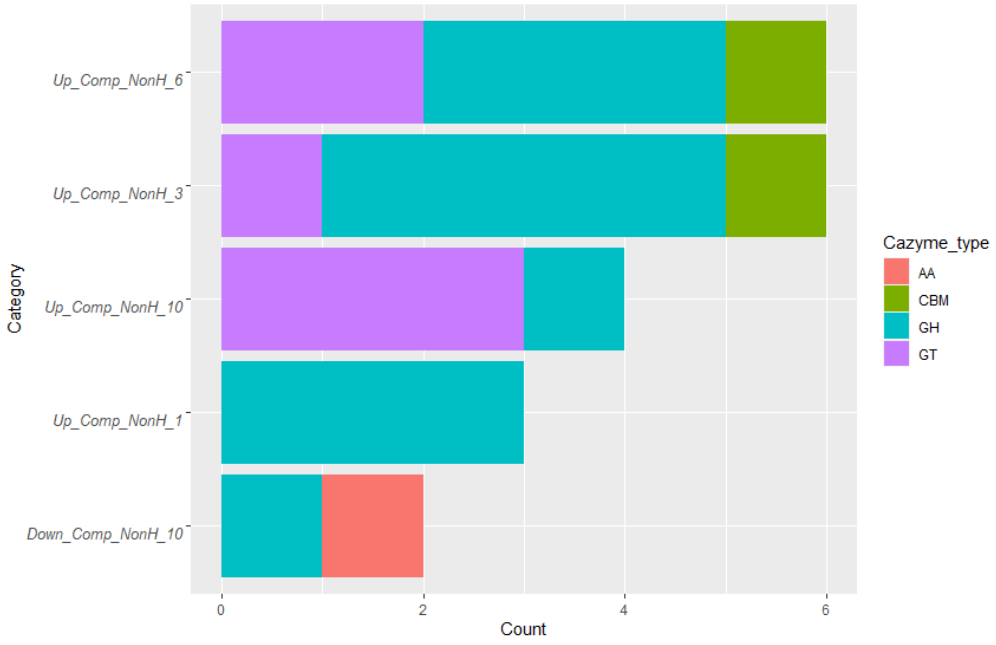

Supplementary Fig. S3. Carbohydrate-active enzymes of *Zymoseptoria tritici* identified at 6, 3, 10, 1 and 10 days post inoculation (from top to bottom) in the comparison between susceptible and non-host interactions. Comp = Susceptible, NonH= Non-Host.

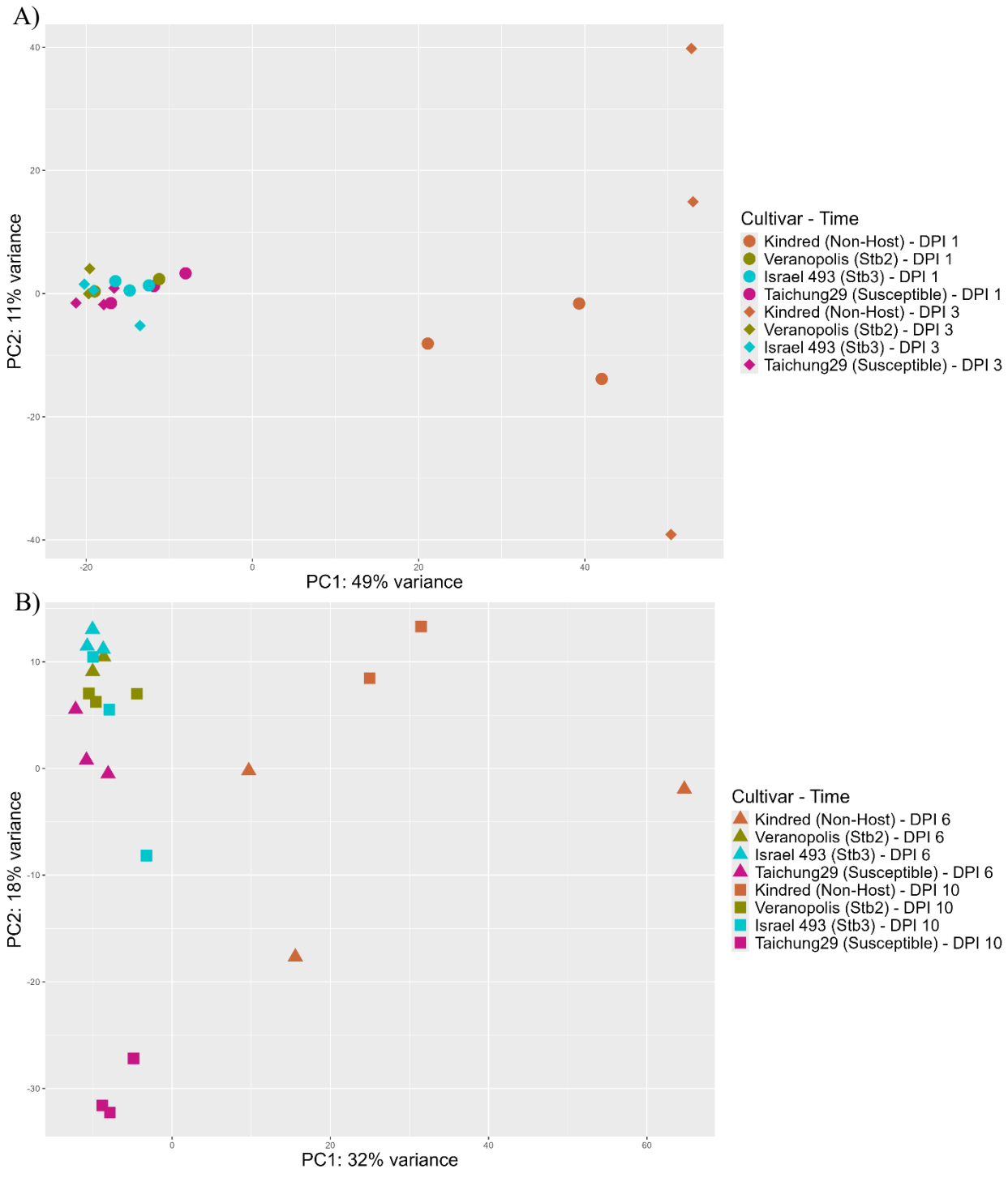

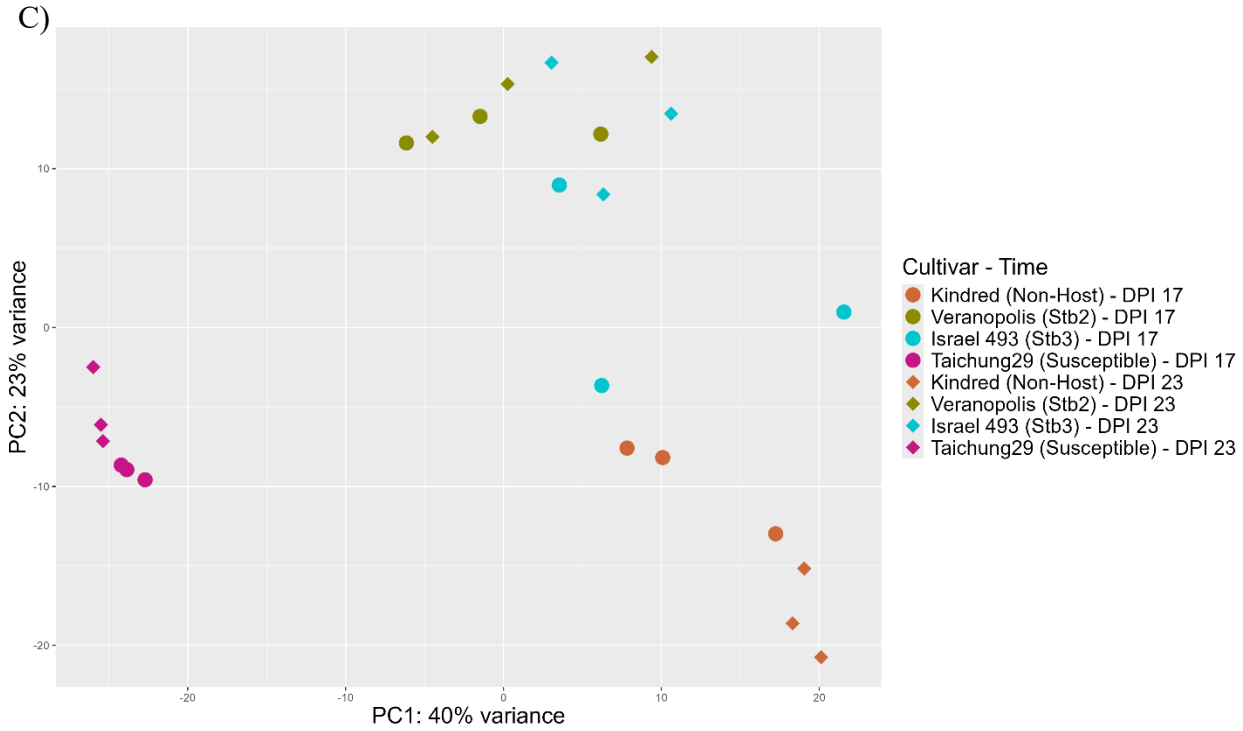

Supplementary Fig. S4. Principal component analysis (PCA) of the normalized filtered read counts for RNA of *Zymoseptoria tritici* inoculated onto the highly susceptible wheat cultivar Taichung 29 (Susceptible) or the R-gene-containing resistant wheat cultivars Veranopolis (*Stb2*) or Israel 493 (*Stb3*) or the non-host barley at: A) 1 and 3; B) 6 and 10; and C) 17 and 23 days post inoculation (DPI).

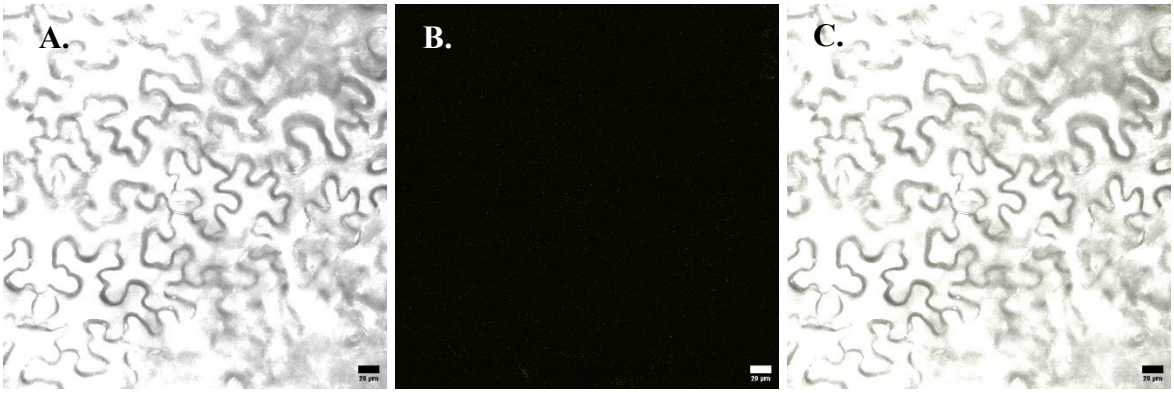

Supplementary Fig. S5. Image of a *Nicotiana benthamiana* leaf infiltrated with *Agrobacterium* expressing a protein with an -HA tag showing: A) brightfield; B) wavelength used for sYFP (514 nm) excitation; and C) the composite image. The gain was increased on the confocal microscope to enhance the detection of any potential low-level fluorescence observed in the leaf tissue.

1582

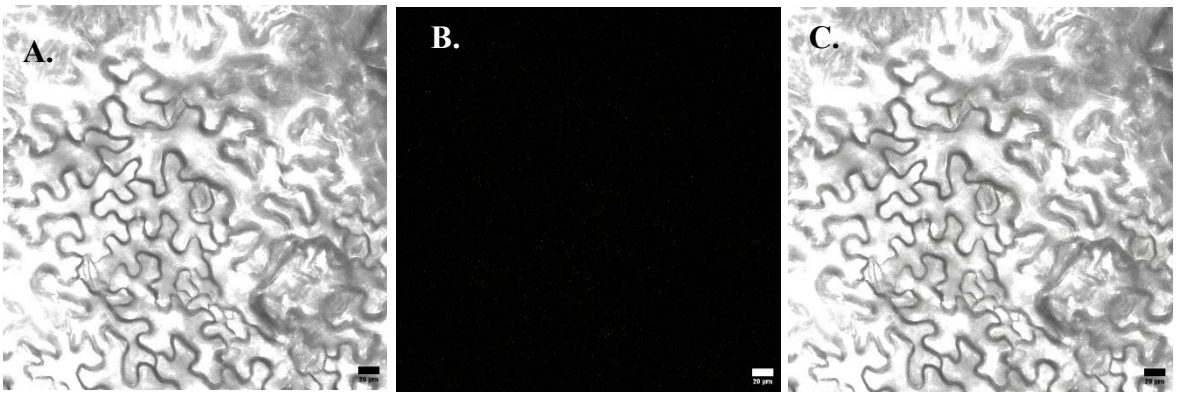

1583
1584 **Supplementary Fig. S6.** Image of a non-infiltrated *Nicotiana benthamiana* leaf showing: A)
1585 brightfield; B) wavelength used for sYFP (514 nm) excitation; and C) the composite image. The
1586 gain was increased on the confocal microscope to enhance the detection of any potential low-
1587 level autofluorescence in the leaf tissue.

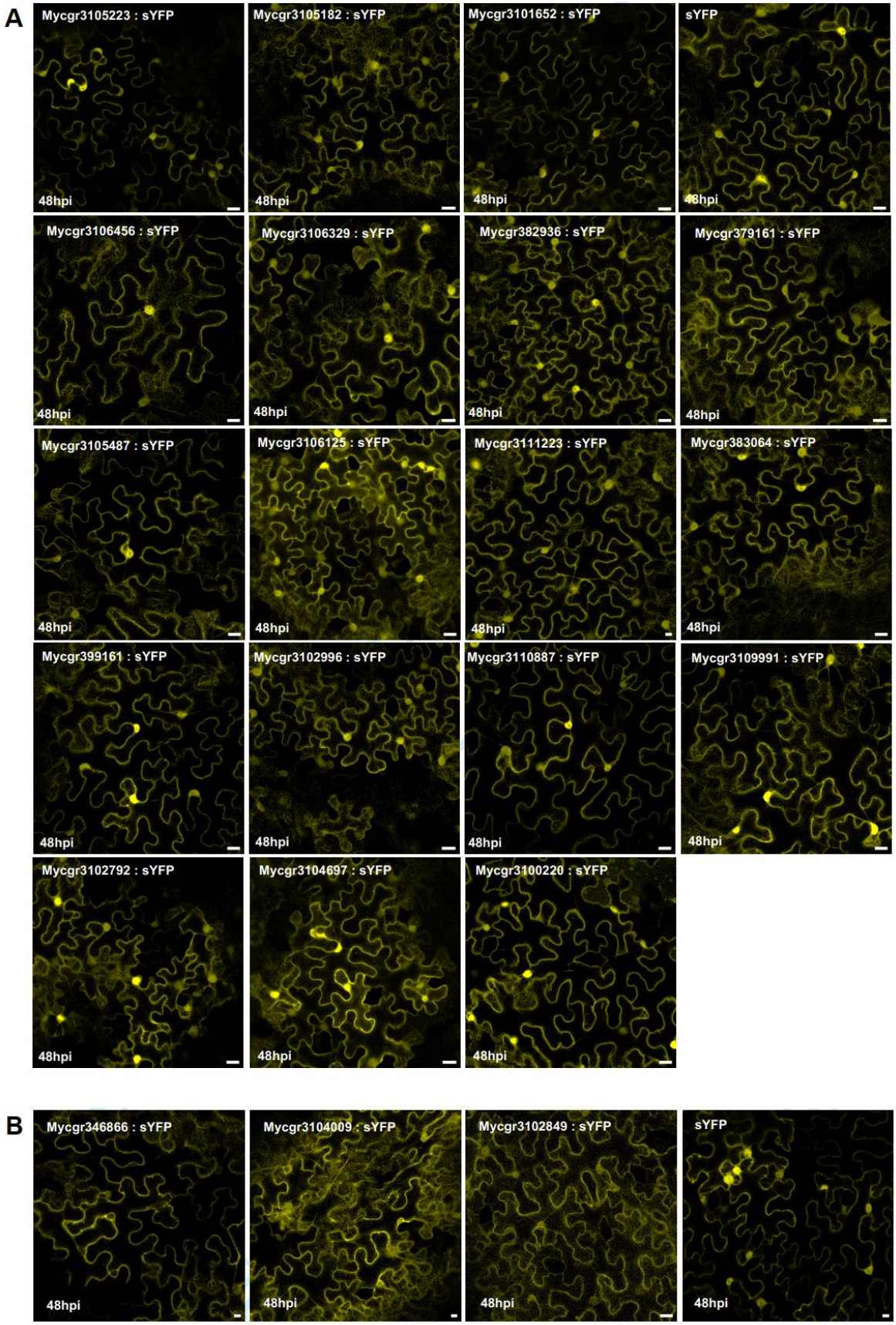
A
Mycgr3105223 : sYFP
48hpi
Mycgr3105182 : sYFP
48hpi
Mycgr3101652 : sYFP
48hpi
sYFP
48hpi
Mycgr3106456 : sYFP
48hpi
Mycgr3106329 : sYFP
48hpi
Mycgr382936 : sYFP
48hpi
Mycgr379161 : sYFP
48hpi
Mycgr3105487 : sYFP
48hpi
Mycgr3106125 : sYFP
48hpi
Mycgr3111223 : sYFP
48hpi
Mycgr383064 : sYFP
48hpi
Mycgr399161 : sYFP
48hpi
Mycgr3102996 : sYFP
48hpi
Mycgr3110887 : sYFP
48hpi
Mycgr3109991 : sYFP
48hpi
Mycgr3102792 : sYFP
48hpi
Mycgr3104697 : sYFP
48hpi
Mycgr3100220 : sYFP
48hpi
B
Mycgr346866 : sYFP
48hpi
Mycgr3104009 : sYFP
48hpi
Mycgr3102849 : sYFP
48hpi
sYFP
48hpi

1588

Supplementary Fig. S7. Subcellular localization of *Zymoseptoria tritici* effectors in *Nicotiana benthamiana* leaf cells expressed without their putative signal peptides. **A)** *Zymoseptoria tritici* candidate effectors display a non-informative nucleus-cytosol localization in *N. benthamiana* that is indistinguishable from the localization of the free sYFP control. **B)** Four *Z. tritici* candidate effectors localize predominantly to the cytosol. sYFP-tagged *Z. tritici* candidate effectors were transiently expressed without their putative signal peptides in *N. benthamiana* leaves using agroinfiltration. Confocal micrographs of leaf epidermal cells were captured 48 hours following agroinfiltration. The scale bars shown represent 20 µm. All confocal micrographs are of single optical sections.

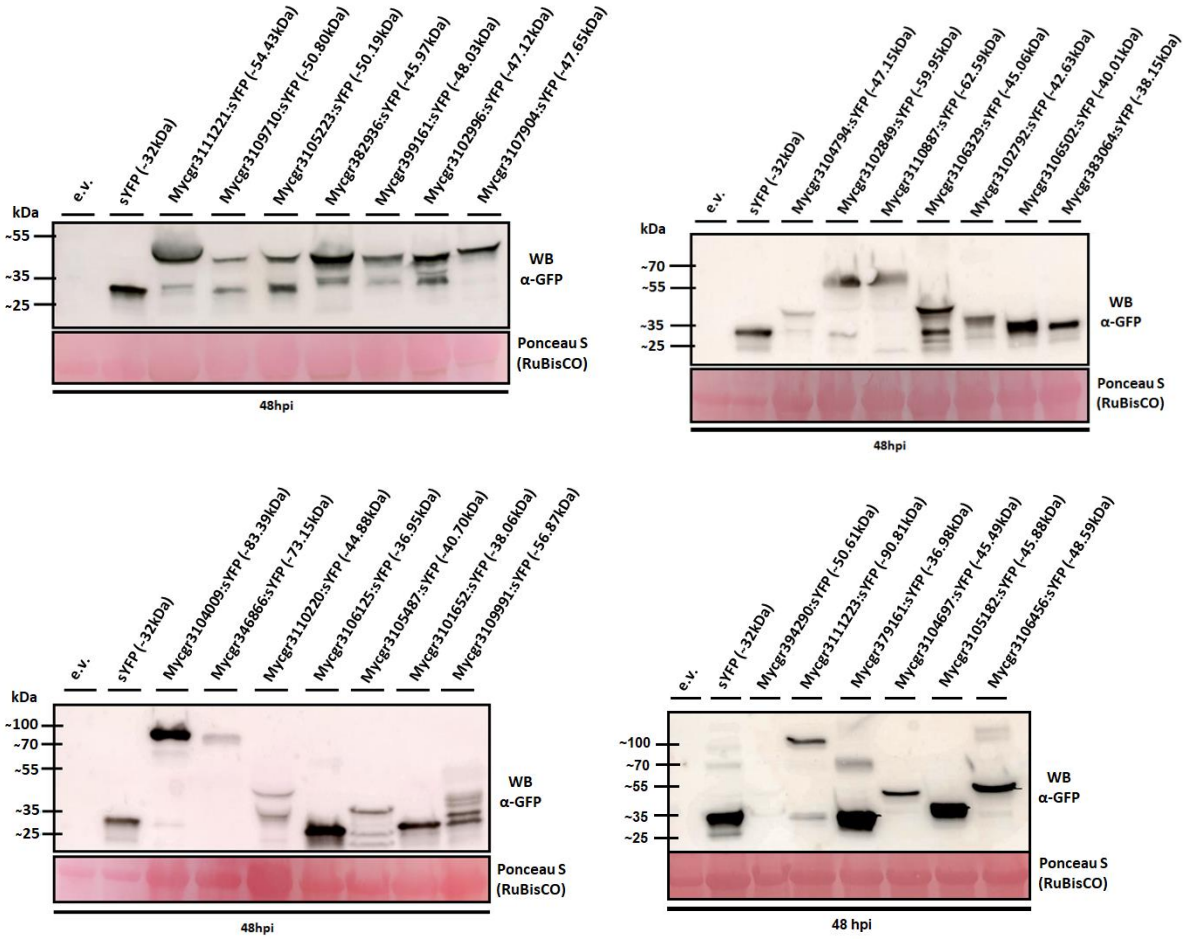

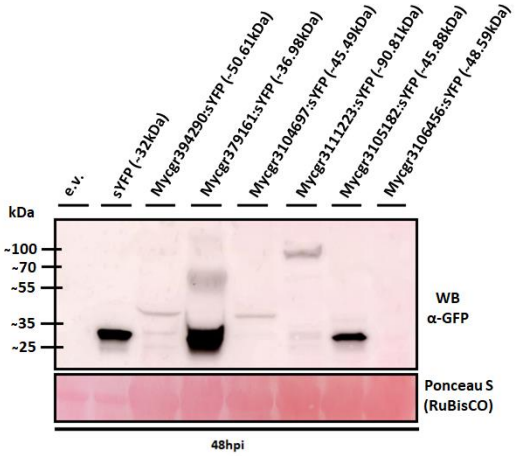

Supplementary Fig. S8. Immunoblot analyses of the *Zymoseptoria tritici* effector-fluorescent protein fusions expressed without their signal peptides. Ponceau staining of the large subunit of RuBisCO served as a loading control.

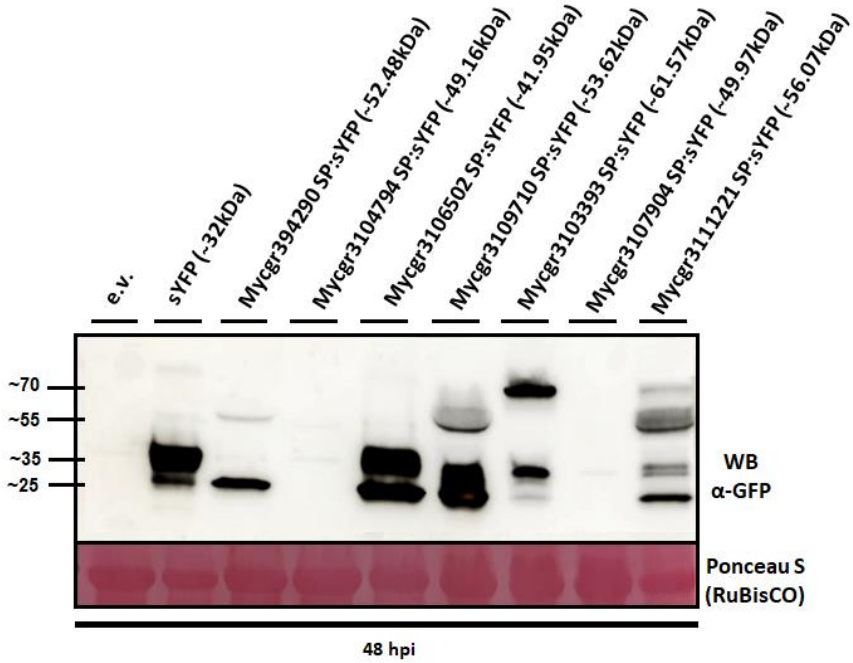

Supplementary Fig. S9. Immunoblot of the *Zymoseptoria tritici* effector-fluorescent protein fusions expressed with their signal peptides. Ponceau staining of the large subunit of RuBisCO served as a loading control. Candidate effector Mycgr3103393 was not included in the selected set of thirty-one candidate effectors, but it is shown in this immunoblot. This figure was previ-

ously published in “Functional characterization of *Zymoseptoria tritici* candidate effectors reveals their role in modulating immunity in *Nicotiana benthamiana*” by S. V. Gomez-Gutierrez et al., 2025 (bioRxiv preprint: https://doi.org/10.1101/2025.05.20.655180). Reprinted with permission.